# Transport Theorie für wechselwirkende Quantenpunkte

Habilitationsschrift
von
Herbert Schoeller

März 1997

# Contents

# Chapter 1

# Introduction

In the last few years the progress in microfabrication technology has led to an enhanced interest in studying transport properties of ultrasmall conducting islands coupled weakly to leads (for reviews see Refs. [5, 101, 48, 124, 149, 115] and popular articles can be found in Refs. [70, 120, 55, 93, 23]). Quantization of charge and tunneling through zero-dimensional states lead to many interesting phenomena in these systems. Adding a single charge to a small system costs the charging energy $E_C \sim e^2/(\epsilon L) \sim e^2/2C$ ($L$ being the length scale of the island, $\epsilon$ the dielectric constant, and $C$ the self-capacitance) and, second, the level spacing $\delta E$ of the single-particle states. For system lengths in the nanoscale regime, charging energies can be reached of order $1-10K$. For temperatures below $1K$ this implies that (dependent on the electrochemical potential of the island and the bias voltage) electron transport can be completely blocked (Coulomb blockade) or restricted to a small number of possible charge states. The latter induces constraints which are very similiar to the role of the strong onsite Coulomb repulsion in a variety of models discussed within the theory of strongly correlated fermions. In the same way electron transport can be influenced by the discrete level structure on the island. Especially in 2d semiconductor quantum dots the level spacing is large (typically 1/10 of the charging energy). This implies the interesting possibility to identify quantum dots with artificial atoms or molecules

whose properties can be measured by attaching macroscopic leads.

The study of physical properties of these systems is important for several reasons. Their sensitivity to adding a single charge can be used for measurement applications, e.g. for the detection of single charges [86, 97, 138, 25] or for setting up current standards [97, 92]. Electronic applications are the subject of intensive research and could become of technological interest if the operating temperature of quantum dots can be increased up to room temperature [120, 25, 90, 94, 62, 95]. Experimentalists can use single-electron phenomena as spectroscopic tools. For theoreticians quantum dots are interesting systems for studying models of strongly correlated systems in equilibrium or nonequilibrium. Various approximations in the low-temperature regime can be tested by comparism with experiment. Certain quantum dots are completely analog to Kondo- and generalized Anderson models. These systems are of fundamental interest in the theory of strongly correlated fermions. Furthermore, arrays of quantum dots can be used to model Hubbard chains. The coupling of quantum dots to macroscopic leads and heat baths is one of the basic problems of statistical mechanics, namely destruction of coherence in a mesoscopic system due to exchange of particles and energy with its environment.

Many phenomena in single-electron devices can be understood within perturbation or golden rule theory. This means that tunneling between system and reservoirs is so weak that the spectral density of the island is not influenced and transport can be described by classical master equations. This approach is called the "orthodox theory" and basically describes incoherent transport through the whole device by sequential tunneling processes [5, 48]. A crucial assumption in justifying perturbation theory is a small intrinsic broadening of the island excitations compared to temperature $T$ (we always set $k_B = 1$). Experimentally this can easily be achieved by using tunneling barriers with resistances $R_T$ much higher than the quantum resistance

$R_K = h/e^2 = 25.81281...k\Omega$. Thus, there exists a well-defined experimental regime where perturbation theory can describe single-electron tunneling processes through zero-dimensional states.

It is important to notice that a master equation with golden rule tunneling rates is a perturbative approach in the coupling to the reservoirs but not in the interaction within the island. Therefore, this approach has to be distinguished from the well-known scattering formalism [88, 16] which can describe coherent transport through mesoscopic devices for arbitrary tunneling barriers and temperatures but is restricted to noninteracting systems. It is therefore very important to formulate theories which can interpolate between both limits. It is one of the purposes of this paper to present a technique which is capabable of describing coherent transport through interacting islands.

There are several experimental motivations to study coherent transport through strongly interacting quantum dots. First of all there are regimes where sequential tunneling is exponentially suppressed. This happens in the Coulomb blockade regime where the current is dominated by higher order processes such as coherent "cotunneling" processes of electrons through several junctions [6]. In interference geometries where quantum dots are part of an Aharonov-Bohm ring, only higher order processes beyond sequential tunneling show a flux dependence and lead to Aharonov-Bohm oscillations[13]. Experiments can be performed in the limit where the tunneling barriers are so low that even the case of perfect transmission can be reached without destroying the effect of Coulomb blockade. This leads to a significant deviation from "orthodox theory" even in regimes where sequential tunneling contributes. This has been observed in single one-channel dots [83], coupled dots [139, 12, 105, 137, 121], and, most recently, in single multi-channel metallic islands [69]. Corresponding theories have been developed in Refs. [33, 99, 38], Refs. [100, 46, 82], and Refs. [123, 76, 80]. For

weak tranmission, deviations from golden rule theory will occur in the low-temperature region where quantum fluctuations and renormalization effects set on. In both cases, the spectral density of the island will be strongly affected by the coupling to the leads, and the broadening of levels will approach temperature or level spacing upon continuously increasing tunneling. For noninteracting systems it is very easy to incorporate these complications just by replacing the energy conservation law of golden rule by a lorentzian function with half-width , . For $T \sim$ , $<< \delta E$, the line shape of conductance maxima is then described by the well-known Breit-Wigner formula [17]. However, in interacting systems, the broadening itself can be a complicated function of energy, temperature and bias voltage. This induces strong renormalization effects of the levels and the system parameters. For quantum dots described by one degenerate low-lying level it can even lead to new resonances in the spectral density in the form of Kondo resonances [43, 109, 118]. They show up in various anomalies in the differential conductance as function of the bias voltage [58, 103, 59, 77, 78]. Quantum dots with continuous level spectra are, in the two charge-state approximation, equivalent to multichannel Kondo models [98]. Again, this gives rise to anomalous temperature dependences of the conductance as function of gate or bias voltage [123, 76, 80, 69]. By varying the level spacing, level position or using multi-dot systems an enormous variety of interesting many-body systems can be created. Their low-temperature scaling behaviour is still not known for most cases.

When the transmission per channel of the barriers approaches unity it is no longer possible to distinguish between electrons in the dot and the leads. This is a problem not treated within this paper. It would require a complete interacting theory for the total system, i.e. dot and leads, describing e.g. problems how screening properties of a perfect metall evolve continuously into a mesoscopic region. Some preliminary but important fundamental steps in this direction can be found e.g. in [18, 99, 38]. Here

we are interested in the case where the transmission per channel is still much less than unity so that a well-defined description via a tunneling Hamiltonian is justified. One should recognize that, for large channel number, this includes the possibility of total transmission being larger than unity. Experiments in this regime have recently been performed in metallic dots with clear signs for deviations from classical behaviour [69]. Furthermore, as already mentioned before, quantum fluctuations become also visible by lowering the temperature. Especially vertical quantum dots [134], ultrasmall metallic particles [117], carbon nanotubes [27] or molecules [74], where the level spacing and , can be very large, are promising candidates for the observation of quantum fluctuations in the weak transmission limit at realistic temperatures.

The transport theory presented here is based on a recently developed real-time diagrammatic approach [123, 76, 77, 78] closely related to path-integral methods formulated in connection with dissipation [31, 19, 140] or tunneling in metallic junctions [28, 125, 124]. The idea is to integrate out the reservoir degrees of freedom and to set up a formally exact kinetic equation for the reduced density matrix of the dot. The kernel of this integro-differential equation is represented as a sum over all irreducible diagrams and can be calculated in a systematic perturbation expansion in tunneling. In this way the strong correlations on the island are fully taken into account. Furthermore, the golden rule theory, which is reproduced by using the kernel in lowest order perturbation theory, can be systematically generalized to higher orders including time-dependent fields, heat baths and transient phenomena. We will formulate an approximation for an explicit calculation of the kernel which reproduces the Landauer-Büttiker theory in the noninteracting limit but provides also a good description for coherent transport in the strongly interacting case.

# Chapter 2

# Single-electron devices

## 2.1 Basic system

We consider a small island containing interacting electrons in a uniform positive background charge. The island is coupled electrostatically to macroscopic metallic reservoirs and can exchange electrons with the reservoirs via tunnel junctions. A schematic view of such an arrangement is shown in Fig. 2.1. The total charge on the island is given by $Q = eN$, where N denotes the excess electron number relative to the positive background and $e < 0$ is the elementary charge of a single-electron. The charge can change by tunneling to the left or right reservoir and a current will flow through the island when the electrostatic potentials $eV_r$, $r = L, R$, of the left and right reservoir are different (the chemical potentials of the reservoirs are assumed to be identical and serve as zero reference point for excitation energies). Due to the electrostatic coupling, the electrochemical potential of the island is not independent of the voltages $V_r$ on the reservoirs. However, by means of a third terminal, called the gate, which is coupled electrostatically to the island, one can change the electrochemical potential of the island independent of $V_L$ and $V_R$. In this way it is possible to control the particle number on the island. Such a system is called a single-electron transistor (SET) in the general nonequilibrium situation where $V_L \neq V_R$, or a single-electron box (SEB) for the equilibrium case where $V_L = V_R$.

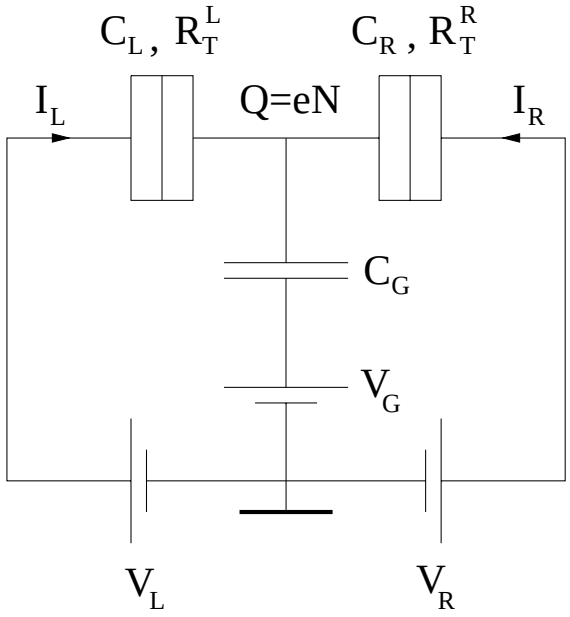


Figure 2.1: The SET transistor. All three terminals are coupled capacitively to the island. Two tunnel junctions allow transport from the left reservoir to the right one.

The length $L$ of the island is typically of order $0.1 - 1\mu m$. This is large compared to atomic scales. Therefore it is possible to couple the island to macroscopic voltage sources. On the other hand, the system size is so small that single charge-transfer processes can be measured on a $meV$ voltage scale. Adding one single charge to the neutral island will cost the charging energy

$$E_C \sim e^2/(\epsilon L) \tag{2.1}$$

due to the Coulomb interaction. This gives $E_C \sim 0.1 - 1meV \sim 1 - 10K$ where we have assumed $\epsilon \sim 10$ for typical semiconductor quantum dots. Therefore, single-electron transport becomes visible in the sub-Kelvin regime. The level spacing $\delta E$ between the single particle states of the island defines the second energy scale for adding one electron. It is given by the inverse density of states of the island

$$\delta E \sim L^{-d} N_F^{-1} \sim (k_F L)^{2-d} \frac{\hbar^2 \pi^2}{m^* L^2} \tag{2.2}$$

where $k_F$ is the Fermi wave vector, $d$ the dimension, $N_F$ the density of states per

volume at the Fermi level, and $m^*$ the effective electron mass. To achieve $\delta E \sim 1K$, one has to reduce the dimension $d$ or use smaller system sizes. For a 3d metallic system with Fermi wave length $\lambda_F \sim 10\mathring{A}$, one needs $L \sim 10nm$. For a 2d electron gas it is sufficient to take $L \sim 100nm$. Furthermore, the level spacing is increased in systems with small effective mass.

Modern lithographic techniques make it possible to produce such systems in a variety of ways. Here we mention some characteristic examples (for more details see Refs. [48, 101]). Tunnel junctions between metallic 3d systems consist of a thin insulating oxide layer between two metallic Al-lines [48]. Two junctions in series together with a gate form the single-electron transistor. The width and length of the island is about $0.1 - 1\mu m$. Therefore, the level spacing is rather small in these systems (typically of order $10^{-3}E_C$). More recent techniques [117] use metallic quantum point contacts with a small hole in the insulating layer. The island is formed by evaporation of Al-particles of size $\sim 10nm$ between oxyd layers. Here the level spacing together with the charging energy is important. Small islands can also be realized by atoms between a substrat and an STM tip [126] or by molecules [74]. The standard system characterized by large charging energy and level spacing is realized by a two-dimensional electron gas (2DEG) at the interface of a GaAs/AlGaAs heterostructure [101]. The tunnel barriers and the quantum dot are formed by top gates which deplete the electron gas. These systems are especially characterized by high mobility, the elastic mean free path is of order $10 - 100\mu m$ and exceeds the system size $L \sim 100nm$. Besides these lateral structures also vertical structures are used [134, 121]. They are characterized by very large level spacing in transport direction due to the vertical confinement of the 2DEG. Single-electron transport can be used here to measure atomic or molecule like spectra of quantum dots.

## 2.2 Motivation: The Coulomb blockade model

In this section we discuss the basic physical properties of quantum dots. We introduce a simplified model and discuss the conditions for various energy scales when Coulomb blockade phenomena and tunneling through zero-dimensional states are observable.

We start with the concept of charging energy. Without using any assumption about the screening properties of the island, it is usually quite complicated to calculate the electrostatic work $E_{pot}$ to build up an arbitrary charge distribution on the island for fixed voltage distribution on the reservoirs and the gate. Therefore, one usually assumes the so-called Coulomb blockade model which contains the essential physics. It means that the island is treated like a metal, i.e. the electrostatic potential on the island is assumed to be homogeneous. Strictly speaking this is only justified if the Thomas-Fermi screening length $\lambda_{TF}$ is much smaller than the system size $L$. According to Eqs. (2.1) and (2.2) this implies for a 3d system

$$\lambda_{TF} \sim (e^2 N_F)^{-1/2} \sim L\,(\frac{\delta E}{E_C})^{1/2} \ll L\,. \tag{2.3}$$

For a 3d metallic system with $\delta E \ll E_C$ this can easily be achieved. However, as discussed in the previous section, this assumption will break down for 3d systems smaller than $L \sim 10nm$. In 2d semiconductor quantum dots there is no exponential screening and the screening length is given by the Bohr radius $a_B$. Here it depends on the particle number and the distance to the gates whether the Coulomb blockade model can be used. Nevertheless we will use a capacitive model in this section since it explains the qualitative features very satisfactory in most cases and follows the standard approach. The general theory set up in the following sections does not rely on any assumption about the dot Hamiltonian. For further details about screening properties of mesoscopic systems we refer to Ref. [18].

Within the capacitive model the electrostatic work $E_{pot}(Q)$ to build up the total

charge $Q$ on the island is given by

$$E_{pot}(Q) = \int_0^Q dQ' V(Q') \tag{2.4}$$

where $V(Q)$ is the electrostatic potential of the island for given island charge $Q$. It depends on the fixed voltages $V_i$, $i = L, R, g$, of the metallic reservoirs and the gate, and follows from $C_i(V_i - V) = Q_i$, where $Q_i$ is the screening charge on capacitor $i$ (see Fig. 2.1 for notations). Using $-Q = Q_L + Q_R + Q_g$ together with the definitions $C = C_L + C_R + C_g$ and

$$q_x = -en_x = \sum_{i=L,R,g} C_i V_i \,, \tag{2.5}$$

we obtain $V(Q) = (Q + q_x)/C$ and from (2.4)

$$E_{pot}(Q = eN) = E_C(N - n_x)^2 \,, \tag{2.6}$$

where we have added the irrelevant constant $E_C n_x^2$. The charging energy $E_C$ is given by

$$E_C = \frac{e^2}{2C} \tag{2.7}$$

and defines the energy scale from the Coulomb interaction to add one particle to the neutral island (i.e. the transition from $N = 0$ to $N = \pm 1$). Compared with (2.1), we see that the total capacitance $C$ replaces the system size $L$ multiplied with the dielectric constant $\epsilon$. For typical lengths $L \sim 0.1 - 1\mu m$ and a dielectric constant $\epsilon \sim 10$, the capacitance is of order $C \sim 10^{-16} - 10^{-15} F$.

In the preceeding derivation the capacitance $C$ results as the sum of the capacitances between the dot and the metallic reservoirs (gates). Hereby we have assumed that the charge is locally screened at all tunnel junctions and at the connection between dot and gate. The capacitances $C_i$ are then determined by the area and thickness of the junctions. A more general interpretation of $q_x$ and $C$ can be given by using the capacitance matrix of the system. If the dot behaves like a metal we have $Q = CV +$

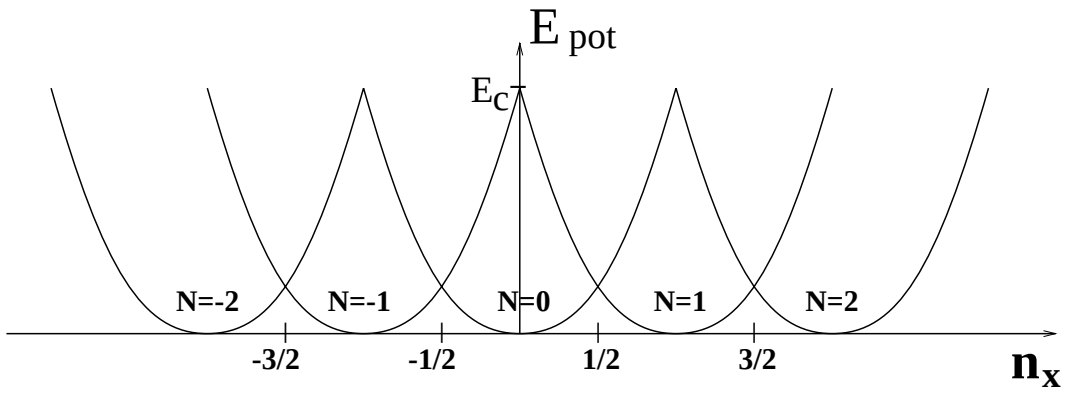


Figure 2.2: The electrostatic energy within the capacitive model for different particle numbers $N$. At the intersection point of two adjacent parabolas transport is possible.

$\sum_i \bar{C}_i V_i$, where $C$ is the self-capacitance of the dot and $\bar{C}_i$ the capacitance coefficients between dot and reservoir (gate) $i$. Again we get $V = (Q + q_x)/C$, with $q_x = -\sum_i \bar{C}_i V_i$, leading to the same result as above for the electrostatic energy. Thus, the capacitance entering the charging energy $E_C = e^2/(2C)$ can very generally be interpreted as the self-capacitance of the dot.

The system tries to minimize its electrostatic energy. Therefore, the integer particle number $N$ tends to be as close as possible to the continuous variable $n_x$. As a consequence, the particle number on the island can be controlled in discrete units by varying $n_x$ via the gate voltage $V_g$. For half-integer values of $n_x$, two adjacent particle numbers $N = n_x \pm 1/2$ lead to the same electrostatic energy and transport is possible (see Fig. 2.2). Away from the degeneracy points, transport is suppressed up to smearing due to temperature, bias voltage and quantum fluctuations. This is the phenomenon of Coulomb-blockade. The current as function of gate voltage shows a series of resonances, the so-called Coulomb oscillations. In metallic junctions, where the charging energy is dominant, they are periodic and have been first observed by Fulton and Dolan [37]. Later, many more controlled measurements have been performed which are summarized in Ref. [48].

So far we have considered only the Coulomb interaction. The total energy $E$ of the

island is given by

$$E = \sum_k \epsilon_{kD} n_{kD} + E_C (N - n_x)^2 \,, \tag{2.8}$$

where $|kD>$ are single-particle states of the dot with occupation $n_{kD}$ and energy $\epsilon_{kD}$. $k$ is the wave vector numerating the states. Furthermore, the total excess particle number is given by

$$N = \sum_k n_{kD} - N_0 \,, \tag{2.9}$$

where $N_0$ is the number of electrons on the neutral island. The ground state energy of the island corresponding to $N$ excess electrons reads

$$E_N = \sum_{k=1}^{N+N_0} \epsilon_{kD} + E_C (N - n_x)^2 \,. \tag{2.10}$$

If the particle number increases by one from $N$ to $N+1$, the ground state energy changes by the amount

$$\Delta_N = E_{N+1} - E_N = \epsilon_{N+N_0+1,D} + 2E_C (N - n_x) + E_C \,. \tag{2.11}$$

It describes a one-particle excitation energy (often called "addition energy") of the island corresponding to a transition between ground state energies with different particle numbers. The quantities $\Delta_N$ can also be regarded as the definition of the electrochemical potential of the island. Of course there are other excitations involving excited states, which become important if the level spacing $\delta E$ is smaller than temperature or bias voltage.

We are now able to set up the conditions when transport is possible. In Fig. 2.3 we have shown an energy profile of the double barrier structure indicating all electrochemical potentials of the reservoirs and the island. For constant level spacing $\delta E$, all excitations of the island are equidistant

$$\Delta = \Delta_{N+1} - \Delta_N = \delta E + 2E_C \,. \tag{2.12}$$

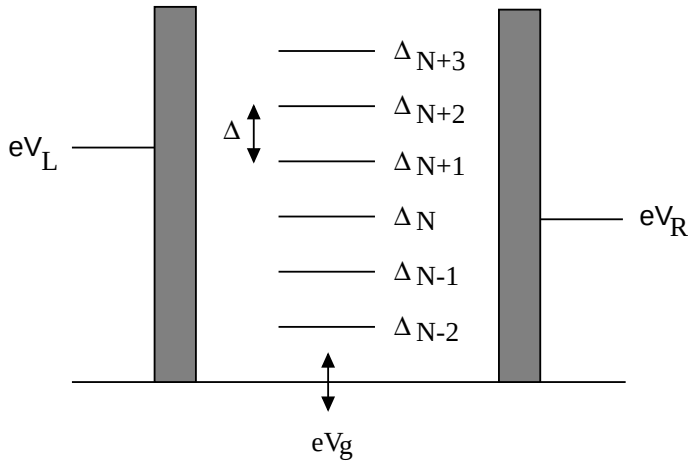


Figure 2.3: One-particle excitation energies of the Coulomb blockade model. For simplicity it is assumed that the level spacing is a constant. If an excitation $\Delta_N$ falls into the window of the electrochemical potentials of the reservoirs, transport can occur. The position of $\Delta_N$ depends linearly on the gate voltage $V_g$.

In the presence of spin, the excitations are two-fold degenerate and the distance will alternate between $\delta E + 2E_C$ and $2E_C$. Furthermore, according to (2.5) and (2.11), their absolute position can be shifted linearly by the gate voltage

$$\frac{\partial \Delta_N}{\partial V_g} = eC_g/C\,. \tag{2.13}$$

In lowest order perturbation theory in the tunneling barriers, where golden rule applies, energy conservation and the Pauli principle restrict tunneling. This means that one of the excitations $\Delta_N$ has to lie within the window of the electrochemical potentials of the reservoirs

$$eV_R < \Delta_N < eV_L\,. \tag{2.14}$$

For finite temperatures, this condition has to be fulfilled only within the smearing defined by the Fermi distribution function. If no excitation lies between $eV_R$ and $eV_L$, transport is suppressed. Thus, in order to observe a significant modulation of the current due to single-electron processes, we need $T, eV = eV_L - eV_R \ll \Delta$ which, using (2.12), is equivalent to

$$T, eV \ll \delta E \qquad \text{or} \qquad T, eV \ll E_C\,. \tag{2.15}$$

The first condition guarantees transport through zero-dimensional states, whereas the second one implies the occurence of Coulomb-blockade phenomena.

As in the case of metallic islands, the current as function of gate voltage will show a series of resonances but their distance (2.12) depends not only on the charging energy but also on the level spacing. Transport through zero-dimensional states has first been observed in vertical structures [119, 132, 52]. In the presence of charging effects the Coulomb oscillations have first been measured in narrow wires where accidental impurities formed the "dot" [128]. Using lateral quantum dots in GaAs/AlGaAs heterostructures more controlled experiments were performed in Ref. [104] for the linear conductance and, including measurements in nonlinear response, in Refs. [68, 35, 143, 144, 136]. Most recently, Coulomb blockade phenomena in the presence of discrete single particle states have been analysed in ultrasmall metallic particles [117] and in disk-shaped vertical quantum dots [134, 121].

In realistic dots, where $\delta E$ and $E_C$ are of the same order of magnitude, it is no longer possible to separate the two energy scales. The Coulomb blockade model breaks down, and the wave functions are of many-body nature [114, 141, 142, 66, 54]. Nevertheless, the qualitative considerations from this section still apply. The possible one-particle excitations of the island are still well separated by a typical distance $\Delta \sim \delta E + E_C$. Of course, $\Delta$ will no longer be a constant and, due to spin or orbital degeneracies, many excitations can lie close to each other. A theoretical analysis of the general situation together with the discussion of tunneling via excited states will be presented in the following sections.

Within golden rule theory it is sufficient to consider the excitation spectrum of the isolated dot as shown in Fig. 2.3. This means that we have neglected the fact that the spectral density of the dot itself can be changed by the presence of the reservoirs. Due to the finite life-time $\tau$ of the excitations there will be a corresponding broadening $\sim \hbar/\tau$

and via Kramers-Kronig also a renormalization. We denote the temperature where the renormalization becomes significant by $T_K$ and call it "Kondo temperature" since the models we will study are similiar to Kondo and Anderson models. The broadening and renormalization has two important consequences. First, in the low-temperature region where $T < \hbar/\tau$ or $T < T_K$, golden rule theory breaks down, higher order processes become important and nonperturbative methods have to be applied. This is the region where quantum fluctuations are important but single electron tunneling still persists. Secondly, if the broadening approaches the distance $\Delta$ of the excitations, single-electron phenomena will no longer be visible. This is the regime of strong tunneling.

Let us start with the case of large level spacing $\delta E \gg T$. Although the life-time of an excitation involving many-body states is strongly influenced by interactions (see chapter 4), a rough estimate for the energy scale of the broadening can be obtained by comparing with the noninteracting case. A single state in a double barrier has a Breit-Wigner broadening , of the order [17]

$$, \sim |t|^2 \delta E \,, \tag{2.16}$$

where $|t|^2$ is the transmission probability of a single barrier. For the Kondo temperature $T_K$, no general estimate is possible since it depends on the spectrum of the dot (see section 4.3). As already stated above, deviations from golden rule theory occur in the low-temperature region $T <$ , or $T < T_K$ (see section 4.2 and 4.3). The regime of strong tunneling $\hbar/\tau \sim \delta E$ cannot be achieved here since, for high tunneling barriers, $|t|^2 \ll 1$, and consequently $\hbar/\tau \sim$ , $\ll \delta E$.

For 3d metallic systems, where the level spacing $\delta E$ is very small, the situation is more complicated. Here, tunneling can happen through many excited states and the broadening of the charge excitations turns out to be , multiplied with the number of

available states for tunneling into or out of the island (see section 4.4)

$$\frac{\hbar}{\tau} \sim \, , \, Z \frac{\max(\Delta_N, T, eV)}{\delta E} \, , \tag{2.17}$$

where $Z$ is the number of transverse channels. Using $\, , \, \sim |t|^2 \delta E$, this expression can also be written in the form

$$\frac{\hbar}{\tau} \sim \alpha_0 \max(\Delta_N, T, eV) \, , \tag{2.18}$$

where

$$\alpha_0 = \frac{1}{4\pi^2} \frac{R_K}{R_T} = \frac{1}{4\pi^2} Z|t|^2 \sim Z \frac{\, , \,}{\delta E} \tag{2.19}$$

is, up to a conventional factor $1/(4\pi^2)$, the dimensionless conductance of a single barrier. $R_K = h/e^2$ is the quantum resistance and $G_T = 1/R_T = Z(e^2/h)|t|^2$ the tunneling conductance of a single barrier. For $\Delta_N \sim E_C \gg T, eV$, (2.19) allows for a simple interpretation since $\hbar/\tau \sim \alpha_0 E_C \sim \hbar/(R_T C)$ gives the classical relaxation time $\tau \sim R_T C$ for a charge on a capacitor in a $RC$-circuit. Single electron phenomena persist if the broadening $\hbar/\tau$ is much less than the distance $\Delta \sim E_C$ between the excitations. This is fulfilled for

$$\alpha_0 \ll 1 \quad \leftrightarrow \quad Z, \, \ll \delta E \, . \tag{2.20}$$

In contrast to the case of large level spacing, this condition is not automatically fulfilled for large tunneling barriers. For large transverse channel number $Z$, $\alpha_0$ can be of order unity even if $\, , \, \ll \delta E$. This is the regime of strong tunneling where quantum fluctuations are enhanced by lowering the tunneling barriers. They can destroy single electron phenomena but, as explained in section 4.4, the Coulomb blockade can be recovered for low enough temperatures due to a renormalization of $\alpha_0$. When the condition (2.20) is fulfilled, single-electron phenomena are visible, but, due to renormalization of charge excitations, golden rule theory again has to be improved in the low-temperature regime (see chapter 4).

## 2.3 Hamiltonian and current operator

In this section we will set up the general Hamiltonian under consideration together with the current operator. We distinguish between two different cases: Quantum dots with discrete quantum states and metallic islands with a continuous single-particle spectrum. We use the convention $\hbar = k_B = 1$ and $e < 0$.

### 2.3.1 Quantum dots

We consider a small island coupled to several metallic reservoirs and to an external heat bath. The bath can be represented by an environment or by internal bosonic degrees of fredom like, e.g., phonons or plasmons. For the general theory we need no assumption for the island Hamiltonian and include the possibility that the voltages on the reservoirs are time-dependent. The coupling to the reservoirs includes an electrostatic interaction as well as tunneling of electrons through high barriers. Let us first state the obvious form of the Hamiltonian and the current operator. For the interested reader, the explicit derivations are presented at the end of this section.

The model Hamiltonian reads $H(t) = H_0 + H_T(t)$ with $H_0 = H_R + H_B + H_D$. Here, $H_R$, $H_B$ and $H_D$ denote the Hamiltonians for the reservoirs, the heat bath, and the dot, respectively, and $H_T(t)$ describes the tunneling between dot and reservoirs. Explicitly, we have

$$\begin{aligned} H_0 &= H_R + H_B + H_D \\ &= \sum_{r=L,R} \sum_k \epsilon_{kr} a_{kr}^\dagger a_{kr} + \sum_q \omega_q b_q^\dagger b_q + \sum_s E_s \hat{P}_s \,, \qquad (2.21) \\ H_T(t) &= \sum_{r=L,R} \sum_{k,ss'} \bar{T}^r_{k,ss'}(t) a_{kr}^\dagger \hat{P}_{ss'} e^{-i\hat{\phi}} + (h.c.) \,. \qquad (2.22) \end{aligned}$$

All terms have an obvious interpretation. $|kr>$ denotes a single particle state in reservoir $r$ with energy $\epsilon_{kr}$, $\omega_q$ are the frequency modes of the heat bath, $E_s$ are the energy eigenvalues of the many-body states $|s>$ of the isolated dot, and $\hat{P}_s = |s><s|$

is the projector on state $|s>$. For the Coulomb blockade model (2.8), the states $|s>$ of the dot are specified by the set of all occupation numbers for the single particle states: $|s>=|\{n_{kD}\}_k>$. The more general notation is introduced here since we want to include cases where the states of the dot cannot be described by single particle states, see e.g. Refs. [114, 141, 142, 66, 54]. Furthermore, the states $|s>$ can represent charge states (see section 2.3.2), spin states, or states of multiple dots. This allows a unified treatment of many possibilities.

The tunneling part (2.22) describes charge transfer processes where the tunneling matrix element $\bar{T}^r_{k,ss'}$ corresponds to a transition of the dot state from $|s'>$ to $|s>$ when an electron tunnels from the dot to reservoir $r$. Therefore, we have introduced the operators $\hat{P}_{ss'}=|s><s'|$. Due to particle number conservation, we have $\bar{T}^r_{k,ss'}=0$ unless $N_s=N_{s'}-1$, where $N_s$ is the particle number on the dot for state $|s>$. The electrostatic interaction between dot and reservoirs is described by the effective time dependence

$$\bar{T}^r_{k,ss'}(t)=T^r_{k,ss'}e^{ie\int_{t_0}^{t}dt'\bar{V}_r(t')}\,, \tag{2.23}$$

where

$$\bar{V}_r(t)=V_r(t)-V_D(t) \tag{2.24}$$

is the change of the electrostatic energy of a particle entering reservoir $r$. $V_r(t)$ denotes the time-dependent voltage on reservoir $r$, and $V_D(t)$ is the spatial average of the external electrostatic potential taken over the dot. The part of the electrostatic energy which remains for zero voltage on all reservoirs is included in $H_D$. E.g. for the Coulomb blockade model (2.8), we have

$$V_D(t)=-\frac{1}{e}2E_C\,n_x(t)=\frac{1}{C}q_x(t)=\sum_{i=L,R,g}\frac{C_i}{C}V_i(t)\,, \tag{2.25}$$

whereas the part $E_C\hat{N}^2$ of the electrostatic energy is included in $H_D$. We see that gauge invariance is fulfilled since a change of all electrostatic potentials of the reservoirs by

the same amount does not change $\bar{V}_r(t)$. For convenience we will split off the effective average electrochemical potential $\mu_r$ of reservoir $r$ by the decomposition

$$e\bar{V}_r(t) = \mu_r + e\bar{V}_r^1(t)\,, \tag{2.26}$$

where, for the time-dependent part, we will often assume the harmonic form

$$e\bar{V}_r^1(t) = \bar{\Delta}_r \sin(\Omega t)\,. \tag{2.27}$$

The tunneling matrix elements (2.23) are conveniently described by their corresponding spectral function

$$\bar{,}^r_{s_1 s_1', s_2 s_2'}(t_1, t_2; \omega) = e^{i\mu_r(t_1 - t_2)} 2\pi \sum_k \bar{T}^r_{k,s_1' s_1}(t_1)^* \, \bar{T}^r_{k,s_2 s_2'}(t_2) \delta(\omega - \epsilon_{kr})\,, \tag{2.28}$$

$$= e^{-ie\int_{t_2}^{t_1} dt' \bar{V}_r^1(t')} \, {}^r_{s_1 s_1', s_2 s_2'}(\omega)\,, \tag{2.29}$$

with

$${}^r_{s_1 s_1', s_2 s_2'}(\omega) = 2\pi \sum_k T^{r*}_{k,s_1' s_1} T^r_{k,s_2 s_2'} \delta(\omega - \epsilon_{kr})\,, \tag{2.30}$$

By convention we have cancelled the dependence of the tunneling matrix elements on the static part $\mu_r$ by the exponential prefactor in (2.28). This is convenient since, for harmonic voltages of the form (2.27), the spectral function $\bar{,}$ is periodic in $t_1$ and $t_2$.

Finally, the bosonic phase factor $\exp(-i\hat{\phi})$ in (2.22) describes the energy exchange with the heat bath due to absorption or emission of bosonic modes. The linear bosonic field $\hat{\phi}$ is defined by

$$\hat{\phi} = i \sum_q \frac{g_q}{\omega_q} (b_q - b_q^\dagger)\,, \tag{2.31}$$

where $g_q$ is the coupling constant to the heat bath for mode $q$. This model has been used widely in the literature, either to describe optical phonons in semiconductor quantum dots [145, 44, 67] or voltage fluctuations in metallic systems [22, 110, 34, 63]. In the latter case, the relation between the spectral function $J(\omega)$ of the coupling constants

$g_q$, and the impedance $Z(\omega)$ of the external circuit is given by [63]

$$J(\omega) = \pi \sum_q g_q^2 \delta(\omega - \omega_q) = e^2 \omega \mathrm{Re} Z(\omega)\,, \tag{2.32}$$

where $\omega > 0$, since the bosonic modes $\omega_q$ are all positive. For an environment characterized by a resistance $R$, a capacitance $C$, and an inductance $L$, we have $Z(\omega) = (i\omega C + 1/(i\omega L) + 1/R)^{-1}$ and

$$J(\omega) = 2E_C \frac{\omega \omega_C}{\omega_C^2 + \omega^2 (1 - \omega_L^2/\omega^2)^2}\,, \tag{2.33}$$

where $E_C = e^2/(2C)$, $\omega_C = 1/(RC)$ and $\omega_L = 1/(LC)^{1/2}$. For a resistive environment ($C = 0$ and $L = \infty$), we get ohmic dissipation

$$J(\omega) = e^2 R \omega\,, \tag{2.34}$$

which is equivalent to the Caldeira-Leggett model [19]. For an $LC$-circuit ($R = \infty$) a one-mode bath is realized with

$$J(\omega) = \pi E_C \omega_L \delta(\omega - \omega_L)\,. \tag{2.35}$$

For a more extended discussion of various kinds of possible environments we refer the reader to Ref. [64].

The physical observable which can be measured experimentally is the current $I_r$ flowing in reservoir $r$. This current consists of two contributions: a tunneling current $I_r^{tun}(t)$ from electrons hopping to or from the island and a displacement current $I_r^{dis}(t) = \frac{d}{dt} Q_r(t)$ arising from the change of the time-dependent screening charge $Q_r(t)$ on reservoir $r$. For given charge distribution on the island the latter can be calculated by solving the Poisson equation with the appropriate boundary conditions for the electrostatic potentials on the metallic reservoirs. The charge distribution itself is a dynamic quantity and will result from the solution of the nonequilibrium problem. Let us show how $Q_r(t)$ can be calculated for the simplified Coulomb blockade

model introduced in section 2.2. For given charge $Q(t)$ on the island and given potentials $V_r(t)$, $r = L, R, g$, on the reservoirs and the gate we get for the screening charge $Q_r = C_r(V_r - V)$ with $V = (Q + q_x)/C$ being the potential on the island. Inserting the definition $q_x = \sum_r C_r V_r$ and taking the time derivative we get for the displacement current

$$I_r^{dis} = C_r \dot{V}_r - \frac{C_r}{C}(\dot{Q} + \sum_{r'} C_{r'} \dot{V}_{r'}) \,. \tag{2.36}$$

The time-derivative of the island charge $\dot{Q} = \sum_r I_r^{tun}$ is known after we have calculated the tunneling currents. Summing (2.36) over $r$ we find total current conservation

$$\sum_r I_r(t) = \sum_r [I_r^{dis}(t) + I_r^{tun}(t)] = 0 \tag{2.37}$$

for all times $t$ (see also a detailed discussion of this property in Ref. [18]). The displacement currents are only important for the calculation of AC-currents since the time average of $I_r^{dis}$ is usually zero except for cases where $\int \dot{V}_r \neq 0$.

The tunneling current operator $\hat{I}_r^{tun}(t)$, where t denotes an explicit time dependence, is given by the time derivative of the particle number operator in reservoir $r$, $\hat{I}_r^{tun}(t) = -e\frac{d}{dt}\hat{N}_r = -ie[H(t), \hat{N}_r]$ (note that $N_r$ denotes the total electron number in reservoir $r$ which is independent of the screening charge $Q_r$ sitting on the capacitor connecting island and reservoir). Inserting for $H(t)$ from (2.21) and (2.22) we find

$$\hat{I}_r^{tun}(t) = ie \sum_{k,ss'} \bar{T}_{k,ss'}^r(t) a_{kr}^\dagger \hat{P}_{ss'} e^{-i\hat{\phi}} \; + \; (h.c.) \,, \tag{2.38}$$

where the explicit time dependence stems from the time dependent tunneling matrix elements.

Let us now turn to the derivation of the Hamiltonian (2.21) and (2.22). The microscopic starting point is

$$H(t) = H_R(t) + H_B + H_D(t) + V_{DB} + H_T \,, \tag{2.39}$$

where $H_R(t)$, $H_B$ and $H_D(t)$ denote the Hamiltonians for the reservoirs, the heat bath, and the dot, respectively. $V_{DB}$ describes the interaction between dot and heat bath, and $H_T$ the tunneling between dot and reservoirs.

For the reservoir Hamiltonian $H_R(t)$ we use a noninteracting Fermi liquid with perfect screening properties like in an ideal metal

$$H_R(t) = \sum_{kr} \epsilon_{kr} a_{kr}^\dagger a_{kr} + e \sum_r V_r(t) \hat{N}_r \,, \tag{2.40}$$

where $V_r(t)$ is the electrostatic potential of reservoir $r$, and $\hat{N}_r$ is the particle number operator.

The heat bath $H_B$ is modelled by a set of harmonic oscillators

$$H_B = \sum_q \omega_q b_q^\dagger b_q \,. \tag{2.41}$$

which couple to the particle number operator $\hat{N}$ of the island by the interaction term

$$V_{DB} = \hat{N} \sum_q g_q (b_q + b_q^\dagger) + \hat{N}^2 \sum_q \frac{g_q^2}{\omega_q} \,. \tag{2.42}$$

The second term is a counter-term which is necessary to avoid an unphysical renormalization of the dot energies $E_s$ (see below). The first term describes a fluctuating electrochemical potential on the island.

The general form of the dot Hamiltonian is

$$H_D(t) = H_D^0 + e V_{ex}(t) \,, \tag{2.43}$$

where $V_{ex}(t) = \sum_i v_{ex}(\hat{\vec{x}}_i, t)$, with $\hat{\vec{x}}_i$ being the position operator for particle $i$ on the dot. $v_{ex}(\vec{x}, t)$ denotes the external electrostatic potential calculated from the fixed (and possibly time-dependent) voltage distribution on the reservoirs. The electrostatic work to build up the island charge distribution for zero voltage on all reservoirs is included in $H_D^0$. In the general case, i.e. without assuming any screening properties, $v_{ex}$ will have the form of an oscillating dipole field causing also transitions between the island states.

However, in typical experimental situations, the gate voltage is coupled so strongly to the dot that $v_{ex}$ will be nearly homogeneous and only the time-dependent modulation of the dot states is dominant. Therefore we use in the following the form

$$V_{ex}(t) = V_D(t)\hat{N}\,, \tag{2.44}$$

where $V_D(t)$ is the spatial average of the external electrostatic potential taken over the dot. Time-dependent transitions can also be included within the general framework of the theory and are described at the end of this section.

We denote the normalized and orthogonal many-body eigenfunctions of $H_D^0$ by $|s>$ with energy $E_s$ and obtain

$$H_D(t) = \sum_s E_s \hat{P}_s + eV_D(t)\hat{N}\,. \tag{2.45}$$

Tunneling between reservoirs and island is described by

$$H_T = \sum_{r,kl} T_{kl}^r a_{kr}^\dagger a_{lD} \; + \; (h.c.)\,, \tag{2.46}$$

where $T_{kl}^r$ are the tunneling matrix elements and $a_{lD}$ is a field operator corresponding to any set of single particle states $|lD>$ on the dot. The form of the tunneling matrix elements is usually described in terms of their correponding spectral function

$$, \,{}_{ll'}^{r}(\omega) = 2\pi \sum_k T_{kl}^{r^*} T_{kl'}^r \delta(\omega - \epsilon_{kr})\,, \tag{2.47}$$

Often one neglects the energy dependence of the spectral function and its dependence on the states $l, l'$ by using

$$, \,{}_{ll'}^{r}(\omega) \approx \delta_{ll'}, \,{}^{r}\,. \tag{2.48}$$

This assumes constant density of states in the reservoirs as well as the neglect of interference phenomena in higher order perturbation theory in , . For a detailed discussion of the latter point see e.g. Ref. [6].

Expressed in the basis of the eigenfunctions $|s>$ of $H_D^0$ we can write the tunneling part as

$$H_T = \sum_{r,k,ss'} T^r_{k,ss'} a^\dagger_{kr} \hat{P}_{ss'} + (h.c.)\,, \tag{2.49}$$

where the transformed tunneling matrix elements

$$T^r_{k,ss'} = \sum_l T^r_{kl} < s|a_{lD}|s' > \tag{2.50}$$

involve matrix elements of the field operators $a_{lD}$ between many-body states of the island. They can lead to exclusion rules [141, 142, 66, 113] (see also section 2.4). Using this form of the tunneling matrix elements we obtain for the spectral function (2.30) in the new basis

$$,^{\ r}_{s_1 s_1', s_2 s_2'}(\omega) = \sum_{l_1 l_2} ,^{\ r}_{l_1 l_2}(\omega) < s_1|a^\dagger_{l_1 D}|s_1' >< s_2|a_{l_2 D}|s_2' > \ . \tag{2.51}$$

Among all the parts of the Hamiltonian, especially $V_{DB}$ and $H_T$ are nontrivial. The rest of the Hamiltonian is already in diagonalized form and is known if the island Hamiltonian $H_D^0$ can be solved. The latter solution depends on many geometrical details but can often be found, at least for simple models or in certain approximations [114, 141, 142, 66, 54]. Therefore we assume in the following that the evolution operator of the dot Hamiltonian $H_D(t)$ is known and concentrate ourselves on finding a transport theory which can treat the interaction between dot, reservoirs and heat bath.

Let us first perform a standard time-dependent unitary transformation $U(t)$ to bring the Hamiltonian into the most convenient form. We choose

$$U(t) = e^{-ie\int_{t_0}^t dt' (\sum_r V_r(t')\hat{N}_r + V_D(t)\hat{N})} e^{-i\hat{N}\hat{\phi}}\,, \tag{2.52}$$

where $t_0$ is the initial time and the hermitian bosonic field $\hat{\phi}$ is defined by (2.31). The transformation creates a shift of the bosonic field operators $U^\dagger b_q U = b_q - \hat{N}\frac{g_q}{\omega_q}$ together with phase factors for the projectors and the reservoir field operators. The transformed

Hamiltonian $\bar{H} = U^\dagger H U - iU^\dagger \frac{d}{dt} U$ reads $\bar{H}(t) = \bar{H}_0 + \bar{H}_T(t)$ where $\bar{H}_0$ and $\bar{H}_T(t)$ are given by (2.21) and (2.22), respectively. We see that the second term on the r.h.s. of (2.42) has been chosen in such a way that it has cancelled out.

For convenience we drop finally the bar on all operators and imply implicitly that all operators $A(t) \equiv \bar{A}(t) = U(t)^\dagger A(t) U(t)$ are the transformed ones after the unitary transformation. The states $|s>$ together with the projectors $\hat{P}_{ss'}$ are kept unchanged. Furthermore we keep the bar on the tunneling matrix elements (2.23) and the corresponding spectral function (2.28).

Without tunneling the problem is now solved, i.e. the interaction between island and bosons can be treated exactly in the absence of the fermionic reservoirs (see also Ref. [96]). The phase factor $e^{-i\hat{\phi}}$ in (2.22) describes the effect of boson-assisted tunneling and is the only place where the heat bath occurs. The tunneling term is still nontrivial and therefore the diagrammatic technique set up in chapter 3 is based on an expansion in the tunneling vertex.

Finally let us treat the case when the external potential term $V_{ex}(t)$ in (2.43) is periodic in time with period $T$ and induces transitions between the states $s$ of the dot. This can easily be included by using Floquet's theory [129]. First we look for a periodic and unitary operator $W(t) = W(t+T)$ which diagonalizes the dot Hamiltonian

$$\bar{H}_D = \sum_s \bar{E}_s \hat{P}_s \tag{2.53}$$

$$= W(t)^\dagger H_D(t) W(t) - iW(t)^\dagger \frac{d}{dt} W(t)\,. \tag{2.54}$$

This means that the wave functions

$$\psi_s(t) = e^{-i\bar{E}_s t} \varphi_s(t)\,, \tag{2.55}$$

with $\varphi_s(t) = W(t)|s>$, form a complete orthonormal set of solutions of the time-dependent Schrödinger equation in Bloch form. $\bar{E}_s$ are the quasienergies and $\varphi_s(t)$ the

Floquet states. The operator $W(t)$ can easily be found by applying Fourier transformation to the equation $W(t)\bar{H}_D = H_D(t)W(t) - i\frac{d}{dt}W(t)$. Using the form

$$H_D(t) = \sum_n H_D^n e^{in\Omega t} \quad , \quad W(t) = \sum_n W^n e^{in\Omega t} \, , \tag{2.56}$$

where $\Omega = 2\pi/T$, we find the infinite-dimensional eigenvalue problem

$$\sum_{n_2 s_2} A_{n_1 s_1, n_2 s_2} \, x^{(s)}_{n_2 s_2} = \bar{E}_s \, x^{(s)}_{n_1 s_1} \, , \tag{2.57}$$

with

$$A_{ns,n's'} = H^{n-n'}_{ss'} + n\Omega\delta_{nn'} \, , \tag{2.58}$$

$$x^{(s')}_{ns} = W^n_{ss'} \, , \tag{2.59}$$

where we defined the matrix elements $H^{n-n'}_{ss'} =< s|H^{n-n'}_D|s' >$ and $W^n_{ss'} =< s|W^n|s' >$. The matrix $A$ is hermitian since $< s|H^n_D|s' >^* =< s'|H^{-n}_D|s >$ which follows from the hermiticity of $H_D(t)$. Therefore, we obtain real quasienergies $\bar{E}_s$. Truncating the Fourier components $W^n$ at some finite value, the eigenvalue problem (2.57) can be solved by straighforward numerical analysis.

Once the operator $W(t)$ is known we multiply the unitary transformation $U(t)$, given by Eq. (2.52), with $W(t)$, and omit the exponential part containing $V_D$. We obtain again the Hamiltonian (2.21) and (2.22) with the difference that the quantities $E_s$ denote now the quasienergies and the transformed tunneling matrix elements are given by

$$\bar{T}^r_{k,ss'}(t) = e^{ie\int_{t_0}^t dt' V_r(t')} \sum_{s_1 s_1'} W_{s_1 s}(t)^* \, W_{s_1' s'}(t) T^r_{k,s_1 s_1'} \, , \tag{2.60}$$

with $W_{ss'}(t) =< s|W(t)|s' >$. We note that the spatial average $eV_D(t)\hat{N}$ of the potential of the dot Hamiltonian is included in the Fourier components $H^n_D$. Therefore, this term does not occur in the exponential factor of (2.60). The average part of $V_D(t)$ leads to a shift of the quasienergies $\bar{E}_s$ whereas the time-dependent periodic part influences $W(t)$.

The spectral function is again defined by (2.28). Since the form of the tunneling matrix elements has changed we obtain instead of (2.29)

$$\begin{aligned} \bar{,}^{r}_{s_1 s_1', s_2 s_2'}(t_1, t_2; \omega) &= e^{-ie\int_{t_2}^{t_1} dt' V_r^1(t')} \times \\ &\times \sum_{\bar{s}_1 \bar{s}_1', \bar{s}_2 \bar{s}_2'} {}^{r}_{,\bar{s}_1 \bar{s}_1', \bar{s}_2 \bar{s}_2'} W_{\bar{s}_1' s_1'}(t_1) W_{\bar{s}_1 s_1}(t_1)^* \, W_{\bar{s}_2' s_2'}(t_2) W_{\bar{s}_2 s_2}(t_2)^* \,, \end{aligned} \tag{2.61}$$

which is a periodic function of $t_1$ and $t_2$.

Formally one can also treat the case when the external voltages are not periodic. In this case the unitary transformation $U(t)$ has to be multiplied with the evolution operator $U_D(t, t_0)$ of the isolated dot Hamiltonian. However, the determination of the latter involves the solution of a matrix differential equation which might be quite cumbersome except for special exactly solvable systems. Furthermore, the tunneling matrix elements will then contain complicated non-periodic parts which cannot be treated by discrete Fourier decomposition.

The case of explictly time-dependent tunneling matrix elements can easily be incorporated by writing $T_{k,s_1 s_1'}(t)$ on the r.h.s. of (2.60). However, except for some notational complications, this does not induce any new interesting aspects into the theory since it is difficult to distinguish between the explicit and the effective time dependence of the tunneling matrix elements. Therefore this is omitted in the following but of course can be included in a straightforward manner for the interested reader.

Finally we note that the unitary transformation $U(t)$ is not equal to unity at the initial time since $U(t_0) = \exp(-i\hat{N}\hat{\phi})W(t_0)$. This has to be kept in mind for the treatment of transient phenomena where the initial density matrix has to be transformed as well.

### 2.3.2 Metallic island

A metallic island is characterized by a very dense level spectrum with small level spacing $\delta E$. Although formally possible, it is not very convenient to use the Hamiltonian from the previous section for this case. The reason is that there is an infinite number of possible many-body states $|s>$ of the dot which are relevant. Setting up a kinetic equation for the corresponding probabilities to be in these states, as outlined in chapter 3, is possible but is not tractable due to the large number of degrees of freedom.

Following the standard approach we therefore introduce two approximations from the very beginning. First, like the reservoirs, we treat the island as a Fermi liquid with perfect screening. This means that we use the Coulomb blockade model (2.8) for the dot Hamiltonian

$$\begin{aligned} H_D(t) &= \sum_k \epsilon_{kD} a_{kD}^\dagger a_{kD} + E_C(\hat{N} - n_x(t))^2 \\ &= \sum_k \epsilon_{kD} a_{kD}^\dagger a_{kD} + E_C \hat{N}^2 + eV_D(t)\hat{N}\,, \end{aligned} \tag{2.62}$$

where we have defined $V_D(t)$ according to (2.25). The total Hamiltonian is again of the form (2.39) with $H_R$, $H_B$, $V_{DB}$ and $H_T$ given by (2.40), (2.41), (2.42) and (2.46), respectively. This approximation is justified if the island is not too small as already discussed in section 2.2.

The second approximation we use is the separation of the charge degrees of freedom of the island (described by $N$) from the degrees of freedom describing how the particles on the island are distributed among the single particle states (described by $n_l$). This means that we neglect the condition (2.9) and treat $N$ as an independent degree of freedom. Furthermore we fix the distribution function on the island by a Fermi distribution. This is justified since the time scale for the change of the distribution function is much larger than the time scale for the variation of the total particle number. As will be discussed in detail in section 2.4.2, the rate of change of the distribution function

is given by , , whereas the rate of change of the charge is $\alpha_0 E_C$. Thus, for $\alpha_0 E_C \gg$ , , we can neglect the dependence of the distribution function on the particle number $N$ and take the equilibrium Fermi distribution function provided that additional inelastic processes are present with an energy relaxation rate $\tau_\epsilon^{-1} \gg$ , . Furthermore, for $\alpha_0 E_C \gg \tau_\epsilon^{-1}$, we can neglect the influence of the inelastic processes on the dynamics of the charge degrees of freedom. Thus, under the condition

$$Z, \frac{E_C}{\delta E} \sim \alpha_0 E_C \gg \tau_\epsilon^{-1} \gg , , \tag{2.63}$$

we can treat the island like an electronic reservoir in equilibrium and allow only for a nonequilibrium distribution for the possible values of $N$. Since $Z \sim 10^3$ and $E_C/\delta E \sim 10^3$ in typical metallic devices, there is a wide range for possible values of $1/\tau_\epsilon$ to fulfil this condition.

A formally precise formulation of this approximation can be achieved in the following way. We first enlarge the Hilbert space by introducing formal charge states $|N>$ with $N$ ranging from minus to plus infinity. We define the operator $\hat{N}$ in (2.62) by $\hat{N}|N>= N|N>$ and the projectors $\hat{P}_{NN'} = |N><N'|$. We demand that each time an electron changes its position from some reservoir to the island or vice versa via tunneling, the charge state has to change simultaneously from $|N>$ to $|N \pm 1>$. This is achieved by introducing the projectors $\hat{P}_{N\pm1,N}$ into the tunneling Hamiltonian

$$H_T(t) = \sum_{r,kl,N} T_{kl}^r(t) a_{kr}^\dagger a_{lD} \hat{P}_{N-1,N} + (h.c.)\,. \tag{2.64}$$

By construction, the new Hamiltonian is exactly equivalent to the old one provided we enforce the constraint (2.9) to restrict ourselves to the original physical Hilbert space. The approximation formulated above corresponds to the neglect of the latter constraint.

As in the previous section, we simplify the treatment of the interaction with the heat bath and the time-dependent fields by applying the same unitary transformation

$U(t)$ given by Eq. (2.52). Dropping all bars on the transformed Hamiltonians, we find $H(t) = H_0 + H_T(t)$ with

$$\begin{aligned} H_0 &= H_R + H_B + H_C \,, \\ &= \sum_{r=L,R,D} \sum_k \epsilon_{kr} a^\dagger_{kr} a_{kr} + \sum_q \omega_q b^\dagger_q b_q + \sum_N E_N \hat{P}_N \,, \qquad (2.65) \\ H_T(t) &= \sum_{r=L,R} \sum_{kl,N} \bar{T}^r_{kl}(t) a^\dagger_{kr} a_{lD} \hat{P}_{N-1,N} e^{-i\hat{\phi}} + (h.c.) \,, \qquad (2.66) \end{aligned}$$

where $E_N = E_C \hat{N}^2$, and $\bar{T}^r_{kl}(t)$ is defined analog to (2.23). As indicated we decomposed the dot Hamiltonian (2.62) into a "reservoir" part $\sum_k \epsilon_{kD} a^\dagger_{kD} a_{kD}$, which has been included in $H_R$, and a charge part $H_C$, which contains the strong correlations and interacts with all reservoirs, the heat bath and time-dependent fields via $H_T$.

Using the same derivation as for the quantum dot case, we obtain for the tunneling current operator

$$\hat{I}^{tun}_r(t) = ie \sum_{kl,N} \bar{T}^r_{kl}(t) a^\dagger_{kr} a_{lD} \hat{P}_{N-1,N} e^{-i\hat{\phi}} + (h.c.) \,, \qquad (2.67)$$

whereas the displacement current can be calculated from (2.36).

Comparing the Hamiltonians for the metallic case, given by (2.65) and (2.66), with the corresponding one for the quantum dot case, given by (2.21) and (2.22), we recognize the same formal structure if we interchange dot states $|s>$ with charge states $|N>$. The only new feature for the metallic case is that particle-hole excitations of the dot serve as another "reservoir". If the charge state changes by tunneling, the electron changes simultaneously its position from one reservoir to the other expressed by the additional field operator $a^{lD}$ in (2.66).

Finally, we note that it is sometimes convenient to express the projectors in Eq. (2.66) in terms of the phase operator $\hat{\varphi}$ which is canonically conjugate to $\hat{N}$, i.e. $[\hat{\varphi}, \hat{N}] = i$ (note that the eigenvalues of $\hat{N}$ are running from minus to plus infinity here). The change of the charge by $\pm 1$ can then be achieved by application of the unitary opera-

tors

$$e^{\pm i\hat{\varphi}} = \sum_N \hat{P}_{N\pm 1,N} \,, \tag{2.68}$$

yielding

$$H_T(t) = \sum_{r,kl} \bar{T}^r_{kl}(t) a^\dagger_{kr} a_{lD} e^{-i\hat{\varphi}} e^{-i\hat{\phi}} \; + \; (h.c.) \,. \tag{2.69}$$

This form is especially useful for the derivation of effective actions in phase or charge representation using path integral methods [28, 125, 76, 79].

### 2.3.3 Relation to other models

The Hamiltonians discussed in the previous sections have many similiarities to models discussed within the theory of strongly correlated fermions and dissipative systems, like Kondo-, Anderson-, and spin boson models. The subject of this section is to set up some of these relationships.

(a) **Quantum dots**. Omitting the bosonic heat bath, the quantum dot Hamiltonian (2.21) and (2.22) can be regarded as a generalization of the Anderson impurity model [72, 11, 60]. The local strongly correlated system (the impurity atom) is here the dot and the conduction band electrons correspond to the electronic reservoirs. Depending on the spectrum of the dot and the form of the tunneling matrix elements, an enormous variety of different systems can be realized which can show completely different behaviour in the low-temperature regime.

Let us start with the simplest case, namely a quantum dot where only one excitation energy $E_{s_1} - E_{s_0}$ is relevant, with $|s_0>$ and $|s_1>$ being two ground states of the dot corresponding to particle numbers $N$ and $N+1$, respectively (without loss of generality we can set $N = 0$). This means that all the other excitations involving ground state energies are far away from the electrochemical potentials of the reservoirs. In this case,

the Hamiltonian reads

$$H(t) = \sum_{kr} \epsilon_{kr} a^\dagger_{kr} a_{kr} + (E_{s_1} - E_{s_0}) \hat{P}_{s_1} + \sum_{kr} (\bar{T}^r_{k,s_0 s_1}(t) a^\dagger_{kr} \hat{P}_{s_0 s_1} \; + \; h.c.) \,, \tag{2.70}$$

where we have used $\hat{P}_{s_0} + \hat{P}_{s_1} = 1$ and omitted an overall constant. This Hamiltonian is equivalent to an effective noninteracting resonant level or Fano-Anderson model [30, 1] with a dot consisting of one single-particle state

$$H(t) = \sum_{kr} \epsilon_{kr} a^\dagger_{kr} a_{kr} + \epsilon \, c^\dagger c + \sum_{kr} (\bar{T}^r_k(t) a^\dagger_{kr} c \; + \; h.c.) \,, \tag{2.71}$$

where $c, c^\dagger$ are the field operators of the dot, and we have identified $\hat{P}_{s_1 s_0} = c^\dagger$, $|s_0> = |0>$, $|s_1> = |1>$, $T^r_{k,s_0 s_1} = T^r_k$, and $\epsilon = E_{s_1} - E_{s_0}$. Obviously the Hamiltonian has the form of a noninteracting system which can be solved exactly. Only the presence of the effective potential $\bar{V}_r = V_r - V_D$ within the tunneling matrix elements reminds of the Coulomb interaction. Here, the latter has only the effect of shifting the band buttoms of the reservoirs and the dot. This means that there exists a well-defined limit where an interacting quantum dot can effectively be described by a noninteracting Hamiltonian [130]. However, in a realistic situation degeneracies of excitations can hardly be excluded due to spin and orbital effects, at least in the absence of high magnetic fields. It is only this case where interaction effects become important and will change the qualitative behaviour of the noninteracting case completely in the whole temperature regime (see section 2.4 and 4.3).

Let us now consider a more realistic and interesting case, namely the presence of two relevant excitation energies $\epsilon_\sigma = E_{s_\sigma} - E_{s_0}$, with $\sigma = \uparrow, \downarrow$ being the spin. This means that we consider the transition between a singlet and a doublet state of the dot. If the incoming electron has spin up or down we consider the transition $s_0 \to s_\uparrow$ or $s_0 \to s_\downarrow$, respectively. Due to spin conservation the corresponding Hamiltonian is given

by

$$H(t) = \sum_{k\sigma r} \epsilon_{k\sigma r} a^\dagger_{k\sigma r} a_{k\sigma r} + \sum_\sigma \epsilon_\sigma \hat{P}_{s_\sigma} + \sum_{k\sigma r} (\bar{T}^r_k a^\dagger_{k\sigma r} \hat{P}_{s_0,s_\sigma} \; + \; h.c.)\,, \tag{2.72}$$

where we have assumed spin independent tunneling matrix elements and used $\hat{P}_{s_0} = 1 - \sum_\sigma \hat{P}_{s_\sigma}$. Each reservoir field operator carries now a spin index in addition to the reservoir index. This model has a very interesting analog in the theory of strongly correlated fermions, namely the so-called infinite-U impurity Anderson model which is described by the Hamiltonian

$$H(t) = \sum_{k\sigma r} \epsilon_{k\sigma r} a^\dagger_{k\sigma r} a_{k\sigma r} + \sum_\sigma \epsilon_\sigma c^\dagger_\sigma c_\sigma + U n_\uparrow n_\downarrow + \sum_{k\sigma r} (\bar{T}^r_k(t) a^\dagger_{k\sigma r} c_\sigma \; + \; h.c.)\,, \tag{2.73}$$

with $U \to \infty$ being assumed to be the largest energy scale of the system. The role of the dot is here taken over by the role of a local impurity with one single state and spin 1/2. $U$ is the on-site Coulomb repulsion and takes over the role of the charging energy. Since $U$ is assumed to be large, double occupancy of the impurity level is suppressed and only the three states $|0>$, $|\uparrow>$, and $|\downarrow>$ are possible. They are identified with the states $|s_0>$, $|s_\uparrow>$, and $|s_\downarrow>$, corresponding to the Hamiltonian (2.72), respectively. This gives $c^\dagger_\sigma \equiv \hat{P}_{s_\sigma s_0}$, and we can see that the two Hamiltonians are equivalent.

In the Kondo-regime, i.e. for $-\epsilon_\sigma \ll \, , \; \ll \epsilon_\sigma + U$, the empty or doubly occupied dot is only possible as a virtual intermediate state, and the Anderson model can be mapped onto the Kondo model via a standard Schrieffer-Wolff transformation [127, 96, 60]. Here, the two singly occupied states of the dot are identified with the two states of a localized spin-1/2 impurity. Without magnetic field and in equilibrium, the result is

$$H = \sum_{k\sigma} \epsilon_k a^\dagger_{k\sigma} a_{k\sigma} + \sum_{kk'} J_{kk'} (a^\dagger_{k\downarrow} a_{k'\uparrow} S^+ + a^\dagger_{k\uparrow} a_{k'\downarrow} S^- + (a^\dagger_{k\uparrow} a_{k'\uparrow} + a^\dagger_{k\downarrow} a_{k'\downarrow}) S_z)\,, \tag{2.74}$$

where $\vec{S}$ denotes the impurity spin operator, and the effective antiferromagnetic coupling constants are given by

$$J_{kk'} = T^*_k T_{k'} (\frac{1}{\epsilon_k - \epsilon} + \frac{1}{\epsilon + U - \epsilon_{k'}})\,. \tag{2.75}$$

As can be seen we have taken both reservoirs together and omitted the reservoir index $r$ everywhere. We note that the reservoir index is not allowed to be interpreted as a channel index used within the two-channel Kondo model. There the channel index of the conduction electrons is conserved by scattering at the local impurity spin which is not the case here.

Even the finite-U impurity Anderson model can be realized in experimental situations. The many-body states $s = (N, S, M)$ of the dot can be classified according to the particle number $N$, the total spin $S$, and the magnetic quantum number $M$ together with additional quantum numbers from spatial symmetries. The infinite-U impurity Anderson model corresponds to the transitions

$$s_0 = (0, 0, 0) \leftrightarrow s_\pm = (1, 1/2, \pm 1/2)\,, \tag{2.76}$$

whereas the finite-U impurity Anderson model includes the transition

$$s_\pm = (1, 1/2, \pm 1/2) \leftrightarrow s_{\uparrow\downarrow} = (2, 0, 0)\,. \tag{2.77}$$

The Coulomb repulsion $U$ is determined by $E_{s_{\uparrow\downarrow}} - E_{s_\sigma} = \epsilon_{-\sigma} + U$. Without magnetic field the doublet consists of two degenerate states and we have $\epsilon_\sigma = \epsilon$. In this case, only two excitation energies $\Delta_0 = E_{s_\sigma} - E_{s_0} = \epsilon$ and $\Delta_1 = E_{s_{\uparrow\downarrow}} - E_{s_\sigma} = \epsilon + U$ are possible. Comparing with Eq. (2.12), derived within the Coulomb blockade model, we find $\Delta = \Delta_1 - \Delta_0 = U = 2E_C$, i.e. the on-site Coulomb repulsion $U$ has to be identified with twice the charging energy.

To find experimental realizations of the finite-U Anderson model, transitions to the triplet state $(N = 2, S = 1, M)$ have to be excluded . This is possible if the triplet state has higher energy than the singlet state which is often the case. Exact diagonalization studies of one-dimensional [141, 142, 66, 54] or parabolic [113, 114, 133] quantum dots provide criteria for the relevant transitions as function of particle number and energy.

Due to spin conservation, the tunneling matrix elements $T^r_{k,ss'}$ are only nonzero when the total spin and the magnetic quantum number have changed by $\pm 1/2$.

For higher particle numbers $N > 2$ an extremely rich structure arises and many possible situations can be realized. This is the reason why quantum dots or quantum dot arrays are very interesting strongly correlated systems. Especially the low-temperature behaviour, where quantum fluctuations are important, is dominated by Kondo-type behaviour but with many subtle differences due to the different kinds of possible transitions between the states. As an example let us consider the situation where two particles are already in the dot forming a singlet state $(2,0,0)$. We now consider the transition to a three particle doublet state $(3,1/2,\pm 1/2)$. Especially in parabolic [114, 133] or square-shaped [54] dots there are two degenerate doublet states due to rotational symmetries. In a magnetic field these two states can be splitted. If the bias voltage is low enough and the gate voltage adjusted appropriately, only the transitions

$$(2,0,0) \leftrightarrow (3,1/2,\pm 1/2) \quad \text{and} \quad (2,0,0) \leftrightarrow (3,1/2,\pm 1/2)^* \tag{2.78}$$

are relevant. Again, we can map this situation onto a single-particle model. We consider two spin-degenerate single-particle levels with energies $\epsilon_{i\sigma}$, $i = 1,2$, $\sigma = \uparrow, \downarrow$. An on-site Coulomb repulsion $U$ suppresses all states with $N > 1$. The Hamiltonian is similiar to the infinite-U Anderson model, but with two states

$$\begin{aligned} H(t) &= \sum_{k\sigma r} \epsilon_{k\sigma r} a^\dagger_{k\sigma r} a_{k\sigma r} + \sum_{i\sigma} \epsilon_{i\sigma} c^\dagger_{i\sigma} c_{i\sigma} \\ &\quad + \frac{U}{2} \sum_{(i\sigma)\neq(i'\sigma')} n_{i\sigma} n_{i'\sigma'} + \sum_{kr,i\sigma} (\bar{T}^r_{ki}(t) a^\dagger_{k\sigma r} c_{i\sigma} \; + \; h.c.)\,. \end{aligned} \tag{2.79}$$

Obviously, we identify $(2,0,0)$ with the empty dot, and $(3,1/2,\pm 1/2)$, $(3,1/2,\pm 1/2)^*$ with the singly occupied dot either with level 1 or with level 2 filled. We note that the wave vector $k$, characterizing the states in the reservoirs, can as well contain the

level index $i$ which is approximately conserved by tunneling. This corresponds to a realistic experimental situation [134] since, for a vertical parabolic dot, the index $i$ denotes an orbital angular quantum number which is also present in the leads. The low-temperature behaviour of this model has been discussed in Ref. [116]. We emphasize that, for low lying levels $i = 1, 2$, a Schrieffer-Wolff transformation does not result in a 2-impurity $S = 1/2$- or a 1-impurity $S = 3/2$-Kondo model. These models are characterized by singlet-, triplet- or quartet-spin states whereas the above model with one electron is characterized by a doublet in two possible realizations which exclude each other. As a consequence, we see that new and experimental accessible models with interesting low-temperature behaviour can arise here.

(b) **Metallic islands**. The metallic case, described by (2.65) and (2.66) (or (2.69), has many similiarities to Kondo models. If we restrict ourselves to two possible charge states $N = 0, 1$, we can write $\hat{N} = S_z + 1/2$, where $S_z$ is the z-component of a spin-1/2 operator. The operators $e^{\pm i\hat{\varphi}}$, which increase (decrease) the charge on the island, can then be identified with the spin raising (lowering) operators $S^{\pm}$ yielding

$$H_T(t) = \sum_{r,kl} \bar{T}^r_{kl}(t) a^\dagger_{kr} a_{lD} S^- \, e^{-i\hat{\phi}} \; + \; (h.c.)\,, \tag{2.80}$$

and

$$H_C = E_C (S_z + \frac{1}{2})^2 = E_C S_z + const\,. \tag{2.81}$$

Without the heat bath we have obtained a Hamiltonian similiar to a spin-1/2 Kondo model where $a_{kr}$, $r = L, R, D$,1 correspond to the "conduction" electrons which change their pseudospin $r$ by scattering at the local "impurity spin" $\vec{S}$. The coupling is anisotropic because there is no scattering term which leaves the pseudospin of the local "impurity" unchanged. Differences occur since there are three possible values $r = L, R, D$ for the pseudospin of the "conduction" electrons. However, in the equilibrium case, where the electrochemical potentials of the reservoirs $r = L, R$ are identical,

we can take both reservoirs together and introduce a pseudospin label $\sigma =\uparrow$ for $r = L, R$ and $\sigma =\downarrow$ for $r = D$. The phase factor $\exp(-ie\int_{t_0}^{t} dt' V_D(t'))$, occuring within the tunneling matrix element (2.23) for $V_r = 0$ $(r = L, R)$, corresponds to a magnetic field term $-2E_C n_x(t) S_z$ by reversing the unitary transformation (2.52). This formal exact mapping of the two charge state metallic dot model in equilibrium onto the anisotropic Kondo model in a magnetic field has first been established in Ref. [98].

Furthermore, we can also introduce a channel index by considering transverse channels in the leads connecting the reservoirs to the dot. The channel index is conserved by tunneling and the Hamiltonian becomes the analog of the multichannel Kondo model. For metallic single-electron transistors the typical number $Z$ of transverse channels is of order $Z \sim 10^3$ which is very large so that corrections of order $1/Z$ can be neglected. In the limit $Z \to \infty$, the pair $a_{kr}^\dagger a_{lD}$ can formally be replaced by the sum of two independent bosonic operators $c_{qr}^\dagger + d_{qr}$ which means that $H_0$, $H_T(t)$, and $\hat{I}_r^{tun}(t)$ are replaced by

$$\begin{aligned} H_0 &= H_R + H_B + H_C \\ &= \sum_{r=L,R} \sum_q \omega_q^r (c_{qr}^\dagger c_{qr} + d_{qr}^\dagger d_{qr}) + \sum_q \omega_q b_q^\dagger b_q + \sum_N E_N \hat{P}_N \,, \qquad (2.82) \\ H_T(t) &= \sum_{r=L,R} \sum_{q,N} \bar{g}_q^r(t) (c_{qr}^\dagger + d_{qr}) \hat{P}_{N-1,N}\, e^{-i\hat{\phi}} \;+\; (h.c.)\,, \qquad (2.83) \\ \hat{I}_r^{tun}(t) &= ie \sum_{q,N} \bar{g}_q^r(t) (c_{qr}^\dagger + d_{qr}) \hat{P}_{N-1,N} e^{-i\hat{\phi}} \;+\; (h.c.)\,, \qquad (2.84) \end{aligned}$$

with new coupling constants $\bar{g}_q^r$ defined analog to (2.23) by

$$\bar{g}_q^r(t) = g_q^r e^{ie\int_{t_0}^{t} dt' \bar{V}_r(t')} \,. \qquad (2.85)$$

In analogy to (2.28) and (2.29) they are characterized by the spectral function

$$\begin{aligned} \frac{1}{\pi} \bar{D}_r(t_1, t_2; \omega) &= e^{i\mu_r(t_1 - t_2)} \sum_q \bar{g}_q^r(t_1)^* \, \bar{g}_q^r(t_2) [\delta(\omega - \omega_q^r) - \delta(\omega + \omega_q^r)] \qquad (2.86) \\ &= e^{-ie\int_{t_2}^{t_1} dt' \bar{V}_r^1(t')} D_r(\omega) \,, \qquad (2.87) \end{aligned}$$

where

$$\begin{aligned}\frac{1}{\pi}D_r(\omega) &= \sum_q |g_q^r|^2[\delta(\omega-\omega_q^r)-\delta(\omega+\omega_q^r)] \\ &= \frac{1}{2\pi}\sum_l ,_{ll}^r(\omega+\epsilon_{lD})[f(\epsilon_{lD})-f(\epsilon_{lD}+\omega)]\,. \end{aligned} \tag{2.88}$$

Here, $,_{ll}^r$ is defined in (2.47), and $f(E)=(e^{\beta E}+1)^{-1}$ is the Fermi distribution function.

The proof of the equivalence of the two Hamiltonians is given in section 3.2 by comparing all possible Wick contractions in real time.

The spectral function can be written in a more elegant way if we assume a constant density of states $\nu_D$ on the island, and use approximately $,_{ll}^r(\omega)\approx ,^r$ independent of $l$ and $\omega$. We obtain

$$\frac{1}{\pi}D_r(\omega)=\alpha_0^r\omega\,, \tag{2.89}$$

where

$$\alpha_0^r=\frac{1}{2\pi},^r\nu_D=\frac{1}{4\pi^2}\frac{R_K}{R_T^r} \tag{2.90}$$

is proportional to the conductance $G_T^r=1/R_T^r$ of a single barrier connecting the island to reservoir $r=L,R$ in units of the quantum conductance $G_K=1/R_K=e^2/h$. For two charge states, the relation (2.90) expresses an ohmic coupling of the auxiliary boson baths to the local spin $S$. However, even without the heat bath $H_B$, the Hamiltonian is not equivalent to the well-known spin boson model [89, 140] since the two boson operator $c_{qr}$ and $d_{qr}$ are not identical. Therefore, bosonic contractions between two vertices both refering to $S^-$ or $S^+$ are forbidden here. The above Hamiltonian results by applying the rotating wave approximation to the spin boson model with ohmic dissipation. Although this is not a justified approximation for the spin boson model, we have shown here that the resulting model has a realization in connection with single-electron devices.

## 2.4 Golden rule theory

Many of the experiments showing single-electron effects can be explained by lowest order perturbation theory in tunneling. The theory is based on classical master equations with golden rule rates and describes basically incoherent transport through the device. This means that the electrons tunnel sequentially, i.e. after each single tunneling process the particle or hole excitation created in the reservoir relaxes to the equilibrium state. For metallic islands the theory was developed in Ref. [85, 5], in the literature referred as "orthodox theory", and later was used for quantum dots with discrete spectra [4, 9, 102, 14]. We will describe golden rule theory already in this section because it can be derived without using diagrammatic many-body methods and gives results which can be understood in terms of simple concepts like energy conservation and the Pauli principle. A more rigorous and powerful theory will be presented in chapter 3 which allows a consistent treatment of higher order tunneling processes as well and generalizes the results of this section.

The master equation with golden rule rates has been studied extensively in the literature. We mention Ref. [5] for the metallic case, Refs. [85, 42, 9, 102, 61, 4] for the Coulomb blockade model, Ref. [141, 142, 66, 113] for the quantum dot case with exact many-body wave functions in the few electron limit, Ref. [12, 75] for coupled quantum dots, Refs [84, 24] for the metallic case in time-dependent fields, Ref. [14] for the Coulomb blockade model in time-dependent fields, and Refs. [64, 110, 34] for the metallic case in the presence of a heat bath. For thermal transport we refer to Ref. [10] and for quantum dots in the fractional quantum Hall regime to Ref. [73].

### 2.4.1 General formalism

We use the Hamiltonian $H(t) = H_0 + H_T(t)$ which was derived in the previous sections. $H_0 = H_R + H_B + H_D$ contains the reservoirs, the heat bath and the dot, whereas $H_T(t)$

describes the interaction due to tunneling and energy exchange. For metallic islands, the dot part is replaced by the charge part $H_C$. We denote the eigenfunctions of $H_0$ by $|\chi s>$ with energy $E_{\chi s} = E_\chi + E_s$. $\chi = \chi_R \chi_B$ includes the reservoir and heat bath part whereas $s$ corresponds to the dot (charge) part. We will take here harmonic voltages on the reservoirs of the form (2.26) and (2.27). The reservoirs and the heat bath are treated as large systems in equilibrium described by the grandcanonical density matrix $\rho^{eq}_{RB} = \rho^{eq}_R \rho^{eq}_B$.

The golden rule tunneling rate for a transition of the dot from state $|s'>$ to $|s>$ when $p = \pm 1$ particles have been added from reservoir $r$ is given by

$$\begin{aligned}\Sigma^{rp}_{ss'} &= 2\pi \sum_{\substack{\chi\chi' \\ N_r(\chi)=N_r(\chi')-p}} \sum_{m=-\infty}^{\infty} \rho^{eq}_{RB}(\chi') J_m(\frac{\bar{\Delta}_r}{\Omega})^2 | < \chi s|H_T(t_0)|\chi' s' > |^2 \times \\ &\qquad \times \delta(E_s - E_{s'} + E_\chi - E_{\chi'} - p\mu_r + m\Omega)\,, \qquad (2.91)\end{aligned}$$

where $N_r(\chi)$ denotes the number of particles in reservoir $r$ for state $\chi$. The energy conservation law includes the change $\mu_r = eV_r - eV_D$ of the DC-part of the electrostatic energy as well as the possibility to absorb the energy $m\Omega$ from the oscillating voltage. This means, that the time-dependent periodic part of the voltage has been described within the physics of photon assisted tunneling [135]. $J_m(\frac{\bar{\Delta}_r}{\Omega})^2$ is the probability to absorb (emit) $m$ energy quanta $\Omega$, where $J_m$ denotes the Bessel function of order $m$. This can easily be understood since a solution of the time-dependent Schrödinger equation for a state with energy $E$ subject to a time-dependent external field $\Delta(t) = \Delta_0 \sin(\Omega t)$ is given by

$$\begin{aligned}|\psi(t)> &= e^{-iE(t-t_0)} e^{-i\int_{t_0}^{t} d\tau \Delta(\tau)} |\psi(t_0)> \\ &= e^{-iE(t-t_0)} e^{-i\frac{\Delta_0}{\Omega}\cos(\Omega t_0)} \sum_m i^m J_m(\frac{\Delta_0}{\Omega}) e^{im\Omega t} |\psi(t_0)> \,. \qquad (2.92)\end{aligned}$$

As a consequence, $J_m(\frac{\Delta_0}{\Omega})^2$ is interpreted as the probability that the state has changed energy by $\pm m\Omega$.

The tunneling Hamiltonian at the initial time can be written as

$$H_T(t_0) = \sum_{rp} \sum_{ss'} H^{rp}_{T,ss'} e^{ip\hat{\phi}} \hat{P}_{ss'} \,, \tag{2.93}$$

with $H^{rp\dagger}_{T,ss'} = H^{r,-p}_{T,s's}$ acting only in reservoir space. This gives for the rate

$$\begin{aligned} \Sigma^{rp}_{ss'} &= 2\pi \int d\omega P^p_r(\omega) \sum_{\chi_R \chi'_R} \rho^{eq}_R(\chi'_R)| < \chi_R|H^{rp}_{T,ss'}|\chi'_R > |^2 \times \\ &\quad \times \delta(E_s - E_{s'} + E_{\chi_R} - E_{\chi'_R} - p\mu_r - p\omega) \,, \end{aligned} \tag{2.94}$$

where we define by

$$P^{\pm}_r(\omega) = \sum_{m=-\infty}^{\infty} J_m(\frac{\bar{\Delta}_r}{\Omega})^2 \, P^{\pm}(\omega + m\Omega) \tag{2.95}$$

the probability to absorb (emit) the energy $\omega$ from the environment including heat bath and time-dependent fields, and by

$$P^p(\omega) = \sum_{\chi_B \chi'_B} \rho^{eq}_B(\chi'_B)| < \chi_B|e^{ip\hat{\phi}}|\chi'_B > |^2 \delta(p\omega + E_{\chi_B} - E_{\chi'_B}) \,, \tag{2.96}$$

the probability to absorb (emit) the energy $\omega$ from the heat bath only. The latter quantity obviously fulfils $P^+(\omega) = P^-(-\omega)$, and the condition of detailed balance

$$P^-(\omega) = e^{\beta_B \omega} P^+(\omega) \,, \tag{2.97}$$

with $\beta_B = 1/T_B$ being the inverse temperature of the heat bath. Using $2\pi\delta(\omega) = \int dt \exp(i\omega t)$, defining the interaction picture $A(t)_I$ with respect to $H_0$, and introducing the Fourier transform $P^{\pm}(\omega) = \frac{1}{2\pi} \int e^{i\omega t} P^{\pm}(t)$, we obtain explicitly the well-known result [22, 110, 34, 64]

$$P^-(t) = P^+(-t) = < e^{i\hat{\phi}(t)_I} e^{-i\hat{\phi}} >_{\rho^{eq}_B} = e^{-W(t)} \,, \tag{2.98}$$

with $W(t) = S(t) + iR(t)$ and

$$S(t) = \frac{1}{\pi} \int_0^{\infty} d\omega \frac{J(\omega)}{\omega^2} (1 - \cos(\omega t)) \coth(\frac{\beta_B \omega}{2}) \,, \tag{2.99}$$

$$R(t) = \frac{1}{\pi} \int_0^{\infty} d\omega \frac{J(\omega)}{\omega^2} \sin(\omega t) \,. \tag{2.100}$$

The total probability $P_r^{\pm}(\omega)$ to exchange energy with the heat bath and the time-dependent fields has the two properties

$$P_r^-(\omega) = P_r^+(-\omega) \quad , \quad \int d\omega P_r^{\pm}(\omega) = 1 \, , \tag{2.101}$$

but does not fulfil detailed balance in general. Classical fields fulfil $P_r^- = P_r^+$ which is equivalent to an infinite bath temperature in the detailed balance property (2.97). For bosonic baths, the probability for absorption and emission is always different. This is an important difference between time-dependent classical fields and quantum mechanically treated boson baths.

For later purpose, we note that, by using again the representation of the $\delta$-function, the golden rule rate can also be written as

$$\Sigma_{ss'}^{rp} = \int d\omega P_r^p(\omega) \int dt \, e^{i(E_s - E_{s'} - p\mu_r - p\omega)t} < H_{T,s's}^{r,-p} \, H_{T,ss'}^{rp}(t)_I >_{\rho_R^{eq}} \, . \tag{2.102}$$

The rates can be used as an input for a master equation. Consequently, the stationary DC-probability distribution $P_s$ for the dot and the stationary DC-tunneling current in reservoir $r$ can be calculated from

$$0 = \sum_{s'} (\Sigma_{ss'} P_{s'} - \Sigma_{s's} P_s) \, , \tag{2.103}$$

$$I_r = e \sum_{ss'} (\Sigma_{ss'}^{r+} P_{s'} - \Sigma_{s's}^{r-} P_s) \, , \tag{2.104}$$

with $\Sigma_{ss'} = \sum_{rp} \Sigma_{ss'}^{rp}$. We note that the DC-component of the displacement current is zero. Therefore the DC-tunneling current is identical to the total DC-current. Current conservation $\sum_r I_r = 0$ follows from the property

$$\sum_r (\Sigma_{ss'}^{r+} - \Sigma_{ss'}^{r-}) = \Sigma_{ss'}(N_s - N_{s'}) \, . \tag{2.105}$$

The above linear set of equations can be solved by straightforward numerical evaluation. However, analytical progress can be achieved by using the property of detailed

balance. The latter holds if the time-dependent fields are absent ($\bar{\Delta}_r = 0$) and if the temperature of the heat bath is identical to the temperature of the system ($\beta_B = \beta$). In this case, we obtain directly from (2.91)

$$\Sigma^{r-}_{s's} = \Sigma^{r+}_{ss'}\, e^{\beta(E_s - E_{s'} - \mu_r)}\,, \tag{2.106}$$

As a consequence, the equilibrium solution of the master equation (2.103) is the grandcanonical distribution

$$P^{eq}_s = \frac{1}{Z} e^{-\beta(E_s - \mu N_s)}\,, \tag{2.107}$$

which applies when all electrochemical potentials are the same $\mu_r = \mu$. In this case, the DC-current (2.104) is zero. In coincidence with the general theory of equilibrium statistical mechanics, the environment enters only via the temperature $T$ and the electrochemical potential $\mu$. This applies when the tunneling coupling is weak enough. In contrast, the coupling to the heat bath can be arbitrarily strong here without destroying the grandcanonical distribution. This is due to the fact that we have not allowed for the environment to induce transitions between the dot states as it is the case, e.g., in spin boson models [89, 140].

Using detailed balance we can write the tunneling rates as

$$\Sigma^{r+}_{ss'} = f^+_r(E_s - E_{s'})A^r_{ss'} \quad , \quad \Sigma^{r-}_{s's} = f^-_r(E_s - E_{s'})A^r_{ss'}\,, \tag{2.108}$$

where $f_r(\omega) = f(\omega - \mu_r)$ is the effective Fermi distribution of reservoir $r$, $f^+_r = f_r$, $f^-_r = 1 - f^+_r$, and

$$A^r_{ss'} = \Sigma^{r+}_{ss'} + \Sigma^{r-}_{s's} \tag{2.109}$$

is the sum of tunneling "in" and tunneling "out" rates. As a consequence the current (2.104) is given by

$$I_r = e \sum_{ss'} A^r_{ss'} \left[ f^+_r(E_s - E_{s'})P_{s'} - f^-_r(E_s - E_{s'})P_s \right]\,. \tag{2.110}$$

This expresses already energy conservation and the Pauli principle. The first term represents the tunneling "in" process, i.e. an electron has to be present in reservoir $r$ with energy $E_s - E_{s'}$, whereas the second term represents the corresponding tunneling "out" process, i.e. the state with energy $E_s - E_{s'}$ has to be free in reservoir $r$.

Under certain circumstances, this equation can be written in a more convenient way. Let us assume that $A^r_{ss'}$ depends on the reservoir index only via a constant factor

$$A^r_{ss'} = , ^r\lambda_{ss'} . \tag{2.111}$$

As we will see in the next section this is a good approximation for many quantum dots without heat bath since the Fermi functions of the reservoirs cancel out. Inserting this form in (2.110) and using current conservation $\sum_r I_r = 0$, we obtain

$$\sum_{ss'} A^r_{ss'} P_s = \sum_{r'ss'} \frac{A^r_{ss'} A^{r'}_{ss'}}{A_{ss'}} (P_s + P_{s'}) f_r(E_s - E_{s'}) , \tag{2.112}$$

with $A_{ss'} = \sum_r A^r_{ss'}$. Using this relation again in (2.110), we obtain for the current

$$I_r = e \sum_{r'ss'} \frac{A^r_{ss'} A^{r'}_{ss'}}{A_{ss'}} (P_s + P_{s'}) [f_r(E_s - E_{s'}) - f_{r'}(E_s - E_{s'})] . \tag{2.113}$$

This equation has a very obvious structure and reflects the qualitative physics we have already discussed in section 2.2. For a current to flow we need that the excitation energy $E_s - E_{s'}$ of the dot lies in the window between the effective Fermi levels of the reservoirs. The probability distribution still depends on the Fermi functions of the reservoirs and, consequently, the equation is not identical to the Landauer-Büttiker formula [88, 16]. This is due to the Coulomb interaction on the dot.

In linear response, we set $\mu_r = \mu + \delta\mu_r$ and define $e\delta\bar{V}_r = \delta\mu_r$. After linearization, Eq. (2.113) reduces to

$$I_r = \sum_{r'} G_{rr'} (\delta\bar{V}_r - \delta\bar{V}_{r'}) , \tag{2.114}$$

$$G_{rr'} = -e^2 \sum_{ss'} \frac{A^{r,eq}_{ss'} A^{r',eq}_{ss'}}{A^{eq}_{ss'}} (P^{eq}_s + P^{eq}_{s'}) f'(E_s - E_{s'} - \mu) , \tag{2.115}$$

where $A^{r,eq}_{ss'} = \Sigma^{r+,eq}_{ss'} + \Sigma^{r-,eq}_{s's}$ denotes the sum of the rates in equilibrium and $f'$ is the derivative of the Fermi function.

The current formula (2.113) can also be proven under different conditions. In certain cases all terms in the sum of the master equation (2.103) are separately zero, i.e. we can use an iteration scheme from the generalized detailed balance condition

$$P_s \sum_r \Sigma^{r-}_{s's} = P_{s'} \sum_r \Sigma^{r+}_{ss'} \,. \tag{2.116}$$

This is correct when all possible transitions between states of the dot form a "tree". This means that no loops are allowed to occur where transitions starting from a state $s$ can return to the same state in a different way than just by reversing all transitions. Thereby we can identify all degenerate states which have the same probability. Trivially we can use this for the metallic case where each particle sector consists only of one single charge state. Furthermore it can often be used for quantum dots with very few states and special selection rules for the transitions. If (2.116) holds, we can use (2.108) and find that (2.112) now holds even for each term of the sum separately. Thus, we obtain again the current formula (2.113).

The generalized detailed balance condition (2.116) is valid under more general conditions in linear response. To discuss this, we linearize the probability distribution for $\beta\delta\mu_r \ll 1$

$$P_s = P^{eq}_s(1 + \beta \sum_r \psi^r_s \delta\mu_r) \,. \tag{2.117}$$

A straightforward linearization of (2.116) gives the condition

$$\psi^r_s - \psi^r_{s'} = \frac{A^{r,eq}_{ss'}}{A^{eq}_{ss'}} \,. \tag{2.118}$$

Again, this ansatz can only work if the rates have special properties. First, as already discussed above, it is valid when all possible transitions form a "tree". Second, if (2.111) holds, we can fulfil (2.118) by $\psi^r_s = \text{const} + N_s, {}^r/, ,$ with $, = \sum_r , {}^r$. Third,

within the Coulomb blockade model, any eigenstate $s = \{n_l(s)\}_l$ of the dot is given by a set of occupation numbers $n_l(s)$ of the single particle states $l$ . If, in addition, we have the factorized form

$$A^{r,eq}_{s+l,s} = , \, {}^{r}_{l} B^{eq}_{s+l,s} \, , \tag{2.119}$$

with $n_l(s+l) = 1$ and $n_l(s) = 0$, we can solve (2.118) by

$$\psi^r_s = \text{const} + \sum_l n_l(s), \, {}^{r}_{l} /, \, {}_{l} \, , \tag{2.120}$$

with $, \, {}_{l} = \sum_r , \, {}^{r}_{l}$. This solution has first been proposed in Ref. [9].

Finally we discuss the generalization of the current formulas (2.110) and (2.113) to the case when external time-dependent fields are present ($\bar{\Delta}_r \neq 0$) or when the temperature of the boson bath is not necessarily identical to the system temperature. We start from the general formula (2.94) and define frequency dependent rates by

$$\Sigma^{r+}_{ss'} = \int d\omega P^+_r(\omega) \Sigma^{r+}_{ss'}(E_s - E_{s'} - \omega) \, , \tag{2.121}$$

$$\Sigma^{r-}_{s's} = \int d\omega P^-_r(\omega) \Sigma^{r-}_{s's}(E_s - E_{s'} - \omega) \, , \tag{2.122}$$

$$A^r_{ss'}(\omega) = \Sigma^{r+}_{ss'}(\omega) + \Sigma^{r-}_{s's}(\omega) \, . \tag{2.123}$$

The detailed balance condition for the frequency dependent rates reads

$$\Sigma^{r-}_{s's}(\omega) = \Sigma^{r+}_{ss'}(\omega) e^{\beta(\omega - \mu_r)} \, , \tag{2.124}$$

which, in analogy to (2.108) and (2.110), leads to

$$\Sigma^{r+}_{ss'}(\omega) = f^+_r(\omega) A^r_{ss'}(\omega) \quad , \quad \Sigma^{r-}_{s's}(\omega) = f^-_r(\omega) A^r_{ss'}(\omega) \, , \tag{2.125}$$

and

$$\begin{aligned} I_r &= e \sum_{ss'} \int d\omega A^r_{ss'}(E_s - E_{s'} - \omega) \times \\ &\quad \times [P^+_r(\omega) f^+_r(E_s - E_{s'} - \omega) P_{s'} - P^-_r(\omega) f^-_r(E_s - E_{s'} - \omega) P_s] \, . \end{aligned} \tag{2.126}$$

This equation expresses the fact that the dot can exchange energy $\omega$ with the environment. For tunneling "in" ("out") we need the absorption (emission) probability since reversing the tunneling transition means reversing the initial and final states.

As before we can find some cases where the current formula can be written in a more convenient form. The analog condition to (2.111) reads

$$A^r_{ss'}(\omega) = \, , \, ^r B_{ss'}(\omega) \, , \tag{2.127}$$

which again is a good approximation for many quantum dots. If in addition the environment couples symmetrically to the system $P^{\pm}_r = P^{\pm}$ (this includes the case of symmetrically coupled time-dependent fields), we can use an analog derivation to above and find for the current

$$\begin{aligned} I_r &= e \sum_{r'} \sum_{ss'} \frac{\, , \, ^r \, , \, ^{r'}}{\, , \,} \int d\omega B_{ss'}(\omega)[P^-(\omega)P_s + P^+(\omega)P_{s'}] \times \\ &\qquad \times [f_r(E_s - E_{s'} - \omega) - f_{r'}(E_s - E_{s'} - \omega)] \, . \end{aligned} \tag{2.128}$$

We see that the excitation energy $E_s - E_{s'}$ is shifted by $\omega$. Furthermore, we recognize that shifting by $\pm\omega$ is not equivalent for a heat bath, since the probabilities for absorption and emission are not the same.

If the condition (2.116) of generalized detailed balance is fulfilled, we can prove an even more general equation in analogy to (2.113). Using (2.116) together with the definition (2.109), we can write the current (2.104) as

$$I_r = e \sum_{r'} \sum_{ss'} \frac{P_s + P_{s'}}{A_{ss'}} (\Sigma^{r+}_{ss'} \Sigma^{r'-}_{s's} - \Sigma^{r'+}_{ss'} \Sigma^{r-}_{s's}) \, . \tag{2.129}$$

Inserting (2.121), (2.122) and (2.125) we find

$$\begin{aligned} I_r &= e \sum_{r'} \sum_{ss'} \int d\omega \int d\omega' \times \\ &\times \{ A^r_{ss'}(\omega) A^{r'}_{ss'}(\omega') P^+_r(E_s - E_{s'} - \omega) P^-_{r'}(E_s - E_{s'} - \omega) f^+_r(\omega) f^-_{r'}(\omega') - (r \leftrightarrow r') \} \, . \end{aligned} \tag{2.130}$$

Interchanging $\omega \leftrightarrow \omega'$ in the second term allows us to write the current into the form of a generalized "Landauer-Büttiker"-type equation with Pauli-blocking factors

$$I_r = \frac{e}{h}\sum_{r'}\int d\omega \int d\omega' \left\{T_{r'r}(\omega',\omega)f_r^+(\omega)f_{r'}^-(\omega') - T_{rr'}(\omega,\omega')f_r^-(\omega)f_{r'}^+(\omega')\right\}, \quad (2.131)$$

where

$$\begin{aligned} T_{rr'}(\omega,\omega') &= 2\pi\sum_{ss'}\frac{A_{ss'}^r(\omega)A_{ss'}^{r'}(\omega')}{A_{ss'}} \times \\ &\quad \times P_r^-(E_s - E_{s'} - \omega)P_{r'}^+(E_s - E_{s'} - \omega')(P_s + P_{s'}) \end{aligned} \quad (2.132)$$

represents a "transmission coefficient" from reservoir $r'$ to reservoir $r$. Such an equation has been proposed in several contexts [21, 56, 145, 44, 67, 63] to generalize the Landauer-Büttiker formula [88, 16] in the presence of inelastic interactions. However, it is important to notice that, at least in our case of a quantum dot with electron-electron and electron-boson interaction, $T_{rr'}$ will always depend on the Fermi functions of the reservoirs. Even in the case of a single excitation energy, where $P_s + P_{s'} = 1$, and even when the Fermi functions cancel out in $A_{ss'}^r(\omega)$ , the Fermi functions will enter through the quantity $A_{ss'} = \sum_r A_{ss'}^r$ in the denominatror of (2.132) since

$$A_{ss'}^r = \int d\omega [P_r^+(E_s - E_{s'} - \omega)f_r^+(\omega) + P_r^-(E_s - E_{s'} - \omega)f_r^-(\omega)]A_{ss'}^r(\omega)\,. \quad (2.133)$$

Therefore, it is not correct to interpret $T_{rr'}$ as a one-particle transmission coefficient which depends only on the properties of the dot. This is not very suprising since interactions can only be treated correctly within a many-body formalism whereas (2.131) is motivated by the transmission of one-particle scattering waves which exchange energy with an inelastic environment during tunneling through the device. In section 2.4.2 we will discuss an explicit example to demonstrate the influence of correlations on $T_{rr'}$.

From (2.130) we can see that the zero-voltage DC-current can be nonzero in the presence of an environment. This can be the case when the detailed balance condition

(2.106) is violated. It means that the device can act like an electron pump. A "pump"-current will occur when the external fields couple asymmetrically to the reservoirs, i.e. when the probability function $P_r^{\pm}$ depends on the reservoir index $r$. In sections 2.4.2 and 2.4.3 we will discuss several applications and experimental measurements of this effect. As a subtlety we mention that a "pump"-current can also occur due to an asymmetric energy dependence of the quantities $A^r_{ss'}(\omega)$ which might be due to special properties of the tunneling matrix elements. Thus, even a pure bosonic environment with $T_B \neq T$ can create a pump-current due to the violation of detailed balance.

### 2.4.2 Quantum dots

From (2.22) we get $H^{r-}_{T,s's} = \sum_k T^r_{k,s's} a^\dagger_{kr}$. Using (2.102) together with the definition (2.30), we obtain for the rates

$$\Sigma^{r+}_{ss'} = \int d\omega, ^r_{ss',s's}(E_s - E_{s'} - \mu_r - \omega) f_r^+(E_s - E_{s'} - \omega) P_r^+(\omega)\,, \qquad (2.134)$$

$$\Sigma^{r-}_{s's} = \int d\omega, ^r_{ss',s's}(E_s - E_{s'} - \mu_r - \omega) f_r^-(E_s - E_{s'} - \omega) P_r^-(\omega)\,. \qquad (2.135)$$

If we use (2.48), i.e. neglect the dependence of the spectral function $, ^r_{ll'}(\omega) \approx \delta_{ll'}, ^r$ on energy and the single particle states, we obtain

$$, ^r_{ss',s's}(\omega) \approx , ^r \sum_l | < s|a^\dagger_{lD}|s' > |^2\,. \qquad (2.136)$$

In the special case of a single dot described within the Coulomb blockade model, and neglecting the energy dependence of $, ^r_{ll}(\omega) \approx , ^r_l$, we get

$$\Sigma^{r+}_{s+l,s} = , ^r_l \int d\omega f_r^+(\Delta_{N_s l} - \omega) P_r^+(\omega)\,, \qquad (2.137)$$

$$\Sigma^{r-}_{s,s+l} = , ^r_l \int d\omega f_r^-(\Delta_{N_s l} - \omega) P_r^-(\omega)\,, \qquad (2.138)$$

where $n_l(s+l) = 1$, and $n_l(s) = 0$. $\Delta_{Nl} = \epsilon_{lD} + (2N+1)E_C$ describes the energy change of the dot when a particle is added to level $l$.

The physical interpretation of the results for the rates is obvious. They express what we have already discussed qualitatively in section 2.2. For a current to flow through the structure we need that both the tunneling "in" and tunneling "out" rate are nonvanishing. Let us consider a transition between two dot states $s_N \leftrightarrow s_{N+1}$, where $s_N$ corresponds to a state with $N$ particles on the dot. For tunneling "in" from reservoir $r$ we have $s' = s_N$ and $s = s_{N+1}$ in (2.134). This means that $\Delta E = E_{s_{N+1}} - E_{s_N} < \mu_r + \omega$ (up to smearing due to finite temperatures) according to the Fermi function in (2.134). Thereby we have considered an energy absorption $\omega$ with probability $P_r^+(\omega)$ from the environment. For tunneling "out" to reservoir $r'$ we have $s' = s_{N+1}$ and $s = s_N$ in (2.135). This gives $\Delta E > \mu_{r'} + \omega$ where $\omega$ is now the energy which has been emitted to the environment with probability $P_{r'}^-(\omega)$. Both conditions can only be fulfilled simultaneously if the excitation energy $\Delta E$ lies in the window of the effective potentials of the reservoirs shifted by the frequency $\omega$: $\mu_{r'} + \omega < \Delta E < \mu_r + \omega$. This expresses energy conservation from golden rule and the Pauli principle.

Let us start with the case when the heat bath and the time-dependent fields are absent, i.e. for $P_r^{\pm}(\omega) = \delta(\omega)$. Inserting (2.136) in (2.134) and (2.135), we find $A^r_{ss'} = \Sigma^{r+}_{ss'} + \Sigma^{r-}_{s's} = {}^{,\,r}_{,}\sum_l | < s|a^\dagger_{lD}|s' > |^2$, i.e. the condition (2.111) is fulfilled and we can use the current formula (2.113). As a consequence, the nonlinear current and the conductance matrix in linear response read

$$\begin{aligned} I_r &= e \sum_{r's s'} {}^{,\,r,\,r'}_{,} \sum_l | < s|a^\dagger_{lD}|s' > |^2 (P_s + P_{s'}) \times \\ &\qquad \times [f_r(E_s - E_{s'}) - f_{r'}(E_s - E_{s'})] \,, \qquad (2.139) \\ G_{rr'} &= -e^2 \sum_{ss'} {}^{,\,r,\,r'}_{,} \sum_l | < s|a^\dagger_{lD}|s' > |^2 (P^{eq}_s + P^{eq}_{s'}) f'(E_s - E_{s'} - \mu) \,. \qquad (2.140) \end{aligned}$$

For the special case of the Coulomb blockade model we have $\Sigma^{r\pm}_{s\pm l,s} = {}^{,\,r} f^{\pm}_r(\Delta_{Nl})$. This

gives

$$I_r = e \sum_{r'Nl} \frac{\gamma_r \gamma_{r'}}{\gamma} (P_{N+1} F^+_{N+1,l} + P_N F^-_{Nl}) [f_r(\Delta_{Nl}) - f_{r'}(\Delta_{Nl})] , \qquad (2.141)$$

$$G_{rr'} = -e^2 \sum_{Nl} \frac{\gamma_r \gamma_{r'}}{\gamma} (P^{eq}_{N+1} F^{+,eq}_{N+1,l} + P^{eq}_N F^{-,eq}_{Nl}) f'(\Delta_{Nl}) , \qquad (2.142)$$

where $P_N$ is the probability for particle numer $N$ on the dot, and $F^{\pm}_{Nl}$ the conditional probability that level $l$ is filled (empty) provided the dot contains $N$ particles. As will be discussed below, $F^{\pm}_{Nl}$ is generally not identical to the Fermi distribution function due to nonequilibrium, interaction and finite size effects.

In the general case, many excitation energies $E_s - E_{s'}$ can lie between $\mu_r$ and $\mu_{r'}$ and are relevant for transport. However, only those transitions $s' \to s$ will occur for which the initial probability $P_{s'}$ is not too small. For temperatures and bias voltages smaller than the level spacing $\delta E$ and the charging energy $E_C$, only the ground states $s^0_N$ of the dot will have nonzero occupation probability. This means that only the excitation energies

$$\Delta_N = E_{s^0_{N+1}} - E_{s^0_N} \qquad (2.143)$$

are relevant. The transition from $s^0_N$ to an excited state $s^*_{N+1}$ will not occur since, by increasing $\mu_r$ via the gate voltage, the transition $s^0_N \to s^0_{N+1}$ will happen first and afterwards the dot is already in the $N+1$-particle ground state. Thus, we obtain the same physical picture as shown in Fig. 2.3 with the only difference that the distance $\Delta$ between adjacent excitation energies is no longer a constant. This behaviour is reflected in the formula (2.140) for the conductance matrix in linear response. Due to the derivative of the Fermi function, the conductance will be maximal when $\mu$ coincides with one of the excitation energies within temperature. $\mu = -eV_D$ is varied experimentally by the gate voltage (in equilibrium, we set $V_r = 0$). For the Coulomb blockade model we have $\mu = 2E_C n_x = -\frac{C_g}{C} e V_g$ according to (2.25). Thus, the conductance shows a series of resonances with varying distance between the peaks and

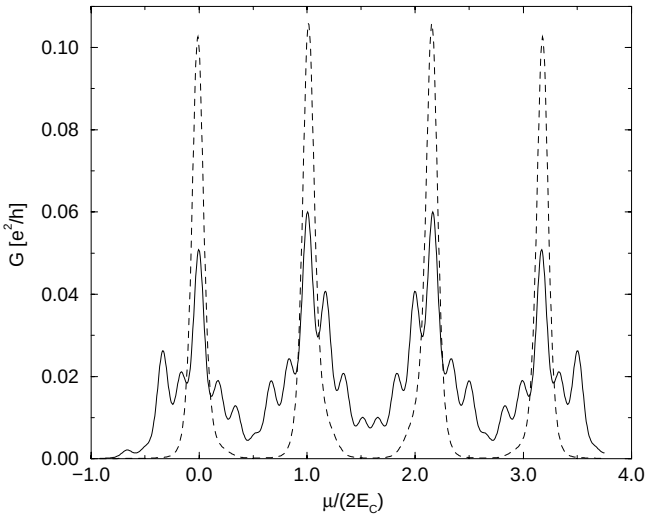


Figure 2.4: Linear conductance versus $\mu$ for two doubly degenerate levels with $\epsilon_1 + E_C = 0$, $\epsilon_2 + E_C = 25$, , for the static case (dashed line) and in the presence of AC-voltages with $\Omega = 50$, and $\bar{\Delta}_L/\Omega = \bar{\Delta}_R/\Omega = 1$ (solid line). The other parameters are $T = 5$, , $E_C = 75$, , and , $^L =$ , $^R =$ , /2. The distance between the second and third main resonance is larger due to the finite level spacing. In the static case all resonances involving excited states are hidden. In the presence of time-dependent fields they become visible together with satellite resonances shifted by $m\Omega$.

a line shape which is approximately given by the derivative of the Fermi distribution function. Between the resonances transport is not possible and the system is in the Coulomb blockade regime. As an example, we have shown these so-called "Coulomb oscillations" in Fig. 2.4 (dashed line) for the Coulomb blockade model with two doubly degenerate levels with energies $\epsilon_1 < \epsilon_2$. We observe four resonances corresponding to the excitation energies $\Delta_{01} = \epsilon_1 + E_C$, $\Delta_{11} = \epsilon_1 + 3E_C$, $\Delta_{22} = \epsilon_2 + 5E_C$, and $\Delta_{32} = \epsilon_2 + 7E_C$. As explained above, all other excitation energies $\Delta_{02} = \epsilon_2 + E_C$, $\Delta_{12} = \epsilon_2 + 3E_C$, $\Delta_{21} = \epsilon_1 + 5E_C$, and $\Delta_{31} = \epsilon_1 + 7E_C$ are hidden because they involve excited states.

At finite bias voltage all excitations are in principle visible since the excited states get finite probability. This holds at least in the absence of certain selection rules arising

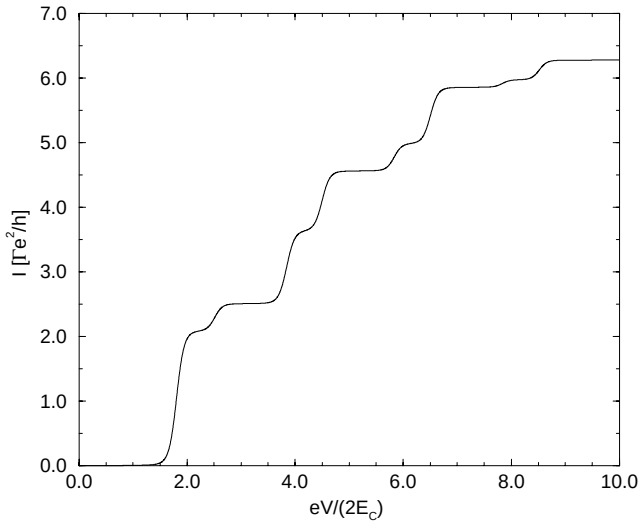


Figure 2.5: DC current in nonlinear response versus $eV = e(V_L - V_R)$, with $V_L = -V_R = V/2$ and $C_g V_g/e = 1$ fixed, for two doubly degenerate levels with $\epsilon_1 + E_C = 0$, $\epsilon_2 + E_C = 50$, . The other parameters are $T = 5$, , $E_C = 75$, , and , $^L$ = , $^R$ = , /2. All one-particle excitations of the dot are visible.

from the matrix element $< s|a_{lD}^\dagger|s' >$ in (2.139). The I-V-characteristic shows steps each time a new excitation becomes relevant. This is commonly called the "Coulomb staircase" and is shown in Fig. 2.5 for the same example as before. Equivalently, the differential conductance $dI/dV$ shows peaks as function of the bias voltage. As can be seen, all eight excitation energies mentioned before are visible.

The effects of strong correlations on the dot are not only reflected by the increase of the distance between adjacent resonances but also show up in the line shape of an individual peak. To show this explicitly, let us consider a singlet-doublet transition which is equivalent to the infinite-U Anderson model (2.73) as discussed in section 2.3. In the degenerate case without magnetic field we get from (2.141), (2.142), and solving the master equation

$$I_r = 2e \sum_{r'} \frac{, ^r, ^{r'}}{,} \frac{1}{1 + \sum_{\bar{r}} \frac{\Gamma^{\bar{r}}}{\Gamma} f_{\bar{r}}(\epsilon)} [f_r(\epsilon) - f_{r'}(\epsilon)] , \qquad (2.144)$$

$$G_{rr'} = -2e^2 \frac{\Gamma^r \Gamma^{r'}}{\Gamma} \frac{1}{1+f(\epsilon-\mu)} f'(\epsilon-\mu)\,. \tag{2.145}$$

The current contains an asymmetry factor $1/(1+\sum_r \frac{\Gamma^r}{\Gamma} f_r(\epsilon))$ which is absent either for a nondegenerate level or for the noninteracting case $U = 2E_C = 0$. This factor arises from correlations since double occupancy of the dot is forbidden. This gives rise to particle-hole asymmetry and, consequently, to an asymmetric line shape of the differential conductance as a function of $\epsilon$ as shown in Fig. 2.6 (dashed curve) for finite bias voltage. The maximal value of the conductance in linear response is given by

$$G_{rr'}^{\max} = 2e^2 \frac{\Gamma^r \Gamma^{r'}}{\Gamma T} \frac{2}{3} = 4\pi \frac{e^2}{h} \frac{\Gamma^r \Gamma^{r'}}{\Gamma T} \frac{2}{3}\,. \tag{2.146}$$

For a nondegenerate level or for the noninteracting case with one degenerate level, the factor 2/3 has to be replaced by 1/2 or 1, respectively. This can easily be understood. At the maximum point, all states of the dot have the same probability. For the infinite-U Anderson model there are two excitations which can be used for transport, and three possible states of the dot (the empty dot and two degenerate states with one electron). Each excitation contributes equally to the current but has to be multiplied with the probability 1/3 of the initial state. This explains the factor 2/3. For a nondegenerate level we have only one excitation and two states, resulting in a factor 1/2. For a noninteracting model with one degenerate level we have four excitations (two for each transition $N = 0 \to N = 1$ and $N = 1 \to N = 2$) and four possible states, giving a factor 1. The reduction of the current by Coulomb repulsion is obvious, since certain processes are blocked. In contrast to the noninteracting case, we have seen that the presence of degenerate states does *not* give rise to a pure multiplicative factor of the degeneracy. The reason is that Coulomb interaction induces a correlation between the levels. When one level is occupied, the other is not allowed to be occupied due to the strong on-site Coulomb repulsion.

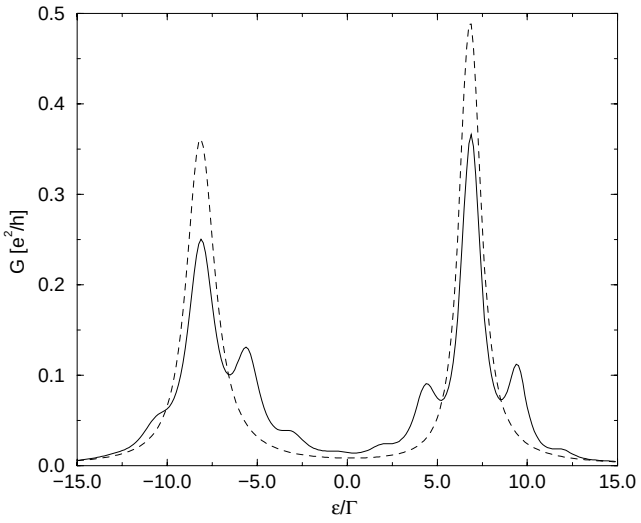


Figure 2.6: The differential conductance as a function of $\epsilon$ for a two-fold degenerate level with infinite Coulomb repulsion $U$, $T = 0.25$, , $\mu_L = -\mu_R = 15$, , and , $^{L} =$ , $^{R} =$ , /2. The dashed line describes the case without heat bath whereas the solid line corresponds to a one-mode bosonic environment with $g = 0.3$, $\Omega = 5$, , and $T_B = \Omega$.

Selection rules occur due to the matrix element $| < s|a_{lD}^{\dagger}|s' > |^2$ in (2.140) [141, 142, 66, 113, 54]. As already mentioned in section 2.3, spin conservation allows only transitions where the total spin $S$ of the states $s$ and $s'$ differs by $\pm 1/2$. In 1d quantum dots, the Lieb-Mattis theorem [91] guarantees that the spins of the ground states are always 0 or 1/2 (depending on the parity). Thus there is no spin selection rule for the transitions (2.143) involving only the ground states. For 2d quantum dots this is no longer the case since the ground states can have spin values larger than 1/2 [142, 54]. Other selection rules arising from the spatial part of the matrix element have been discussed in Ref. [113] for parabolic quantum dots. Although the Coulomb interaction can lead to a very dense excitation spectrum in comparism with the single-particle level spacing, it was shown that most tunneling matrix elements involving excitations of internal degrees of freedom of the dot are suppressed. The most dominant ones are replicas of excitations involving the center of mass coordinates which reflect

approximately the single-particle level spacing. For the discussion of spin blockade effects in connection with the occurence of negative differential conductance we refer to Refs. [141, 142, 66, 54].

The evaluation of the current formulas (2.139) or (2.141) requires the solution of the master equation (2.103). For a finite but not too large number of relevant states this can be done by straightforward numerical analysis or even analytically for special cases. However, if the level spacing decreases, the number of relevant states can become so large that even a numerical analysis is difficult, especially for the determination of the nonequilibrium probability distribution. Let us discuss this problem within the Coulomb blockade model. Here, we need the canonical and nonequilibrium one-particle distribution function $F_{Nl} = F^+_{Nl}$ for given particle number $N$ together with the probability $P_N$ to find $N$ particles in the dot. In principle this can be studied by relating the n-particle distribution function $F_{N,l_1,\ldots,l_n}$ via the master equation (2.103) to the $n+1$-particle distribution function, and finding an appropriate truncation scheme, e.g. in the form of factorization ansatzes or neglecting certain higher-order correlation parts [122, 36]. However, for very small level spacing $\delta E$ and level broadening , such that condition (2.63) is fulfilled, we justified in section 2.3.2 the usage of a Fermi distribution function for $F_{Nl} = f(\epsilon_{lD} - \mu)$. To discuss this more quantitatively, we follow Ref. [3] and sum the master equation (2.103) either over all states $s$ with $N_s = N$ or over all states with $n_l(s) = 1$. Defining $F_l = \sum_N P_N F_{Nl}$, we find the two rate equations

$$0 = \frac{d}{dt}P_N = P_{N+1}\sum_{rl}\{,\, {}^r f^-_r(\Delta_{Nl})F^+_{N+1,l} - P_N\sum_{rl} f^+_r(\Delta_{Nl})F^-_{Nl} - \\ - (N \to N-1)\}\,, \qquad (2.147)$$

$$0 = \frac{d}{dt}F_l = \sum_{rN},\, {}^r[f^+_r(\Delta_{Nl})P_N F^-_{Nl} - f^-_r(\Delta_{Nl})P_{N+1}F^+_{N+1,l}] + W_l\,, \qquad (2.148)$$

where, in addition, we have introduced an energy relaxation term $W_l = (F_l - f(\epsilon_{lD} - \mu))/\tau_\epsilon$ to the second equation. From the first equation we can estimate the rate of

change of $P_N$ as

$$\begin{aligned}\frac{1}{\tau} &\sim , \int d\epsilon[f^-(\epsilon+\Delta_N-\mu)f^+(\epsilon-\mu)+f^+(\epsilon+\Delta_N-\mu)f^-(\epsilon-\mu)] \\ &\sim \alpha_0|\Delta_N-\mu| \sim \alpha_0 E_C \,, \end{aligned} \tag{2.149}$$

for $|\Delta_N-\mu| \sim E_C \gg T, eV, \delta E$, with $\Delta_N = (2N+1)E_C$. Compared with the rate of change of the distribution function $F_l$, which is given by $\max\{, , 1/\tau_\epsilon\}$, we see that the particle number will relax much faster provided that the condition $\alpha_0 E_C \gg \max\{, , 1/\tau_\epsilon\}$, or

$$ZE_C \gg \delta E \, \max\{1, \frac{1}{, \tau_\epsilon}\} \tag{2.150}$$

is fulfilled. Therefore, it was argued in Ref. [3] that the $N$-dependence of $F_{Nl}$ can be neglected. This gives the two equations

$$P_{N+1}\sum_{rl}, {}^r(1-f_r(\Delta_{Nl}))F_l = P_N \sum_{rl}, {}^r f_r(\Delta_{Nl})(1-F_l)\,, \tag{2.151}$$

$$F_l \sum_{rN}, {}^r(1-f_r(\Delta_{Nl}))P_{N+1} = (1-F_l)\sum_{rN}, {}^r f_r(\Delta_{Nl})P_N + W_l\,, \tag{2.152}$$

which can be analysed by a straightforward numerical analysis [3]. In equilibrium, the neglect of the $N$-dependence is equivalent to the neglect of differences between canonical and grandcanonical ensembles. This has been studied numerically in Ref. [9] with the result that $F^{eq}_{Nl}$ approaches a Fermi distribution function when the level spacing is much smaller than temperature and charging energy. In this case, the linear current is identical to the one for metallic islands which will be discussed in the next section. However, in nonequilibrium at finite bias voltages, only an additional energy relaxation rate on the island drives $F_{Nl}$ into a Fermi distribution even if the $N$-dependence can be neglected. Without energy relaxation, i.e. for $\tau_\epsilon^{-1} \ll , ,$ the solution of (2.152) differs considerably from a Fermi function. E.g., when only two charge states $N = 0, 1$ are possible, i.e. $f_r(\Delta_{Nl}) = 0$ $(= 1)$ for $N > 0$ $(N < 0)$, we find at the symmetry point

where $P_0 = P_1 = 1/2$

$$F_l = \sum_r \frac{,^r}{,} f_r(\epsilon_{lD} + \Delta_0)\,. \tag{2.153}$$

For $T = 0$ and two reservoirs with $, ^L = , ^R$, this is a two-step function with $F_l = 1/2$ for all $\mu_L > \epsilon_{lD} + \Delta_0 > \mu_R$.

In summary, we find that for $\alpha_0 E_C \gg \tau_\epsilon^{-1} \gg , ,$ which is the condition (2.63) set up in section 2.3.2, we can take a Fermi distribution for the electrons on the island and can neglect the energy relaxation rate $\tau_\epsilon^{-1}$ for the determination of the charge distribution. For $, \ll \tau_\epsilon^{-1}, T$, we still can use the golden rule equation (2.152) for the determination of $F_l$, but we have to solve this equation with a charge distribution $P_N$ either determined from the golden rule equation (2.151) (for $\alpha_0 \ll 1$) or, in the strong tunneling regime ($\alpha_0 \sim 1$), from a more general kinetic equation including higher order processes as it will be discussed in chapter 3 and 4. This would result in solving a complicated self-consistent problem. Therefore, it is usually assumed that the condition (2.63) is fulfilled which is confirmed experimentally in typical metallic devices.

Next, we will discuss the influence of external fields. Via absorption and emission of photons or bosonic modes, they lead to a shift of the excitation energies of the dot $E_s - E_{s'} \to E_s - E_{s'} - \omega$ and give rise to a finite occupation probability for excited states even in linear response. A heat bath with a continuous spectrum would just smear out the conductance line shapes. Interesting effects occur if the heat bath consists of a single mode or if we treat the case of periodic time-dependent fields with a single frequency. In this case, we can write the probability function as

$$P_r^{\pm}(\omega) = \sum_m p_m^r \delta(\omega \pm m\Omega)\,, \tag{2.154}$$

where $p_m^r$ is the probability for the emission of $m$ energy quanta $\Omega$. For time-dependent

voltages we obtain from (2.95)

$$p_m^r = J_m(\frac{\bar{\Delta}_r}{\Omega})^2 \,, \tag{2.155}$$

which is symmetric under sign change of $m$. A single-mode bosonic environment (Einstein model [96]) can be realized by optical phonons [145, 44, 67] or by fluctuations of an external $LC$-circuit [22, 110, 34, 63] with frequency $\Omega = (LC)^{-1/2}$. Defining

$$g = \sum_q \frac{g_q^2}{\Omega^2} \,, \tag{2.156}$$

we obtain from (2.32) that $J(\omega) = \pi g \Omega^2 \delta(\omega - \Omega)$, and we can calculate $P^{\pm}$ from (2.98)-(2.100) with the result

$$p_m = e^{-g(1+2n(\Omega))} e^{\frac{1}{2}m\beta_B\Omega} I_m(2gn(\Omega)e^{\frac{1}{2}\beta_B\Omega}) \,, \tag{2.157}$$

where $n(\Omega)$ is the Bose function and $I_m$ the modified Bessel function.

We assume that the generalized detailed balance condition (2.116) is fulfilled so that we can apply the current formulas (2.130) or (2.131). Furthermore, we use the form (2.136) for the tunneling matrix elements. As a consequence, we find

$$A_{ss'}^r(\omega) = ,_{ss',s's}^{r}(\omega - \mu_r) \approx ,^r \sum_l | < s|a_{lD}^\dagger|s' > |^2 \,, \tag{2.158}$$

and the condition (2.127) is fulfilled. Thus, for a symmetrically coupled environment, we can also use the current formula (2.128)

We start with the discussion of symmetric coupling of the environment, i.e. the probability function $P_r^{\pm}(\omega) = P^{\pm}(\omega)$ is assumed to be independent of the reservoir index. From (2.128), we get for the current

$$\begin{aligned} I_r \;=\; e \sum_{r'} \sum_{ss'} \frac{,^{r},^{r'}}{,} \sum_l | < s|a_{lD}^\dagger|s' > |^2 \int d\omega [P^-(\omega)P_s + P^+(\omega)P_{s'}] \times \\ \times [f_r(E_s - E_{s'} - \omega) - f_{r'}(E_s - E_{s'} - \omega)] \,. \end{aligned} \tag{2.159}$$

Three interesting effects are worth to be mentioned. First, the shift of the excitation energies implies satellite peaks in the Coulomb oscillations and satellite steps in the

Coulomb staircase. The Coulomb oscillations in the presence of time-dependent fields are shown in Fig. 2.4 (solid curve). Second, in the case of a bosonic heat bath, the satellite peaks of the differential conductance are asymmetric since the probability for absorption and emission are not the same. This is shown in Fig. 2.6. We note that the asymmetry of a single peak in Fig. 2.4 is of different origin since it stems from the presence of the other resonances. Third, and most importantly, the linear conductance now reveals *all* excitations, i.e. also those which are hidden in the case without environment. The reason is that the initial state $s'$ in (2.159) has finite probability even if it is an excited state. This is shown in Fig. 2.4. The effect allows a complete spectroscopy of the dot in linear response and has been confirmed experimentally [111].

If the environment couples asymmetrically to the system but with equal probability for absorption and emission, $P_r^+ = P_r^- = P_r$, we use (2.130) for the current. Together with the normalization (2.101), the expression (2.133) and the property (2.158), we obtain after some elementary manipulations

$$\begin{aligned} I_r &= e\sum_{r'}\sum_{ss'}\frac{{}'_{,}\,{}^{r}_{,}\,{}^{r'}}{}\sum_{l}|<s|a_{lD}^{\dagger}|s'>|^2(P_s+P_{s'})\times \\ &\quad\times\int d\omega[P_r(\omega)f_r(E_s-E_{s'}-\omega)-P_{r'}(\omega)f_{r'}(E_s-E_{s'}-\omega)]\,. \end{aligned} \tag{2.160}$$

An interesting consequence of this result is the possibility to observe a nonvanishing DC-current in the absence of a DC-voltage, i.e. the device can act like an electron pump. For $\mu_r = \mu_{r'} = \mu$ and using again the normalization (2.101), we can write the "pump"-current in the form

$$\begin{aligned} I_r &= e\sum_{r'}\sum_{ss'}\frac{{}'_{,}\,{}^{r}_{,}\,{}^{r'}}{}(P_s+P_{s'})\int d\omega[P_r(\omega)-P_{r'}(\omega)]\times \\ &\quad\times[f^+(E_s-E_{s'}-\omega-\mu)-f^-(E_s-E_{s'}-\omega-\mu)]\,. \end{aligned} \tag{2.161}$$

For an asymmetric coupling, this implies that the current will change sign at the symmetry point where $E_s - E_{s'} = \mu$. The effect can easily be understood since the

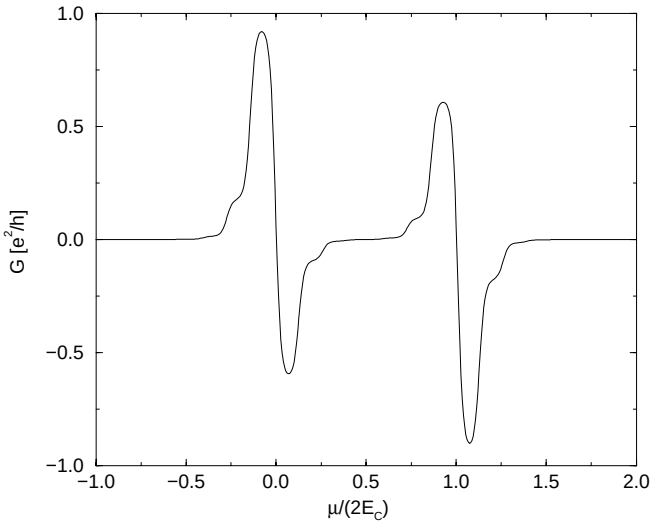


Figure 2.7: Linear conductance versus $\mu$ for a single two-fold degenerate level with $\epsilon + E_C = 0$ in the presence of asymmetric AC-voltages with $\Omega = 20$, , $\bar{\Delta}_L = 30$, , and $\bar{\Delta}_R = 0$. The other parameters are $T = 2$, $E_C = 75$, , and , $^L$ = , $^R$ = , /2. The structure acts as an electron pump.

electrons tunnel from one reservoir to the other via photon assisted tunneling. If the coupling is asymmetric this gives rise to a net current since absorption of energy is favoured in one of the reservoirs. If the excitation $E_s - E_{s'}$ lies above the Fermi level, transport arises from reservoir electrons being shifted up to the excitation energy of the dot, whereas for an excitation lying below $\mu$ absorption processes create holes in the reservoir at $E_s - E_{s'}$ which are filled by electrons from the other reservoir. Therefore the sign of the current is different for the two cases. The Coulomb oscillations in the absence of a transport voltage are shown in Fig. 2.7 and have been observed experimentally [111]. We can easily determine the line shape of the "pump"-current in the linear regime $\bar{\Delta}_r \ll \Omega \ll T$. Using (2.154) together with (2.155), we find by linearizing (2.161)

$$I_r = e \sum_{r'} \sum_{ss'} \frac{, \, ^r, \, ^{r'}}{,} (P_s + P_{s'}) f_r''(E_s - E_{s'}) \frac{\bar{\Delta}_r^2 - \bar{\Delta}_{r'}^2}{4}, \tag{2.162}$$

i.e. the line shape follows the second derivative of the Fermi distribution function.

As already pointed out in section 2.4.1, an interesting question in connection with transport phenomena in mesoscopic devices is wether the current can be written in the generalized "Landauer-Büttiker" form (2.131). We found that this is formally possible when the generalized detailed balance condition (2.116) is fulfilled. However, the transmission coefficient depends on the Fermi functions of the reservoirs. To show this dependence explicitly, let us discuss a specific example, namely the infinite-U Anderson model with two states $\epsilon_\sigma$ which are split by a magnetic field. We denote by $|\sigma>$ the state with one electron in level $\sigma$ and by $|0>$ the empty dot. Furthermore, we define

$$\tilde{\gamma}_r^{\pm}(\omega) = \int d\omega' \gamma_r^{\pm}(\omega') P_r^{\pm}(\omega - \omega') \,, \tag{2.163}$$

$$\gamma_r^{\pm}(\omega) = \frac{1}{2\pi}, ^r(\omega) f_r^{\pm}(\omega) \,, \tag{2.164}$$

where $, ^r(\omega) = , ^r_{\sigma 0,0\sigma}(\omega - \mu_r)$ is assumed to be spin-independent. The golden rule tunneling "in" and " out" rates are given by

$$\Sigma^{r+}_{\sigma 0} = 2\pi \tilde{\gamma}_r^{+}(\epsilon_\sigma) \quad , \quad \Sigma^{r-}_{0\sigma} = 2\pi \tilde{\gamma}_r^{-}(\epsilon_\sigma) \,. \tag{2.165}$$

Solving the master equation we find from the generalized detailed balance condition (2.116) and from the normalization $P_0 + P_\uparrow + P_\downarrow = 1$

$$P_0 = \frac{\tilde{\gamma}^-(\epsilon_\sigma)\tilde{\gamma}^-(\epsilon_{\bar{\sigma}})}{R} \quad , \quad P_\sigma = \frac{\tilde{\gamma}^+(\epsilon_\sigma)\tilde{\gamma}^-(\epsilon_{\bar{\sigma}})}{R} \,, \tag{2.166}$$

where $\bar{\sigma} = -\sigma$, $\tilde{\gamma}^{\pm}(\omega) = \sum_r \tilde{\gamma}_r^{\pm}(\omega)$, and

$$R = \left[\tilde{\gamma}^-(\epsilon_\sigma)\tilde{\gamma}^-(\epsilon_{\bar{\sigma}}) + \tilde{\gamma}^+(\epsilon_\sigma)\tilde{\gamma}^-(\epsilon_{\bar{\sigma}}) + \tilde{\gamma}^-(\epsilon_\sigma)\tilde{\gamma}^+(\epsilon_{\bar{\sigma}})\right]^{-1} . \tag{2.167}$$

Inserting the solution for the probabilities in (2.132), we find for the transmission coefficient

$$T_{rr'}(\omega, \omega') = \frac{1}{R} \sum_\sigma \tilde{\gamma}^-(\epsilon_{\bar{\sigma}}) P_r^-(\epsilon_\sigma - \omega) P_{r'}^+(\epsilon_\sigma - \omega') \,. \tag{2.168}$$

We see that the Fermi functions enter this expression via the factor $\tilde{\gamma}^-(\epsilon_{\bar{\sigma}})/R$. It basically describes a correlation between the two levels and leads to a suppression of the conductance resonance at $\epsilon_\sigma$ when the level $\epsilon_{\bar{\sigma}}$ is below the Fermi level of the reservoirs. In the absence of the environment this means that the linear conductance does not show all excitations as already described above. It is important to notice that not only the Coulomb interaction is responsible for the failure of a one-particle description. If we assume that the Zeeman splitting is so large that we can disregard one of the levels, i.e. $\tilde{\gamma}^+(\epsilon_{\bar{\sigma}}) = 0$, we find

$$\begin{aligned} \frac{\tilde{\gamma}^-(\epsilon_{\bar{\sigma}})}{R} &= \frac{1}{\tilde{\gamma}^+(\epsilon_\sigma) + \tilde{\gamma}^-(\epsilon_\sigma)} \\ &= \frac{1}{\frac{1}{2\pi}\sum_r \int d\omega,^r(\omega)[f_r^+(\epsilon_\sigma - \omega)P_r^+(\omega) + f_r^-(\epsilon_\sigma - \omega)P_r^-(\omega)]}, \end{aligned} \tag{2.169}$$

and, obviously, even here the dependence on the Fermi functions remains since absorption and emission probabilities are generally not the same. This applies especially to the line shape at resonance. Only in the special case when the level $\epsilon_\sigma$ lies very far below the Fermi levels of the reservoirs, i.e. for $f_r^+(\epsilon_\sigma - \omega) \approx 1$, and for $,^r(\omega) \approx ,^r$, we find from the normalization (2.101) that $\tilde{\gamma}^-(\epsilon_{\bar{\sigma}})/R \approx , /(2\pi)$. This is the regime which has been studied in Refs. [145, 44, 67, 63]. There, a second order perturbation theory in , was used since the current from golden rule is exponentially suppressed in the Coulomb blockade regime.

### 2.4.3 Metallic islands

From (2.66) we obtain $H^{r-}_{T,N-1,N} = \sum_{kl} T^r_{kl} a^\dagger_{kr} a_{lD}$. The rates follow from (2.102). Using the definitions (2.47) and (2.88) for the spectral functions, we find

$$\Sigma^{r+}_{N+1,N} = 2\int d\omega D_r(\Delta_N - \mu_r - \omega) n_r^+(\Delta_N - \omega) P_r^+(\omega), \tag{2.170}$$

$$\Sigma^{r-}_{N,N+1} = 2\int d\omega D_r(\Delta_N - \mu_r - \omega) n_r^-(\Delta_N - \omega) P_r^-(\omega), \tag{2.171}$$

where $n_r^+(\omega) = n(\omega - \mu_r)$, $n_r^- = 1 + n_r^+$, and $n(\omega)$ is the Bose distribution. $\Delta_N = E_{N+1} - E_N$, $E_N = E_C N^2$, describes a charge excitation energy of the island. Since only the difference $\Delta_N - \mu_r$, with $\mu_r = eV_r - eV_D$ and $eV_D = -2E_C n_x$, occurs in all expression, we include the potential $eV_D$ of the dot from now on in $\Delta_N$. Equivalently, this means that we choose

$$E_N = E_C(N - n_x)^2\,, \tag{2.172}$$

and set the equilibrium electrochemical potential $\mu = 0$. Furthermore, we treat from now on always the case of two reservoirs $r = L, R$ with $\mu_L = -\mu_R = eV/2$.

The form of the spectral function $D_r$, given by (2.88), depends on the spectral function (2.47) of the tunneling matrix elements. The influence of a discrete spectral function has been analysed in Ref. [4]. Here we assume a continuous spectrum on the island and use the form $D_r(\omega) = \pi\alpha_0^r\omega$ which was introduced in Eq. (2.89). As a consequence, we find for the frequency dependent rates defined by (2.121) and (2.122)

$$\Sigma^{r+}_{N+1,N}(\omega) = 2\pi\alpha_r^+(\omega) \quad , \quad \Sigma^{r-}_{N,N+1}(\omega) = 2\pi\alpha_r^-(\omega)\,, \tag{2.173}$$

where we define

$$\alpha_r^\pm(\omega) = \alpha_0^r(\omega - \mu_r)n_r^\pm(\omega)\,. \tag{2.174}$$

Up to a factor $2\pi$, these are the rates in the absence of the environment if we set $\omega = \Delta_N$. Furthermore, we will use frequently the definitions $\alpha_r = \alpha_r^+ + \alpha_r^-$, $\alpha^\pm = \sum_r \alpha_r^\pm$, and $\alpha = \sum_r \alpha_r$. The rates in the presence of an environment follow from convolution with the probability distribution. Therefore we define

$$\tilde{\alpha}_r^\pm(\omega) = \int d\omega' P_r^\pm(\omega - \omega')\alpha_r^\pm(\omega')\,, \tag{2.175}$$

and the rates are given by

$$\Sigma^{r+}_{N+1,N} = 2\pi\tilde{\alpha}_r^+(\Delta_N) \quad , \quad \Sigma^{r-}_{N,N+1} = 2\pi\tilde{\alpha}_r^-(\Delta_N)\,. \tag{2.176}$$

The low-temperature form of the rates follows from

$$\alpha_r^{\pm}(\omega) \approx \alpha_0^r |\omega - \mu_r| \, \theta(\pm(\mu_r - \omega)) \quad , \quad \text{for} \quad |\omega - \mu_r| \ll T \, . \tag{2.177}$$

Since the condition of generalized detailed balance (2.116) is fulfilled for the metallic case, we can use the current formulas (2.113) and (2.129)-(2.132) as outlined in section 2.4.1.

First we treat the case when the environment is absent $P_r^{\pm}(\omega) = \delta(\omega)$. The nonlinear current in the left junction follows from (2.113)

$$I = 2\pi e \sum_N \frac{\alpha_L(\Delta_N)\alpha_R(\Delta_N)}{\alpha(\Delta_N)} (P_{N+1} + P_N)[f_L(\Delta_N) - f_R(\Delta_N)] \, , \tag{2.178}$$

and shows directly that, at low temperatures, only the excitations

$$\mu_L = \frac{eV}{2} > \Delta_{N\max} > \ldots > \Delta_{N_0} > -\frac{eV}{2} = \mu_R \tag{2.179}$$

will contribute to transport. The probabilities follow from the generalized detailed balance condition (2.116) which gives the recursion relation

$$P_{N+1} = \frac{\alpha^+(\Delta_N)}{\alpha^-(\Delta_N)} P_N \, . \tag{2.180}$$

In the nonlinear response regime, i.e. for $eV \gg T$, only the charge states $N_0, \ldots, N_{\max} + 1$ are occupied, and (2.180) reads

$$P_{N+1} = \frac{\alpha_0^L}{\alpha_0^R} \frac{eV/2 - \Delta_N}{eV/2 + \Delta_N} P_N \quad , \quad \text{for} \quad N_0 < N < N_{\max} \, . \tag{2.181}$$

In this regime, we find from (2.177) and (2.178) for the current

$$I = G_{as}/e \sum_{N=N_0}^{N\max} (P_{N+1} + P_N) \frac{(eV/2)^2 - \Delta_N^2}{eV/2 + \frac{\alpha_0^R - \alpha_0^L}{\alpha_0^R + \alpha_0^L} \Delta_N} \, , \tag{2.182}$$

where

$$G_{as} = 4\pi^2 \frac{\alpha_0^R \alpha_0^L}{\alpha_0^R + \alpha_0^L} \frac{e^2}{h} \tag{2.183}$$

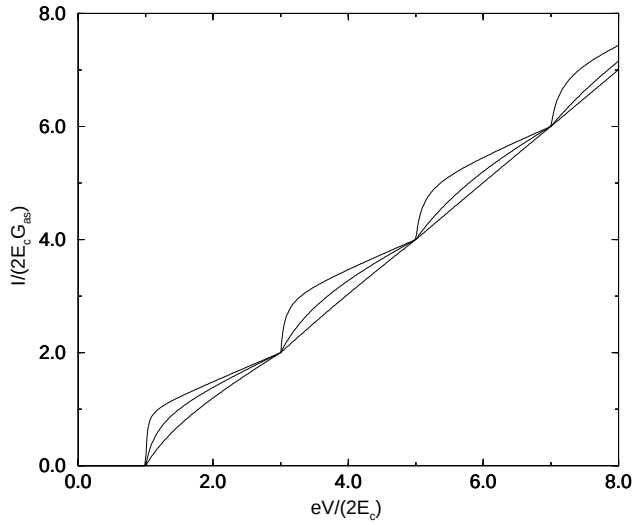


Figure 2.8: The I-V characteristic for the metallic SET-transistor at zero temperature for (from top to bottom) $\alpha_0^L = 100\alpha_0^R, 10\alpha_0^R, \alpha_0^R$ and $\Delta_0 = E_C$.

is the asymptotic differential conductance for $eV \gg E_C$ which agrees with the classical ohmic value $G_{as} = 1/R_T^R + 1/R_T^L$, where $1/R_T^r = 4\pi^2\alpha_0^r e^2/h$.

The line shape of the I-V-characteristic for fixed gate voltage is shown in Fig. 2.8. We note that the positions of the excitations $\Delta_N = 2E_C(N - n_x) + E_C$ are not changed by varying $V$ for symmetric capacitances $C_L = C_R$ and $V_L = -V_R = V/2$. This is due to the form (2.5) of the polarization charge $q_x = -en_x$ which gives the $V$-independent result $-en_x = C_g V_g$. For voltages so small that no excitation falls into the window of the bias voltage, the current is zero. This is the Coulomb blockade regime. For sufficiently high voltage the current starts abruptly and changes its slope discontinuously each time a new charge state can be occupied. However, for $\alpha_0^L = \alpha_0^R$, there is no significant "step" structure as in the quantum dot case with discrete levels. After the current has started, the I-V-characteristic is almost linear and approaches the ohmic form $I = G_{as}V$ for $V \gg E_C$. The reason is that the spectrum of the dot is continuous. This means that the number of single-particle states on the island which can be used

for tunneling increases linearly by increasing $V$. Thus the current will also increase almost linearly with $V$ although the number of possible charge states is constant. The step-like features can be increased by using asymmetric tunnel resistances as shown in Fig. 2.8.

The differential conductance $G = dI/dV$ for values of the bias voltage where only two charge states $N = 0, 1$ are possible follows from (2.182) as

$$G = 2G_{as}\frac{(eV/2)^2 + \Delta_0^2}{(eV)^2}\,\theta(\frac{eV}{2} - |\Delta_0|)\,, \tag{2.184}$$

where we have chosen symmetric barriers with $\alpha_0^R = \alpha_0^L$. The line shape of $G$ as function of $\Delta_0$, or equivalently the gate voltage since $\Delta_0 = \text{const} + eC_gV_g/C$, is shown in Fig. 2.9 for fixed bias voltage. As expected, the conductance falls abruptly to zero when the excitation energy $\Delta_0$ falls out of the window defined by the bias voltage. The differential conductance, i.e. the *change* of the conductance, is maximal when $\Delta_0$ leaves the window. However, in contrast to the quantum dot case, it is nonzero between the maximal values and approaches

$$G(\Delta_0 = 0) = G_{as}/2 \quad , \quad \text{for} \quad T, eV \ll E_C \tag{2.185}$$

at the symmetry point $\Delta_0 = 0$. Again the reason is the continuous spectrum of the single-particle states on the island. For finite temperature the peaks are washed out but the value at the symmetry point remains which can be seen directly from the analytic formula (2.178) when we consider only two charge states. As we will see in section 4.4, this value can only decrease by quantum fluctuations due to higher order tunneling processes.

In linear response, i.e. for $eV \ll T$, we find directly by linearizing (2.178)

$$G = \frac{G_{as}}{2}\sum_N (P_{N+1}^{eq} + P_N^{eq})\frac{\beta\Delta_N}{\sinh(\beta\Delta_N)}\,, \tag{2.186}$$

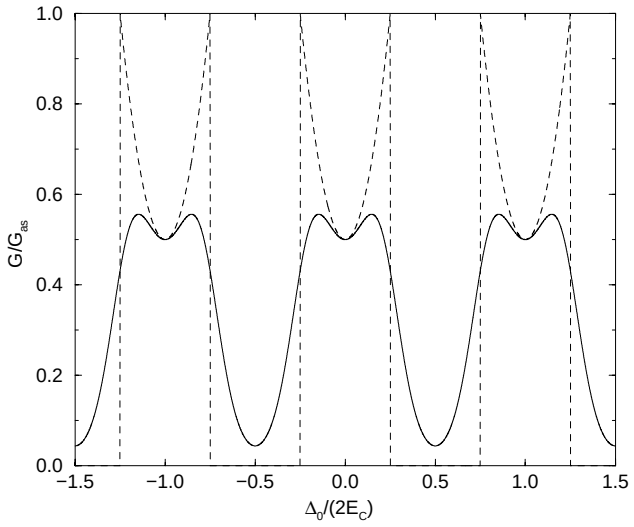


Figure 2.9: Differential conductance as function of the gate voltage for $\alpha_0^L = \alpha_0^R$, $eV = E_C$, $T = 0$ (dashed curve) and $T = 0.1\,E_C$ (solid curve).

with $P_N^{eq} = \exp(-\beta E_N)/Z$ being the equilibrium probability distribution of the charge states. For $T \gg E_C$ the conductance again approaches the ohmic value $G_{as}$. For $T \ll E_C$, the Coulomb blockade sets on and a series of periodic peaks with distance $2E_C$ is observed as shown in Fig. 2.10. This are the so-called Coulomb oscillations which deserve their name here really since the blockade of the current between the peaks is only due to the Coulomb interaction, whereas in the quantum dot case the distance between peaks is as well influenced by the discreteness of the single-particle levels. The line shape of an individual peak for $T \ll E_C$ where only two charge states $N = 0, 1$ are important, is given by

$$G = \frac{G_{as}}{2} \frac{\beta\Delta_0}{\sinh(\beta\Delta_0)}\,. \tag{2.187}$$

The broadening scales linearly with temperature but the height at resonance is again given by the temperature independent value $G_{as}/2$ in accordance with the general result (2.185). The temperature dependence of the maximal conductance is very different from the quantum dot case (2.146) where the peak height scales with inverse temper-

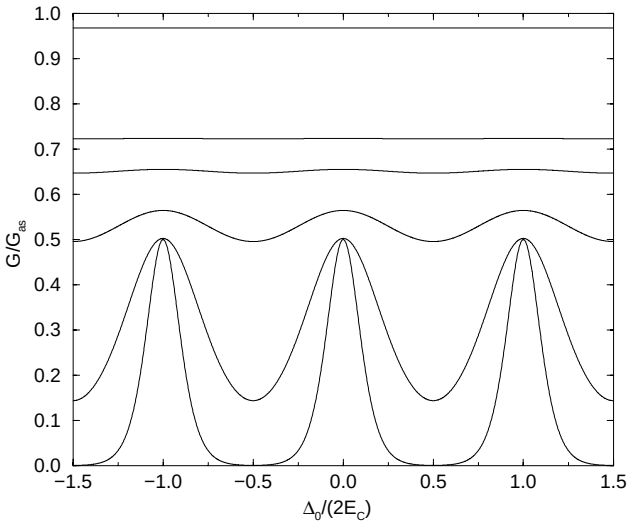


Figure 2.10: The linear conductance of the metallic SET-transistor for $\alpha_0^L = \alpha_0^R$ and (from bottom to top) $T = 0.1, 0.25, 0.5, 0.75, 1, 10\, E_C$.

ature. This is again due to the dense level spectrum on the island. By decreasing temperature the number of available states is decreased but at the same time transport through the available states is enhanced since the Fermi function in the reservoir sharpens. Both effects cancel each other so that the maximal conductance is temperature independent. In contrast, in the quantum dot case, there is no decrease of the number of available states and, therefore, the conductance increases with decreasing temperature.

Finally we turn to the investigation of the influence of the environment. For the current we use Eq. (2.129) and insert the rates from (2.176). This gives the general expression

$$I = 2\pi e \sum_N \frac{P_{N+1} + P_N}{\tilde{\alpha}(\Delta_N)} [\tilde{\alpha}_L^+(\Delta_N)\tilde{\alpha}_R^-(\Delta_N) - \tilde{\alpha}_L^-(\Delta_N)\tilde{\alpha}_R^+(\Delta_N)] \,. \tag{2.188}$$

The probability distribution follows from generalized detailed balance analog to (2.180)

$$P_{N+1} = \frac{\tilde{\alpha}^+(\Delta_N)}{\tilde{\alpha}^-(\Delta_N)} P_N \,. \tag{2.189}$$

In the absence of time-dependent fields and for a bosonic environment which has the same temperature as the system $\beta_B = \beta$, we can use detailed balance (2.106), and the current can be written as

$$I = 2\pi e \sum_N (P_{N+1} + P_N) \frac{\tilde{\alpha}_L^+(\Delta_N)\tilde{\alpha}_R^-(\Delta_N)}{\tilde{\alpha}(\Delta_N)} (1 - e^{-\beta eV}) \,, \tag{2.190}$$

where $\mu_L - \mu_R = eV > 0$. We can see that only those terms contribute where the tunneling "in" rate at the left junction and the tunneling "out" rate at the right junction are both nonzero. However, all effects are now washed out by the bosonic environment at least in the presence of a continuous spectrum of external modes. For a detailed discussion of various bosonic environments in metallic systems we refer to Ref. [64].

Here we will discuss in more detail the influence of time-dependent fields with frequency $\Omega$ which are of recent experimental interest [84, 57]. The probabilities for absorption and emission are here the same $P_r^{\pm} = P_r$, and the explicit expressions are given by (2.154) and (2.155). Inserting the definitions (2.175) and (2.174) for the rates in Eq. (2.188), and using the normalization (2.101), we find after some elementary manipulations

$$I = 2\pi e \sum_N \frac{P_{N+1} + P_N}{\tilde{\alpha}(\Delta_N)} [\alpha_0^R(\Delta_N - \mu_R)\tilde{\alpha}_L^+(\Delta_N) - \alpha_0^L(\Delta_N - \mu_L)\tilde{\alpha}_R^+(\Delta_N)] \,. \tag{2.191}$$

For symmetrically coupled fields, we have $P_r = P$, and a straighforward linearization for $eV \ll T \ll \Omega$ leads to the conductance

$$G = \frac{G_{as}}{2} \sum_N (P_{N+1} + P_N) \frac{\sum_m \theta(m\Omega - |\Delta_N|) m p_m}{\sum_m \theta(m\Omega - |\Delta_N|) m p_m + |\frac{\Delta_N}{\Omega}| \sum_m \theta(|\Delta_N| - m\Omega) p_m} \,. \tag{2.192}$$

The conductance resonances reveal jumps when $\Delta_N$ differs from its resonant value by an integer value of the external frequency. This is shown in Fig. 2.11 and again differs from the behaviour of the quantum dot case where satellite peaks are observed. In

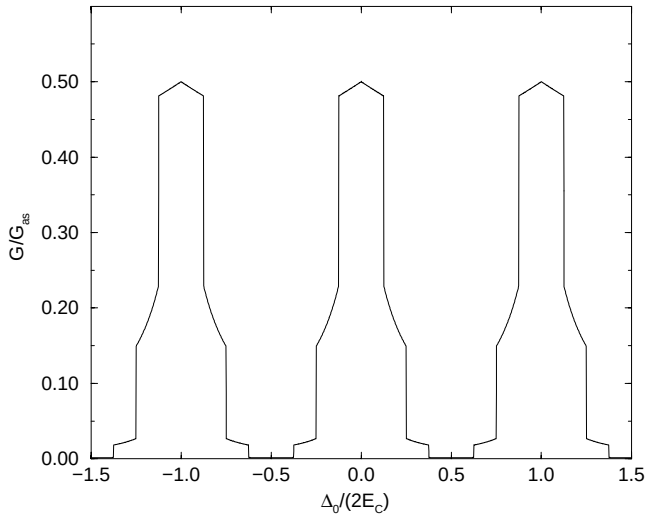


Figure 2.11: The linear conductance of the SET-transistor at $T = 0$ in the presence of time-dependent fields for $\alpha_0^L = \alpha_0^R$, $\Omega = 0.25E_C$ and $\bar{\Delta}_L/\Omega = \bar{\Delta}_R/\Omega = 2$.

the same way one can show from (2.191) that the I-V-characteristic shows side kinks instead of steps. Both effects have been studied theoretically and experimentally in Ref. [84].

As in the quantum dot case we can also find a "pump"-current for $P_L \neq P_R$ and $\mu_L = \mu_R$. Again, by using (2.191), we find for $\bar{\Delta}_r \ll \Omega \ll T$

$$I = G_{as}/e \sum_N (P_{N+1}^{eq} + P_N^{eq}) \left[ \frac{1}{\sinh(\beta\Delta_N)} - \frac{\beta\Delta_N}{4\sinh^2(\beta\Delta_N/2)} \right] \frac{\bar{\Delta}_L^2 - \bar{\Delta}_R^2}{4T}\,, \qquad (2.193)$$

which shows that the qualitative behaviour but not the detailed line shape is identical to the analog formula (2.162) for the quantum dot case. The pump current has been observed in Ref. [84].

# Chapter 3

# Real-time transport theory

## 3.1 General concept

In this section we will explain the general structure of the theory without going into details of technical derivations. The full microscopic approach together with explicit expressions for various quantities introduced here will be presented in the next section 3.2.

The following considerations refer to the quantum dot case but hold as well for metallic islands by the replacement of dot states by charge states (formally $D \to C$, $s \to N$).

### 3.1.1 Kinetic equation

The total Hamiltonian of our system consists of an environment, including particle reservoirs $H_R$ and a heat bath $H_B$, a dot part $H_D$, and a tunneling part $H_T(t)$. The latter describes the coupling between environment and dot and will drive the dot system out of equilibrium. Therefore, we formulate the nonequilibrium problem in the following way. For $t \leq t_0$, we assume $H_T(t)$ to vanish, and the environment to be in equilibrium. This means that the total density matrix can be written in factorized form

$$\rho(t) = \rho_R^{eq} \rho_B^{eq} \hat{P}(t) \qquad \text{for } t \leq t_0\,, \tag{3.1}$$

where

$$\rho_R^{eq} = \frac{e^{-\beta H_R}}{Z_R} \quad , \quad \rho_B^{eq} = \frac{e^{-\beta_B H_B}}{Z_B} \, , \tag{3.2}$$

and $\hat{P}(t)$ is the reduced density matrix of the dot

$$\hat{P}(t) = Tr_{RB}\rho(t) \, , \tag{3.3}$$

with $Tr_{RB} = Tr_R Tr_B$ being the trace over the reservoir and heat bath degrees of freedom.

The matrix elements of $\hat{P}$ with respect to the eigenstates $|s>$ of $H_D$ are denoted by

$$P_{ss'}(t) =< s|\hat{P}(t)|s' >= Tr\rho(t)\hat{P}_{s's} \, , \tag{3.4}$$

and the probability to be in a certain state $|s>$ is given by $P_s(t) = P_{ss}(t)$. $\hat{P}_{s's} = |s' >< s|$ is the projector already used in section 2.3.1. We neither assume here any initial probability distribution $\hat{P}(t_0)$ nor that $\hat{P}$ is diagonal in the states $|s>$, i.e. in principle we can study an arbitrary preparation of the dot at the initial time.

At time $t_0$ we switch on the tunneling between dot and reservoirs. For $t_0 \to -\infty$ this is performed adiabatically. Our first aim is to study the time evolution of $P_{ss'}(t)$. This will be performed in section 3.2 by integrating out the reservoirs and the heat bath with the result of an effective theory in terms of the dot degrees of freedom. The Liouville equation governing the time evolution of the reduced density matrix $\hat{P}$ will turn out to be of the form

$$\frac{d}{dt}\hat{P}(t) + i[H_D, \hat{P}(t)] = \int_{t_0}^{t} dt' \hat{\Sigma}(t,t')\hat{P}(t') \, , \tag{3.5}$$

where $[.,.]$ denotes the commutator and the integral kernel $\hat{\Sigma}$ denotes a Liouville superoperator, i.e. it is defined as a function within the space of all operators. Written in the basis of the eigenstates of $H_D$, we obtain explicitly

$$\frac{d}{dt}P_{ss'}(t) + i(E_s - E_{s'})P_{ss'}(t) = \sum_{s_1 s_1'} \int_{t_0}^{t} dt' \Sigma(t,t')_{ss',s_1 s_1'} P(t')_{s_1 s_1'} \, . \tag{3.6}$$

The second term on the l.h.s. of this equation is a flow term which describes the time evolution of the reduced density matrix in the absence of tunneling. It is not a dissipative source and, in the absence of tunneling, would lead to a coherent time evolution of the dot. Dissipation is described by the r.h.s. of Eq. (3.6). It forces the dot to approach a stationary state and is due to tunneling. We see that the full kinetic equation is of a non-Markovian form, i.e. the r.h.s. depends on the reduced density matrix at all times prior to $t$. An explicit expression for the kernel $\Sigma$ will be provided in section 3.2 in terms of a well-defined perturbation expansion in even powers of $H_T$

$$\hat{\Sigma}(t,t') = \sum_{n=1}^{\infty} \hat{\Sigma}^{(2n)}(t,t') \,. \tag{3.7}$$

Furthermore, we will set up systematic diagrammatic rules how one can calculate each order of $\Sigma$ without being forced to understand the microscopic details where these rules come from.

The kinetic equation (3.6) can be written in a more familiar and transparent form by eliminating the nondiagonal matrix elements of the probability distribution. Using the kinetic equation one can express them iteratively by the diagonal matrix elements leading to an equation of the form

$$\frac{d}{dt}P_s(t) = \sum_{s'} \int_{t_0}^{t} dt' \Sigma_{ss'}(t,t') P_{s'}(t') \,. \tag{3.8}$$

In section 3.2 we will derive an explicit and more constructive expression for the kernel entering this equation. Furthermore, we will prove the property

$$\sum_{s} \Sigma_{ss'}(t,t') = 0 \,, \tag{3.9}$$

which guarantees the conservation of probability $\sum_s \dot{P}_s(t) = 0$. Using it we can rewrite the kinetic equation as

$$\frac{d}{dt}P_s(t) = \sum_{\substack{s' \\ s' \neq s}} \int_{t_0}^{t} dt' \left\{ \Sigma_{ss'}(t,t') P_{s'}(t') - \Sigma_{s's}(t,t') P_s(t') \right\} \,. \tag{3.10}$$

We have obtained the structure of a master equation with a gain and loss term on the r.h.s.. The kernel $\Sigma_{ss'}(t,t')$ can be interpreted as a generalized and formally exact transition rate from the state $s'$ at time $t'$ to the state $s$ at time $t$. In second order in $H_T$, which represents the first term $\Sigma^{(2)}$ of the series (3.7), we obtain the lowest order expression for the rate but for arbitrary time-dependent situations. In the asymptotic limit $t_0 \to -\infty$ it reduces to the golden rule rate when integrated over the time difference $t-t'$ (see section 3.1.3 and 4.1). In the context of Coulomb blockade phenomena, this term is called the transition rate of "sequential tunneling". It corresponds to the physical situation where all tunneling processes are incoherent. The next term $\Sigma^{(4)}$, which is of forth order in $H_T$, is called the cotunneling transition rate. It means that at least two tunneling processes are coherent allowing for coherent transport through the dot from one reservoir to the other. The higher order terms $\Sigma^{(2n)}$ with $n > 2$ contain processes where the electron tunnels coherently back and forth between the dot and the reservoirs and, as we will see in chapter 4, can lead to renormalization and broadening effects. Except for special systems which are exactly solvable (see section 4.2 for an example), it is not possible to calculate $\Sigma$ exactly. However, we will at least formulate a systematic and very general approximation in section 3.2.4 which will be applied to specific examples in chapter 4. We call the summation over all terms within this approximation the resonant tunneling transition rate.

For the special case of a diagonal density matrix $P_{ss'}(t) = \delta_{ss'}P_s(t)$, the kernel is given by $\Sigma_{ss'}(t,t') = \Sigma_{ss,s's'}(t,t')$. As we will see in chapter 4, there are special systems where particle or spin conservation implies the property that $\hat{P}(t)$ will be diagonal for all times $t$ if it is diagonal at the initial time $t_0$. To give a concrete example we note the following property of $P_{ss'}(t)$ which follows from particle number conservation

$$P_{ss'}(t) \sim \delta_{N_s,N_{s'}} , \tag{3.11}$$

which is fulfilled for all times if it is fulfilled initially. This follows directly from the definition (3.3) and the fact that the total particle number $N_{tot} = \sum_{r=L,R} N_r + N$ is a conserved quantity. Thus, for metallic systems, (3.11) implies that $P_{NN'}(t) = \delta_{NN'} P_N(t)$ if this property holds initially. A similiar proof can also be given for quantum dots with a single spin-degenerate state where spin conservation can be used (see section 4.3).

The derivation of closed kinetic equations for the reduced density matrix of small systems coupled to reservoir degrees of freedom is not new. Using the Zwanzig projection operator technique, one can easily set up an equation of the form (3.5) [32, 39]. However, the usage of rather formal projectors does not reveal an important property of the kernel $\Sigma$, namely its well-defined perturbation expansion (3.7) in the coupling to the reservoirs. We will define the kernel in section 3.2 by the property that the total density matrix is never diagonal during any coherent process contained in $\Sigma$. Furthermore, we will always take first the thermodynamic limit of the reservoirs before performing the long time limit. As shown in section 3.2 these criteria together with the adiabatic switching on of $H_T(t)$ lead to well-defined expressions. Furthermore, at least in the absence of accidental degeneracies in the dot, we will also show that the full kernel entering the diagonal equation (3.8) is well-defined.

Our form of the kernel is similiar to the way it is defined within the investigation of spin-bosons models [140, 51] although the detailed way of evaluation is quite different. An essential generalization presented here concerns the inclusion of a coupling to particle reservoirs, whereas within spin-boson models one consideres energy exchange with an external heat bath. To avoid confusion, we mention that within spin-boson models the kinetic equations are always set up in the diagonal form (3.8).

### 3.1.2 Tunneling current

Another quantity of interest is the tunneling current given by the average of the corresponding operator

$$I_r^{tun}(t) = Tr\rho(t)\hat{I}_r^{tun}(t)\,, \tag{3.12}$$

where we note once again that the time dependence of the tunneling current operator is an explicit one due to the time dependence of the tunneling matrix elements. Inserting the form (2.38), (2.67) or (2.84) for the operator and again integrating out the reservoir and heat bath degrees of freedom, we will show in section 3.2 that the tunneling current can be written as

$$\begin{aligned} I_r^{tun}(t) &= -e\int_{t_0}^{t} dt' Tr_D \hat{\Sigma}^r(t,t')\hat{P}(t') \\ &= -e\sum_{ss_1s_1'}\int_{t_0}^{t} dt' \Sigma^r_{ss,s_1s_1'}(t,t')P_{s_1s_1'}(t')\,, \end{aligned} \tag{3.13}$$

or in diagonal form as

$$I_r^{tun}(t) = -e\sum_{ss'}\int_{t_0}^{t} dt' \Sigma^r_{ss'}(t,t')P_{s'}(t')\,, \tag{3.14}$$

where, analog to the discussion in the previous section, $\Sigma^r_{ss'}(t,t') = \Sigma^r_{ss,s's'}(t,t')$ for diagonal density matrices, or, in the general nondiagonal case, the kernel aquires a more complicated structure as outlined in section 3.2.

The physical interpretation of (3.14) is very obvious. To obtain the tunneling current at time $t$, one has to multiply the current rate $\sum_s \Sigma^r_{ss'}(t,t')$, corresponding to the sum over all processes starting at $t'$ in state $s'$ and ending at time t in any state, with the appropriate initial probability $P_{s'}(t')$ and integrate over all initial times $t'$. The index $r$ indicates that during these processes the particle number in reservoir $r$ has changed. As a minor remark we note that, just for formal reasons, only the sum over $s$ of $\Sigma^r_{ss'}(t,t')$ is allowed to be interpreted as the current rate.

The current rate includes all possible processes, i.e. the change of the particle number in reservoir $r$ can take any value. Therefore it is natural to decompose the current rate in the form

$$\sum_s \Sigma^r_{ss'}(t,t') = -\sum_s \sum_{p=-\infty}^{\infty} p\Sigma^{rp}_{ss'}(t,t')\,, \tag{3.15}$$

where $\Sigma^{rp}_{ss'}(t,t')$ corresponds to that part of the total transition rate $\Sigma_{ss'}(t,t')$ where in sum $p$ particles are taken out of reservoir $r$. This allows a decomposition of the tunneling current into a tunneling "in" and a tunneling "out" contribution

$$I^{tun}_r(t) = e\sum_{p=1}^{\infty} p \sum_{ss'} \int_{t_0}^{t} dt' \left\{\Sigma^{r,p}_{ss'}(t,t')P_{s'}(t') - \Sigma^{r,\bar{}p}_{ss'}(t,t')P_{s'}(t')\right\}\,. \tag{3.16}$$

In section 3.2 we will derive explicit diagrammatic rules to evaluate the current rate as well. Like the kernel of the kinetic equation it can be represented as a perturbation expansion in even powers of $H_T$

$$\Sigma^r_{ss'}(t,t') = \sum_{n=1}^{\infty} \Sigma^{r,(2n)}_{ss'}(t,t')\,, \tag{3.17}$$

and analog for $\Sigma^{rp}_{ss'}(t,t')$. The second order term $\Sigma^{rp,(2)}_{ss'}$ correponds to the sequential tunneling current rate and gives only a contribution for $p = \pm 1$. Analog to the kernel $\Sigma$, we call the term in forth order the cotunneling current rate, and the nonperturbative summation of higher order terms within the approximation formulated in section 3.2.4 the resonant tunneling current rate.

The sequential tunneling and cotunneling currents are given by

$$I^{seq}_r(t) = -e\sum_{ss'} \int_{t_0}^{t} dt' \Sigma^{r,(2)}_{ss'}(t,t')P^{(0)}_{s'}(t')\,, \tag{3.18}$$

$$I^{cot}_r(t) = -e\sum_{ss'} \int_{t_0}^{t} dt' \left\{\Sigma^{r,(4)}_{ss'}(t,t')P^{(0)}_{s'}(t') + \Sigma^{r,(2)}_{ss'}(t,t')P^{(2)}_{s'}(t')\right\}\,, \tag{3.19}$$

where we have introduced the perturbation expansion of $P_s(t)$ in even powers of $H_T$ as well

$$P_s(t) = \sum_{n=0}^{\infty} P^{(2n)}_s(t)\,. \tag{3.20}$$

The lowest order term $P_s^{(0)}(t)$ follows just from the kinetic equation with sequential tunneling transition rates. We emphasize that the cotunneling current consists of two contributions. The second one has been considered in Ref. [80] and cannot be neglected since the probability distribution $P_s^{(2)}(t)$ can be finite even in regimes where the sequential tunneling contribution $P_s^{(0)}(t)$ is exponentially small. Furthermore, the second term is often necessary to cancel many contributions arising from the first term on the r.h.s of Eq. (3.19) [80].

### 3.1.3 Relaxation and the stationary state

Provided that we have found a reasonable approximation for the kernels $\Sigma_{ss'}(t,t')$ and $\Sigma^r_{ss'}(t,t')$, we describe in this section the best procedure to find the solution $P_s(t)$ from the kinetic equation (3.8) and the tunneling current $I_r^{tun}(t)$ from (3.14). The technique is based on Fourier-Laplace transformations [140, 51, 50].

We start with the determination of the stationary state. This means that we will set the initial time $t_0 = -\infty$. We assume that the time-dependence of the electrostatic potentials is periodic in time with period $T = 2\pi/\Omega$. This implies $\Sigma_{ss'}(t+T, t'+T) = \Sigma_{ss'}(t,t')$ and the periodicity of the stationary probability distribution and the tunneling current. Thus, we use the Fourier expansion

$$P_s^{st}(t) = \sum_{n=-\infty}^{\infty} P_s^n e^{in\Omega t}\,, \tag{3.21}$$

$$I_r^{st}(t) = \sum_{n=-\infty}^{\infty} I_r^n e^{in\Omega t}\,, \tag{3.22}$$

$$\Sigma_{ss'}(t,t') = \sum_{n=-\infty}^{\infty} \Sigma_{ss'}^n(t-t') e^{in\Omega t'}\,, \tag{3.23}$$

with the inverse given by $\Sigma^n_{ss'}(\tau) = 1/T \int_0^T dt e^{-in\Omega t}\Sigma_{ss'}(t+\tau,t)$. A corresponding representation is used for $\Sigma^r_{ss'}(t,t')$ and $\Sigma^{rp}_{ss'}(t,t')$. Inserting these expansions in the kinetic equation (3.8) and Eq. (3.14) for the tunneling current, and comparing Fourier

components, we find

$$in\Omega P_s^n = \sum_{s'}\sum_m \Sigma_{ss'}^{mn} P_{s'}^{n-m} = \sum_{\substack{s' \\ s'\neq s}}\sum_m (\Sigma_{ss'}^{mn} P_{s'}^{n-m} - \Sigma_{s's}^{mn} P_s^{n-m}), \tag{3.24}$$

$$I_r^n = -e\sum_{ss'}\sum_m \Sigma_{ss'}^{r,mn} P_{s'}^{n-m}, \tag{3.25}$$

where we have defined the Laplace transform

$$\Sigma_{ss'}^{mn} = \Sigma_{ss'}^{m}(z = -n\Omega + i\eta), \tag{3.26}$$

$$\Sigma_{ss'}^{m}(z) = \int_0^\infty d\tau \Sigma_{ss'}^{m}(\tau) e^{iz\tau}, \tag{3.27}$$

and an analog definition for the Laplace transform of $\Sigma_{ss'}^{r,mn}$.

If the period $T$ is much smaller than the characteristic memory time $\tau_\Sigma$ of the kernels, the $n = 0$ component of $\Sigma_{ss'}^{n}(t - t')$ will give the most dominant contribution to (3.8). The reason is that, for $n \neq 0$, the factor $e^{in\Omega t'}$ from (3.23) will oscillate very strongly for $t'$ varying on a range $\tau_\Sigma \gg \Omega^{-1}$. With the same argument one can also neglect the components of $\Sigma_{ss'}^{mn}(t, t')$ for $n \neq 0$. The AC-components of the probability distribution are then much smaller than the DC-components and we obtain

$$0 = \sum_{s'} \Sigma_{ss'} P_{s'} = \sum_{\substack{s' \\ s'\neq s}} (\Sigma_{ss'} P_{s'} - \Sigma_{s's} P_s), \tag{3.28}$$

$$I_r = -e\sum_{ss'} \Sigma_{ss'}^{r} P_{s'}, \tag{3.29}$$

$$\Sigma_{ss'} = \frac{1}{T}\int_0^T dt \int_0^\infty d\tau e^{-\eta\tau} \Sigma_{ss'}(t + \tau, t), \tag{3.30}$$

and an analog equation for $\Sigma_{ss'}^{r}$. By convention, we imply from now on always that we mean the DC-Fourier component $n = m = 0$ if no time argument and no Fourier index is written. For time-translational invariant systems, the kernels depend only on the relative time argument $t - t'$ and Eqs. (3.28)-(3.30) hold exactly.

The full time evolution of the probability distribution and the tunneling current, i.e. the relaxation into the stationary state, can also be studied for an arbitrary initial

state. Here we set $t_0 = 0$ and use again the Fourier expansion (3.23) and the Laplace transformation (3.27) for the rates. Furthermore, we define the Laplace transformation

$$P_s(z) = \int_0^\infty dt e^{izt} P(t)\,, \tag{3.31}$$

with $Im(z) > 0$. In the same way we define $I_r^{tun}(z)$. The master equation and the tunneling current in Fourier-Laplace space read

$$\begin{aligned} -izP_s(z) &= P_s(t=0) + \sum_{s'}\sum_m \Sigma_{ss'}^m(z) P_{s'}(z+m\Omega)\,, & (3.32)\\ I_r^{tun}(z) &= -e\sum_{ss'}\sum_m \Sigma_{ss'}^{r,m}(z) P_{s'}(z+m\Omega)\,. & (3.33) \end{aligned}$$

For given $z$ the master equation defines a linear set of equations for the quantities $P_s(z+m\Omega)$, $m = 0, \pm 1, \pm 2, \ldots$. When the time-dependent fields are absent, i.e. for a time translational invariant system, the master equation is local in Laplace space. The Fourier components describing the stationary state are given by

$$P_s^n = \lim_{\eta\to 0} \eta P(-n\Omega + i\eta)\,, \tag{3.34}$$

and the full time-dependent solution follows from reversing the Laplace transformation

$$P_s(t) = \frac{1}{2\pi}\int_{-\infty+i\eta}^{\infty+i\eta} dz\, e^{-izt} P_s(z)\,. \tag{3.35}$$

Analog relations hold for the tunneling current. The relaxation times can be found from the imaginary parts of the pols of the functions $P_s(z)$ and $I_r^{tun}(z)$ in the complex plane.

## 3.2 Microscopic theory

In this section we provide the microscopic derivation of the kinetic equation and the formulas for the tunneling current introduced in section 3.1. Thereby we will derive an explicit way how to calculate the various kernels entering these equations for a given

perturbation order in tunneling. This will be formulated in terms of diagrammatic rules which can be used as a given tool without knowing about the microscopic background. Furthermore we will formulate an approximation for the kernels which is characterized by a nonperturbative resummation of a certain series of terms in all orders of tunneling.

Again, as in the previous section, we emphasize that all general aspects are completely analog for quantum dots and metallic islands. The only difference occurs for some diagrammatic rules which are stated explicitly at the appropriate place. We will restrict ourselves here to the case of a metallic island with infinite channel number $Z$, i.e. use the form (2.82) and (2.83) for the tunneling Hamiltonian. The generalization to finite $Z$, described by (2.65) and (2.66), is straightforward and can be found in [123].

### 3.2.1 Kinetic equation

We start from the definition (3.4) of the matrix elements of the reduced density matrix of the dot and obtain from the formal solution of the von Neumann equation and cyclic invariance under the trace

$$P_{ss'}(t) = Tr\rho(t_0)U(t_0,t)\hat{P}_{s's}U(t,t_0)\,, \tag{3.36}$$

where $U(t,t')$ is the evolution operator of the total Hamiltonian $H(t) = H_0 + H_T(t)$, with $H_0 = H_R + H_B + H_D$. Denoting by $U_0(t,t')$ the evolution operator of $H_0$, we define the interaction picture of an arbitrary Schrödinger operator $A(t)$ by $A(t)_I = U_0(t_0,t)A(t)U_0(t,t_0)$. Furthermore, we define the evolution operator in interaction picture by $U(t,t_0)_I = U_0(t_0,t)U(t,t_0)$. This gives

$$P_{ss'}(t) = Tr\rho(t_0)U(t_0,t)_I\hat{P}_{s's}(t)_I U(t,t_0)_I\,. \tag{3.37}$$

The evolution operators in interaction picture are given by the time-ordered expressions (valid for $t > t_0$)

$$U(t,t_0)_I = T\, e^{-i\int_{t_0}^{t} dt' H_T(t')_I} \quad , \quad U(t_0,t)_I = \bar{T}\, e^{i\int_{t_0}^{t} dt' H_T(t')_I}\,, \tag{3.38}$$

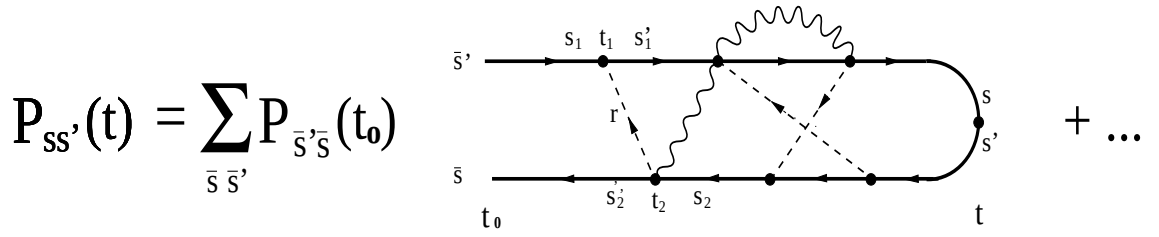


Figure 3.1: An example for a diagram contributing to the matrix element $P_{ss'}(t)$ of the reduced density matrix of the dot. Reservoir (boson) lines are indicated by dashed (wiggly) lines.

where $T$ ($\bar{T}$) denote the (anti-)chronological time ordering operators. Inserting these equations in (3.37), and using the initial condition (3.1), we obtain

$$P_{ss'}(t) = \sum_{\bar{s}\bar{s}'} P_{\bar{s}'\bar{s}}(t_0) < \bar{s}|Tr_{RB}\, \rho_R^{eq} \rho_B^{eq} T_\gamma \left\{ e^{-i\int_\gamma dt' H_T(t')_I} \hat{P}_{s's}(t)_I \right\} |\bar{s}' > \ . \qquad (3.39)$$

Here, $\gamma$ denotes the usual closed Keldysh contour which runs from $t_0$ to $t$ on the real axis and then back again from $t$ to $t_0$. $T_\gamma$ denotes the time ordering along this closed time path.

The next step is to expand (3.39) in $H_T(t)_I$ and insert the form (2.22) or (2.83) for the tunneling Hamiltonian. The tunneling vertices are arranged along the closed time path as indicated in Fig. 3.1. The upper line corresponds to the forward propagator and the lower line to the backward propagator. To each vertex we assign a time variable $t_i$ and, from the tunneling Hamiltonian, a projection operator $\hat{P}_{s_i' s_i}$, where $s_i$ is the incoming state and $s_i'$ the outgoing state at each vertex (see Fig. 3.1). There is one external vertex emerging from the projector $\hat{P}_{s's}$ in Eq. (3.39), which is the rightmost vertex at time t in Fig. 3.1. It is the only vertex which does not contain any reservoir or heat bath field operator.

The procedure is now to perform the trace over the reservoirs and the heat bath, and finally calculate the matrix element with respect to the dot states. The trace can be calculated exactly since $H_0$ is a bilinear form in the reservoir and boson field operators, and $\rho_{R,B}^{eq}$ are equilibrium density matrices. What is left for each term is a c-

number multiplied with the matrix element $<\bar{s}|\ldots|\bar{s}'>$ of a product of dot projection operators in interaction picture. We note that the three steps, i.e. calculating $Tr_R$, $Tr_B$ and the matrix element of the dot operators, can be performed independently since $H_0 = H_R + H_B + H_D$ contains no coupling between reservoirs, heat bath and dot. Furthermore, the reader can convince himself that Fermi statistics does not give rise to any minus sign during the factorization of reservoir from dot field operators if both are kept in the same sequence separately. This is due to the quadratic structure $a^\dagger_{kr}a_{lD}$ or $a^\dagger_{lD}a_{kr}$ of the tunneling vertex. In our convention, the time-ordering operator $T_\gamma$ does not introduce any change of sign.

Let us start with the calculation of $Tr_R$. It can be performed using Wick's theorem with the result that all reservoir field operators are contracted in pairs of creation and annihilation operators. In our convention, a single contraction for the quantum dot case gives the contribution ($\pm$ refers to $t_1 \lessgtr t_2$ with respect to the Keldysh time path)

$$\begin{aligned}\gamma^{r,\pm}_{s_1 s_1', s_2 s_2'}(t_1,t_2) &= \sum_k \bar{T}^r_{k,s_1' s_1}(t_1)^* \bar{T}^r_{k,s_2 s_2'}(t_2) \langle T_\gamma \left\{ a_{kr}(t_1)_I a^\dagger_{kr}(t_2)_I \right\} \rangle_{\rho^{eq}_R} \\ &= \frac{1}{2\pi}\int d\omega, ^-_{s_1 s_1', s_2 s_2'}(t_1,t_2;\omega-\mu_r) f^\pm_r(\omega) e^{-i\omega(t_1-t_2)}\,, \qquad (3.40)\end{aligned}$$

whereas for the infinite-Z metallic case we get

$$\begin{aligned}\alpha^\pm_r(t,t') &= \sum_{kl} \bar{T}^r_{kl}(t)^* \bar{T}^r_{kl}(t') \langle T_\gamma \left\{ (a^\dagger_{lD}a_{kr})(t)_I (a^\dagger_{kr}a_{lD})(t')_I \right\} \rangle_{\rho^{eq}_R} \\ &= \frac{1}{2\pi}\int d\omega \sum_l ,^-_{ll}(t,t';\omega+\epsilon_{lD}-\mu_r) f^\pm_r(\omega+\epsilon_{lD}) f^\mp(\epsilon_{lD}) e^{-i\omega(t-t')}\,, \qquad (3.41)\end{aligned}$$

where $f^\pm_r(\omega) = f^\pm(\omega-\mu_r)$, $f^+ = f$, $f^- = 1-f$, and $f$ is the Fermi distribution. For the metallic case we have used the fact that each loop of Wick contractions is proportional to the channel number $Z$. Therefore, for large channel number, the loops will contain the minimal number of vertices, i.e. they have the form of Eq. (3.41).

On the other hand, the corresponding contraction for the Hamiltonian given by

(2.82) and (2.83) reads

$$\begin{aligned}\alpha_r^{\pm}(t,t') &= \sum_q \bar{g}_q^r(t)^* \bar{g}_q^r(t') \langle T_\gamma \left\{ (c_{qr} + d_{qr}^\dagger)(t)_I (c_{qr}^\dagger + d_{qr})(t')_I \right\} \rangle_{\rho_R^{eq}} \\ &= \frac{1}{\pi} \int d\omega \bar{D}_r(t,t';\omega - \mu_r) n_r^{\pm}(\omega) e^{-i\omega(t-t')} \,, \end{aligned} \tag{3.42}$$

where $n_r^{\pm}(\omega) = n^{\pm}(\omega - \mu_r)$, $n^+ = n$, $n^- = 1 + n$, and $n$ denotes the Bose distribution. We see that (3.41) and (3.42) agree for the spectral function given by (2.88). This proofs the equivalence of the infinite-Z metallic island Hamiltonian, given by (2.65) and (2.66), with the bosonic version, given by (2.82) and (2.83).

For the quantum dot case, we get a minus sign for each crossing of contractions due to Fermi statistics. Diagrammatically, a contraction between reservoir field operators is indicated by a dashed line (see Fig. 3.1). The direction of the line is chosen in such a way that it leaves the vertex where a particle is annihilated on the dot. The time argument of this vertex has to be chosen as the second time argument of the function $\gamma$, i.e. corresponds to $t_2$ in Eq. (3.40). The states $s_{1,2}$ ($s'_{1,2}$) refer to the outgoing (incoming) dot states at both vertices.

The calculation of $Tr_B$ proceeds in a different way since the tunneling vertex contains an exponential $\exp(\pm i\hat{\phi})$ of a linear bosonic field. Here we can use path integral methods or Feynman's disentangling method [96] to get

$$\langle T_\gamma \left\{ e^{-i\hat{\phi}(t_1)_I} e^{i\hat{\phi}(t'_1)_I} \ldots e^{-i\hat{\phi}(t_m)_I} e^{i\hat{\phi}(t'_m)_I} \right\} \rangle_{\rho_B^{eq}} = \prod_{i<j} P^{\pm}(t_i,t_j)^{-1} \prod_{i<j} P^{\pm}(t'_i,t'_j)^{-1} \prod_{i,j} P^{\pm}(t_i,t'_j) \,, \tag{3.43}$$

where, for $t_1 \lessgtr t_2$ with respect to the Keldysh path, we have defined

$$P^{\pm}(t_1,t_2) = \langle T_\gamma \left\{ e^{-i\hat{\phi}(t_1)_I} e^{i\hat{\phi}(t_2)_I} \right\} \rangle_{\rho_B^{eq}} = P^{\pm}(t_1 - t_2) \,, \tag{3.44}$$

with $P^{\pm}(t)$ given by (2.98). Eq. (3.43) is in the form of a product which would mean that all pairs of vertices give a contribution. To be able to distinguish wether a pair

does contribute or not, we write (3.43) formally as a sum by defining

$$L_d^{\pm}(t_1,t_2) = P^{\pm}(t_1,t_2) - 1\,, \tag{3.45}$$

$$L_s^{\pm}(t_1,t_2) = P^{\pm}(t_1,t_2)^{-1} - 1\,. \tag{3.46}$$

Furthermore, using (3.44), we have $L_{d,s}^{\pm}(t_1,t_2) = L_{d,s}^{\pm}(t_1-t_2)$, and we define the Fourier transform

$$L_{d,s}^{\pm}(\omega) = \frac{1}{2\pi}\int dt e^{i\omega t} L_{d,s}^{\pm}(t) \tag{3.47}$$

Here, $L_d^{\pm}$ corresponds to a pair of vertices with different (d) signs of the bosonic phase fields, whereas $L_s^{\pm}$ refers to a pair with the same (s) sign. Both $L_d^{\pm}$ and $L_s^{\pm}$ are zero if the coupling to the environment is absent. Diagrammatically, we represent the bosonic contributions $L_{d,s}^{\pm}$ refering to a certain pair of vertices by a wiggly line connecting these vertices (see Fig. 3.1). In contrast to reservoir lines, an arbitrary number of bosonic lines can be attached to a single vertex. Furthermore, by fixing an arbitrary direction of the bosonic line, the time argument $t_2$ in (3.45) and (3.46) refers to the vertex where the line starts.

The matrix element $<\bar{s}|\ldots|\bar{s}'>$ of products of dot projection operators in interaction picture is given by

$$<\bar{s}|\prod_{i=0}^{m}\hat{P}_{s_i's_i}(t_i)_I|\bar{s}'> = \prod_{i=0}^{m} < s_{i+1}|U_D(t_{i+1},t_i)|s_i'>\,, \tag{3.48}$$

where $U_D(t,t')$ is the evolution operator of $H_D$, and we identified $s_{m+1}=\bar{s}$, $s_0'=\bar{s}'$, and $t_{m+1}=t_0$. This result means that each segment of the Keldysh contour in Fig. 3.1, which connects two vertices, corresponds to a matrix element of the dot evolution operator starting from the outgoing state of the initial vertex to the incoming state of the final vertex. Since $H_D$ is diagonal in the states $|s>$, the matrix elements of the evolution operator are given by

$$<s|U_D(t,t')|s'> = \delta_{ss'}e^{-iE_s(t-t')}\,. \tag{3.49}$$

This means that we can assign a certain dot state to each segment of the Keldysh contour.

Finally, we have to consider that the expansion of the exponentials in Eq. (3.39) gives a factor $(-i)^n i^m$, where $n$ ($m$) is the number of vertices on the forward (backward) propagator. The time integrations are then all performed on the real axis from $t_0$ to $t$. Assigning a factor $(-i)^2$ to each reservoir line, we can alternatively say that each reservoir line and each vertex on the lower part of the Keldysh contour gives rise to a minus sign.

We summarize the diagrammatic rules in time space:

**1.** Each reservoir line running from vertex 2 to vertex 1 gives rise to $\gamma^{r,\pm}_{s_1 s'_1, s_2 s'_2}(t_1, t_2)$ (quantum dot) or $\alpha^{\pm}_r(t_1, t_2)$ (metallic island). $r$ is the index of the reservoir, $\pm$ corresponds to $t_1 \lessgtr t_2$ with respect to the Keldysh contour, and $s_{1,2}$ ($s'_{1,2}$) are the outgoing (incoming) dot states at each vertex. At vertex 2 where the line starts, a particle has to be annihilated on the dot. To each vertex we can at most attach one reservoir line.

**2.** Each boson line running from vertex 2 to vertex 1 gives rise to $L^{\pm}_{d,s}(t_1, t_2)$. $d$ ($s$) correspond to different (the same) signs of the bosonic phase factors at both vertices. $\pm$ corresponds to $t_1 \lessgtr t_2$ with respect to the Keldysh contour. The direction of the boson lines can be chosen arbitrary. To each vertex we can attach an arbitrary number of boson lines.

**3.** Each element of the Keldysh contour running from vertex 2 to vertex 1 gives rise to $< s_1|U_D(t_1, t_2)|s_2 >$, where $s_1$ is the outgoing dot state at vertex 2, and $s_1$ the incoming dot state at vertex 1.

**4.** The prefactor is given by $(-1)^{a+b+c}$, where $a$ is the number of reservoir lines, $b$ the

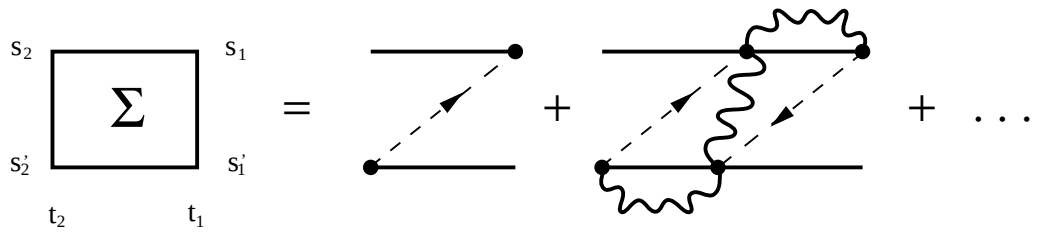


Figure 3.2: The kernel $\Sigma_{s_1 s_1', s_2 s_2'}(t_1, t_2)$ which contains all irreducible diagrams in the sense that an arbitrary vertical line will always cut through some reservoir or boson line.

number of vertices on the lower part of the Keldysh contour, and $c$ the number of crossings of fermionic reservoir lines (quantum dot case).

We add that all reservoir lines can be dressed by boson lines. This means that instead of $\gamma^{r,\pm}$ or $\alpha_r^{\pm}$, the contribution of a reservoir line can be replaced by

$$\tilde{\gamma}^{r,\pm}_{s_1 s_1', s_2 s_2'}(t_1, t_2) = \gamma^{r,\pm}_{s_1 s_1', s_2 s_2'}(t_1, t_2) P^{\pm}(t_1, t_2)\,, \tag{3.50}$$

$$\tilde{\alpha}_r^{\pm}(t_1, t_2) = \alpha_r^{\pm}(t_1, t_2) P^{\pm}(t_1, t_2)\,, \tag{3.51}$$

where we have added the two contribution of the two vertices being connected by a reservoir and a boson line (giving $\gamma L$ or $\alpha L$), and the term where they are only connected by a reservoir line (giving $\gamma$ or $\alpha$), and used (3.45) and (3.46).

We can now proceed to derive the kinetic equation (3.6). Looking at an arbitrary diagram we distinguish between two different time segments. There are "free" time segments in the sense that a vertical line drawn through the diagram will not cut through any reservoir or boson line. These parts correspond to the free evolution of the density matrix of the dot without any coupling to the external environment. All the other time segments are "irreducible", i.e. a vertical line cuts either through a reservoir or a boson line. They reflect the influence of the environment and describe the coupling of the forward and backward propagator. In more physical terms, they can be characterized by the criterium that the total density matrix of the system is no

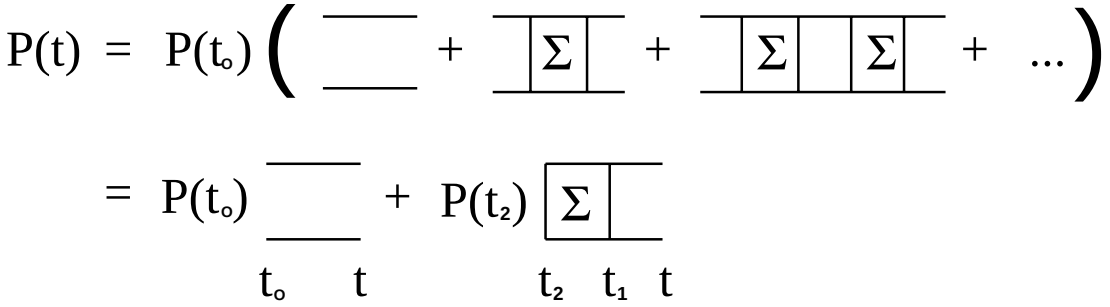


Figure 3.3: The Dyson-like equation for the probability distribution. $\Sigma$ includes all irreducible diagrams in the sense that any vertical line will at least cut one reservoir or boson line.

longer diagonal with respect to the reservoirs or the heat bath during the time interval of the irreducible segment. This means that a coherent process takes place during which the excited quasiparticles of the environment do not relax to their equilibrium state. We denote the sum of all irreducible diagrams by the kernel $\Sigma_{s_1 s_1', s_2 s_2'}(t_1, t_2)$, with arguments as shown in Fig. 3.2. The summation of sequences of irreducible blocks with free parts in between can be performed by an iteration in the style of a Dyson equation (see Fig. 3.3)

$$\hat{P}(t) = \hat{\Pi}^{(0)}(t, t_0)\hat{P}(t_0) + \int_{t_0}^{t} dt_1 \int_{t_0}^{t_1} dt_2\, \hat{\Pi}^{(0)}(t, t_1)\hat{\Sigma}(t_1, t_2)\hat{P}(t_2)\,, \tag{3.52}$$

where

$$\Pi^{(0)}_{s_1 s_1', s_2 s_2'}(t_1, t_2) = < s_1 | U_D(t_1, t_2) | s_2 >< s_2' | U_D(t_2, t_1) | s_1' > \tag{3.53}$$

describes the evolution of the density matrix in the free segments. Differentiating (3.52) with respect to $t$ and using (in superoperator notation with $A$ being an arbitrary Schrödinger operator) $\frac{\partial}{\partial t_1}\hat{\Pi}^{(0)}(t_1, t_2)A = -i[H_D(t_1), \hat{\Pi}^{(0)}(t_1, t_2)A]$, we arrive at the kinetic equation (3.6).

For the diagonal kinetic equation (3.8) we have to define the kernel $\Sigma_{ss'}$ in a different way. We allow for free segments in the kernel as well but with the restriction that the dot states associated with the lower and upper line of the contour are different in the free segments. We denote the contribution of the restricted free part by $\Pi^{(0),ir}$

indicating that it is irreducible in the sense that each vertical line does not cut through two dot states which are identical. $\Sigma_{ss'}$ is then given by the sum over all sequences of kernels $\Sigma_{s_1 s_1', s_2 s_2'}$ with irreducible free parts $\Pi^{(0),ir}$ in between.

The property $\sum_s \Sigma_{ss'}(t,t') = 0$, stated in (3.9), can be easily proven by attaching the rightmost vertex of each diagram $\Sigma$ to the upper and lower proppagator. The minus sign for each vertex on the backward propagator cancels both contributions if we sum over all states $s$.

### 3.2.2 Tunneling current

To calculate the tunneling current (3.12), we have to replace the projector $\hat{P}_{s's}$ in (3.39) by the tunneling current operator (2.38) (quantum dot case) or (2.84) (infinite-Z metallic island). This means that the rightmost vertex of each diagram will be the tunneling current vertex which has the same structure as the other tunneling vertices from $H_T$. Therefore, the first irreducible block $\Sigma^r$ to the right is part of the total kernel $\Sigma$ which enters the kinetic equation. Here $r$ is the index for the reservoir for which we want to calculate the tunneling current. Accounting correctly for the signs of the tunneling current vertex, we find immediately that $\Sigma^r$ is that part of $\Sigma$, where the reservoir line attached to the rightmost vertex corresponds to reservoir $r$ and is an outgoing (ingoing) line if the rightmost vertex lies on the upper (lower) propagator. The other irreducible blocks which follow $\Sigma^r$ to the left are identical to $\Sigma$. Thus, after summing over all sequences of $\Sigma$ which gives the probability distribution $P$, we obtain (3.13) and (3.14).

The proof of (3.15) requires some more technical considerations. The kernel $\Sigma^{rp}$ is defined as that part of $\Sigma$ where $p$ particles are taken out of reservoir $r$. Within our graphical language this means that the number of reservoir lines with reservoir index $r$ running from the backward to the forward propagator minus the number of reservoir

lines with reservoir index $r$ running from the forward to the backward propagator is given by $p$. Let us now consider any diagram of $\Sigma^{rp}_{ss'}$. Changing the vertical position of the rightmost vertex we obtain a diagram of $\Sigma^{rp}_{s''s'}$ if the rightmost reservoir line has a reservoir index different from $r$ or of $\Sigma^{r,p\pm1}_{s'',s'}$ if the rightmost reservoir line has the reservoir index $r$ and if it enters (leaves) the backward propagator or leaves (enters) the forward propagator. This diagram has up to a sign the same value as the diagram from which it was constructed. Multiplying both diagrams with the corresponding factors $p$ or $p \pm 1$, summing over $s$ and $s''$, respectively, and adding them, all terms proportional to $p$ cancel. The remaining contribution is either zero if the rightmost reservoir line has not the reservoir index $r$, or it is that contribution of $-\sum_s \Sigma^r_{ss'}$ where $p \pm 1$ particles have been taken out of reservoir $r$. Thus, summing $p\Sigma^{rp}_{ss'}$ over $s$ and $p$, we obtain exactly all diagrams of $-\sum_s \Sigma^r_{ss'}$ which proves Eq. (3.15).

To proof charge conservation we use a similiar proof as before and find

$$\sum_s N_s \Sigma_{ss'}(t,t') = -\sum_{rs} \Sigma^r_{ss'}(t,t')\,. \tag{3.54}$$

Multiplying the kinetic equation (3.8) with $eN_s$, summing over $s$, and using (3.54) together with the tunneling current formula (3.14), we find charge or particle number conservation

$$\sum_r I^{tun}_r(t) = \frac{d}{dt} Q(t)\,, \tag{3.55}$$

where $Q(t)$ is the total charge on the dot. Comparing with current conservation (2.37) we see that the r.h.s of (3.55) is identical to minus the sum over all displacement currents flowing in the reservoirs.

### 3.2.3 Diagrammatic rules in energy space

For periodic voltages we have shown in section 3.1.3 that it is convenient to study the kinetic equation and the tunneling current in Fourier-Laplace space. Therefore we

will set up in this section diagrammatic rules to calculate directly the Fourier-Laplace transformation of the rates given by (3.23) and (3.27), i.e. we want to calculate the quantity

$$\Sigma^n_{ss'}(z) = \frac{1}{T}\int_0^T d\tau' \int_0^\infty d\tau e^{-in\Omega\tau'} e^{iz\tau}\Sigma_{ss'}(\tau+\tau',\tau')\,. \tag{3.56}$$

For that purpose let us also introduce the Fourier transform of $\gamma$ and $\alpha$ again for the special case when the voltages on the reservoirs and the gate are periodic in time with period $T = 2\pi/\Omega$. Any quantity $A(t_1,t_2)$ which fulfils $A(t_1+T,t_2+T) = A(t_1,t_2)$, like e.g. $A = \gamma$, $\tilde{\gamma}$ or $A = \alpha$, $\tilde{\alpha}$, is Fourier transformed as

$$A(t_1,t_2) = \sum_{n=-\infty}^{\infty}\int d\omega e^{in\Omega t_1} e^{-i\omega(t_1-t_2)} A^n(\omega)\,, \tag{3.57}$$

with the inverse given by

$$A^n(\omega) = \frac{1}{2\pi}\int d\tau e^{i\omega\tau}\frac{1}{T}\int_0^T dt e^{-in\Omega t} A(t,t-\tau)\,. \tag{3.58}$$

Furthermore, any quantity $B(t_1,t_2)$ which is periodic in $t_1$ and $t_2$ separately, like e.g. $B = \bar{,}$, $\bar{D}$, is Fourier transformed as

$$B(t_1,t_2) = \sum_{nm} e^{in\Omega t_1} e^{-im\Omega t_2} B^{nm}\,. \tag{3.59}$$

As a consequence, the Fourier transform of Eqs. (3.40) and (3.42) reads

$$\gamma^{r,\pm,n}_{s_1,s_1',s_2s_2'}(\omega) = \frac{1}{2\pi}\sum_m \bar{,}^{r,n+m,m}_{s_1s_1',s_2s_2'}(\omega-\mu_r+m\Omega) f_r^{\pm}(\omega+m\Omega)\,, \tag{3.60}$$

$$\alpha_r^{\pm,n}(\omega) = \frac{1}{\pi}\sum_m \bar{D}_r^{n+m,m}(\omega-\mu_r+m\Omega) n_r^{\pm}(\omega+m\Omega)\,. \tag{3.61}$$

For AC-voltages of the form (2.27) we find from the Fourier transform of (2.29) and (2.87)

$$\bar{,}^{r,nm}_{s_1s_1',s_2s_2'}(\omega) = {,}^{r}_{s_1s_1',s_2s_2'}(\omega) i^{n-m} J_n(\frac{\bar{\Delta}_r}{\Omega}) J_m(\frac{\bar{\Delta}_r}{\Omega})\,, \tag{3.62}$$

$$\bar{D}_r^{nm}(\omega) = D_r(\omega) i^{n-m} J_n(\frac{\bar{\Delta}_r}{\Omega}) J_m(\frac{\bar{\Delta}_r}{\Omega})\,, \tag{3.63}$$

where $J_n$ denote the Bessel functions.

In the presence of time-dependent transitions between the dot states, discussed at the end of section 2.3.1, we obtain from (2.61)

$$\begin{aligned} {}^{-}_{;\,s_1s_1',s_2s_2'}{}^{r,nm}(\omega) &= \sum_{\bar{s}_1\bar{s}_1',\bar{s}_2\bar{s}_2'} {}^{r}_{;\,\bar{s}_1\bar{s}_1',\bar{s}_2\bar{s}_2'}(\omega) \sum_{n'm'} i^{n'-m'} J_{n'}(\frac{\Delta_r}{\Omega}) J_{m'}(\frac{\Delta_r}{\Omega}) \times \\ &\times \sum_{n_1} W^{n_1}_{\bar{s}_1's_1'} W^{n-n'-n_1}_{s_1\bar{s}_1} \sum_{m_1} W^{m_1}_{\bar{s}_2's_2'} W^{m'-m-m_1}_{s_2\bar{s}_2} \,. \end{aligned} \tag{3.64}$$

The Fourier transform of the dressed reservoir lines, given by (3.50) and (3.51), reads

$$\tilde{\gamma}^{r,\pm,n}_{s_1s_1',s_2s_2'}(\omega) = \int d\omega' \gamma^{r,\pm,n}_{s_1s_1',s_2s_2'}(\omega-\omega') P^{\pm}(\omega') \,, \tag{3.65}$$

$$\tilde{\alpha}^{\pm,n}_{r}(\omega) = \int d\omega' \alpha^{\pm,n}_{r}(\omega-\omega') P^{\pm}(\omega') \,. \tag{3.66}$$

The $n = 0$ components can be written very elegantly for AC-voltages of the form (2.27). Using (3.60)-(3.63), we obtain

$$\tilde{\gamma}^{r,\pm}_{s_1s_1',s_2s_2'}(\omega) = \frac{1}{2\pi} \int d\omega' \, {}^{r}_{;\,s_1s_1',s_2s_2'}(\omega-\omega'-\mu_r) f^{\pm}_r(\omega-\omega') P^{\pm}_r(\omega') \,, \tag{3.67}$$

$$\tilde{\alpha}^{\pm}_{r}(\omega) = \frac{1}{\pi} \int d\omega' D_r(\omega-\omega'-\mu_r) n^{\pm}_r(\omega-\omega') P^{\pm}_r(\omega') \,, \tag{3.68}$$

where again we imply the Fourier component $n = 0$ if no index and no time argument is written, and $P^{\pm}_r(\omega)$ has been defined in (2.95) as the total probability function for absorption or emission of energy arising from the time-dependent fields and the heat bath. Up to a prefactor we have obtained the golden rule rates (2.134), (2.135), (2.170) and (2.171) for appropriately chosen values for $\omega$.

Using these representations together with the Fourier transform (3.47) of $L^{\pm}_{d,s}(t_1,t_2)$ and the representation (3.49) of $U_D(t_1,t_2)$, we can now derive the diagrammatic rules in energy space for the rate (3.56). To each reservoir and boson line we associate a frequency $\omega$, and, in addition, a Fourier index $n$ for reservoir lines. To the dot lines, represented by the segments of the Keldysh contour, we associate the dot energies $E_s$.

In this way we can define for each vertex a quantity $x$ which is defined as the sum of all energies leaving the vertex minus all energies entering the vertex. Thereby we have to consider all reservoir, boson and dot lines. The energy $n\Omega$ from the Fourier index is thereby counted only for reservoir lines entering the vertex but not for those leaving the vertex. With this definition we obtain the following time integral occuring in a certain diagram of (3.56)

$$I = \frac{1}{T}\int_0^T d\tau' \int_0^\infty d\tau \qquad \int_{\tau'}^{\tau+\tau'} d\tau_1 \int_{\tau_1}^{\tau+\tau'} d\tau_2 \cdots \int_{\tau_{m-2}}^{\tau+\tau'} d\tau_{m-1}\, e^{-in\Omega\tau'} e^{iz\tau} \times$$
$$\times e^{ix_0\tau'} e^{ix_1\tau_1} \cdots e^{ix_{m-1}\tau_{m-1}} e^{ix_m(\tau+\tau')}\,, \tag{3.69}$$

where $x_0, \ldots, x_m$ correspond to the energy differences for the vertices at times $\tau_0 = \tau' < \tau_1 < \ldots < \tau_{m-1} < \tau_m = \tau + \tau'$. A straighforward calculation yields for the integral

$$I = \delta_{nl} i^m \frac{1}{x_m + z}\ \frac{1}{x_m + x_{m-1} + z} \cdots \frac{1}{x_m + \ldots + x_1 + z}\ , \tag{3.70}$$

where $l\Omega = x_0 + x_1 + \ldots + x_m$ is the sum over all Fourier energies of the reservoir lines since all other energies will cancel in the sum. The denominators of the resolvents of (3.70) can be calculated from a simple diagrammatic rule. Cutting the diagram by a vertical line between vertex $i-1$ and vertex $i$ we obtain

$$\Delta E_i \equiv x_m + x_{m-1} + \ldots + x_i = y_i + l_i\Omega\,, \tag{3.71}$$

where $y_i$ is the difference off all energies going to the left minus all energies going to the right in each segment limited by $\tau_{i-1}$ and $\tau_i$, and $l_i$ is the sum over all Fourier indices from lines entering vertices which lie to the right of the vertical cut.

We summarize the diagrammatic rules in energy space for the rates $\Sigma^n_{ss'}(z)$ or $\Sigma^{r,n}_{ss'}(z)$

**1.** Each reservoir line running from vertex 2 to vertex 1 with Fourier index $n$ and energy $\omega$ gives rise to $\gamma^{r,\pm,n}_{s_1 s'_1, s_2 s'_2}(\omega)$ (quantum dot) or $\alpha^{\pm,n}_r(\omega)$ (metallic island). $r$ is the index of the reservoir, $\pm$ corresponds to $t_1 \lessgtr t_2$ with respect to the Keldysh

contour, and $s_{1,2}$ ($s'_{1,2}$) are the outgoing (incoming) dot states at each vertex. At vertex 2 where the line starts, a particle has to be annihilated on the dot. To each vertex we can at most attach one reservoir line.

**2.** Each boson line running from vertex 2 to vertex 1 with energy $\omega$ gives rise to $L^{\pm}_{d,s}(\omega)$. $d$ ($s$) correspond to different (the same) signs of the bosonic phase factors at both vertices. $\pm$ corresponds to $t_1 \lessgtr t_2$ with respect to the Keldysh contour. The direction of the boson lines can be chosen arbitrary. To each vertex we can attach an arbitrary number of boson lines.

**3.** For each vertical cut between vertex $i-1$ and vertex $i$ we obtain a resolvent $1/(y_i + l_i\Omega + z)$. $y_i$ is the difference of the leftgoing minus the rightgoing energies (including the energies of reservoir, boson and dot lines). $l_i$ is the sum over all Fourier indices of reservoir lines which are cut by the vertical line or lie right to it.

**4.** The sum over all Fourier indices of reservoir lines has to be identical to $n$.

**5.** The prefactor is given by $-i(-1)^{b+c}$, where $b$ is the number of vertices on the lower part of the Keldysh contour, and $c$ the number of crossings of fermionic reservoir lines (quantum dot case).

As already mentioned at the end of section 3.1.1, an important mathematical property of the irreducible kernels $\Sigma(t,t')$ is that they are well-defined objects. For finite times $t$ and $t'$ this is a trivial statement. However, for the calculation of stationary transport properties, i.e. for $t_0 \to -\infty$, one needs time integrals over the kernels ranging to infinity as can be seen from Eq. (3.30). There are two reasons why the time integral is well-defined. First, due to the adiabatic switching on of the tunneling term, we can add a factor $\exp(-\eta\tau)$ to the integrand, where $\eta = 0^+$. Secondly, by calculating

the time integrals as outlined above, we obtain resolvents with energy differences $\Delta E_i$ of the form (3.71) in the denominator. Since the kernel for the nondiagonal kinetic equation (3.6) is defined to be irreducible, the energy differences $\Delta E_i$ will all involve energies of the reservoir or boson lines, i.e. they are not zero but integration variables. Therefore, the energy integrals will exist at least if the spectral functions (2.30) and (2.88) together with $L_{d,s}(E)$ are smooth functions of energy and will fall off rapidly enough for high energies. To guarantee the smoothness, it is crucial to perform first the thermodynamic limit with the environment before performing the long time limit $\eta \to 0^+$.

For the kernel of the diagonal kinetic equation (3.8), a problem may arise for the irreducible free time segment $\Pi^{(0),ir}$, where no reservoir or boson line is present. Here, the energy difference $\Delta E_i$ is given by $E_{s_i'} - E_{s_i} + l_i\Omega$, where $s_i'$ and $s_i$ are the different dot states associated with the lower and upper part of the contour. Thus, $\Delta E_i$ can be exactly zero if the two states are degenerate, leading to a $1/\eta$-divergence in (3.70). In such a case it is no longer possible to work with the diagonal kinetic equation but one should use the more general nondiagonal one, at least in the subspaces of degenerate dot states. However, due to conservation laws, the reduced density matrix is often exactly diagonal in these subspaces.

### 3.2.4 Resonant tunneling approximation

For a given model it is straightforward to calculate the lowest orders of the kernels $\Sigma$ and $\Sigma^r$. However, as we will see in chapter 4, renormalization and broadening effects due to quantum fluctuations can only be described by considering an infinite series of higher order diagrams. Therefore it is necessary to set up a systematic approximation which defines the diagrams being the most important ones.

The approximation is formulated in terms of the extend we allow the total density

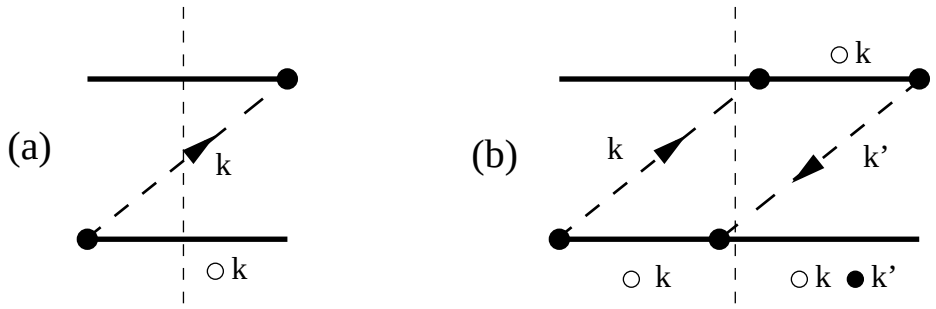


Figure 3.4: Diagrams contributing to (a) sequential and (b) resonant tunneling. At each reservoir line we have indicated which state $k$ of the reservoir is involved at the tunneling vertices. This creates holes (open circles) or particles (filled circles) on the propagators.

matrix to be nondiagonal with respect to the reservoir degrees of freedom. For this let us disregard the bosonic heat bath for a moment and consider first the lowest order contribution to the kernels. This is the contribution to the sequential tunneling or golden rule rate and consists diagrammatically of one single reservoir line. An example is shown in Fig.3.4a. If the reservoir field operator at the tunneling vertices is $a^{(\dagger)}_{kr}$, we see that one hole in reservoir $r$ is created on the backward propagator. This means that we have considered a matrix element of the total density matrix which is offdiagonal only up to one hole excitation. If we consider all diagrams in lowest order, we find that sequential tunneling can be characterized by offdiagonal elements up to one hole or one electron excitation. This shows that the density matrix tries to be as close as possible to a diagonal matrix with respect to the reservoir states. Therefore it is natural to improve the approximation of sequential tunneling by considering the next possibility of nondiagonal matrix elements, namely allowing for offdiagonal elements up to one electron-hole, electron-electron or hole-hole excitation. An example is shown in Fig.3.4b. It shows that this approximation can be characterized diagrammatically by the condition that any vertical line can cut at most two reservoir lines.

This approximation is essentially nonperturbative in the tunneling coupling. It con-

tains the physics of resonant tunneling, i.e. describes renormalization and broadening of the excitation energies of the dot. This is testet and explicitly shown in section 4.2 for the simplest model of a dot containing one single excitation energy where the approximation turns out to be exact. Of course, for an arbitrary model, the approximation does not provide us with some parameter to define the temperature range when it can be applied. This has to be analysed by comparing with other known solutions in equilibrium or using additional techniques like renormalization group analysis. However, as we will see in chapter 4, for certain models the leading zero-temperature divergencies are even included within our approximation, or, if not completely, the results are at least qualitatively good. The spirit of our approach is very similiar to variational wave function ansatzes for strongly correlated systems [53], but we have found here a real-time formulation which is based on the density matrix and therefore allows the treatment of nonequilibrium phenomena in nonlinear response at finite temperatures.

Without the heat bath it can be shown that the sum over all diagrams within the resonant tunneling approximation can be written in the form of a self-consistent integral equation. For special models this integral equation can be solved analytically, otherwise one has to find the solution numerically. For the technical details we refer the reader to [123, 78, 79]. In the presence of a heat bath, one can use the same solution by dressing the reservoir lines. The inclusion of bosonic lines between vertices which are not connected by reservoir lines is very difficult and is still an open problem.

# Chapter 4

# Applications

In this section we will describe several applications using the formalism we have developed in chapter 3. We start with two well-known limits which are standardly used in the literature to describe most of the experiments of transport through small devices: golden rule theory (sequential tunneling) and the noninteracting case (Landauer-Büttiker theory). Golden rule theory treats the tunneling in lowest order whereas interaction effects are incorporated in all orders. The noninteracting case disregards interaction effects whereas the tunneling is treated in all orders. In section 4.3 we describe resonant tunneling in a quantum dot with large charging energy and two possible spin excitations, and in section 4.4 resonant tunneling for the infinite-Z metallic island in the two state approximation. Here tunneling is considered in all orders within the approximation set up in section 3.4, and interaction effects are treated exactly. In this sense we are able to interpolate between the two known limits described in section 4.1 and 4.2.

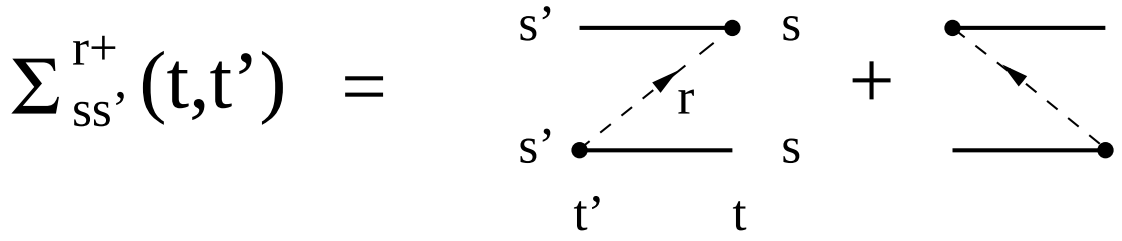


Figure 4.1: The diagrams for the rates in lowest order perturbation theory to tunnel from reservoir $r$ to the dot. The rate to tunnel from the dot to reservoir $r$ is obtained from the same diagrams by inverting the direction of the reservoir lines.

## 4.1 Sequential tunneling

The rates $\Sigma^{rp}_{ss'}(t,t')$ in second order in $H_T$ are shown in Fig. 4.1 for $s \neq s'$. They enter the current formula (3.16) which reads in lowest order

$$I^{tun}_r(t) = e \sum_{s \neq s'} \int_{t_0}^{t} dt' \left\{ \Sigma^{r+}_{ss'}(t,t') P_{s'}(t') - \Sigma^{r-}_{s's}(t,t') P_s(t') \right\} , \tag{4.1}$$

where $\Sigma^{r\pm}_{ss'} \equiv \Sigma^{r,\pm 1}_{ss'}$. The case $s = s'$ does not contribute since it corresponds to $p = 0$, i.e. no electron has been transferred between the dot and the reservoirs. Thus this does not give any contribution to the current. Furthermore, for $s \neq s'$, we get for the kernels entering the kinetic equation (3.10)

$$\Sigma_{ss'}(t,t') = \sum_r \sum_{p=\pm 1} \Sigma^{rp}_{ss'}(t,t') . \tag{4.2}$$

Here, the terms with $p = 0$ do not contribute since the corresponding diagrams have no vertices on the forward or the backward propagator. This implies $s = s'$ since the isolated dot evolution operator (3.49) is diagonal.

The diagrammatic rules give

$$\Sigma^{r+}_{ss'}(t,t') = e^{i(E_s - E_{s'})(t-t')} \tilde{\gamma}^{r+}_{ss',s's}(t,t') + (t \leftrightarrow t') , \tag{4.3}$$

$$\Sigma^{r-}_{s's}(t,t') = e^{i(E_s - E_{s'})(t-t')} \tilde{\gamma}^{r-}_{ss',s's}(t,t') + (t \leftrightarrow t') , \tag{4.4}$$

for the quantum dot case, and

$$\Sigma^{r+}_{N+1,N}(t,t') = e^{i\Delta_N(t-t')} \tilde{\alpha}^{r+}(t,t') + (t \leftrightarrow t') , \tag{4.5}$$

$$\Sigma^{r-}_{N,N+1}(t,t') \;=\; e^{i\Delta_N(t-t')}\tilde{\alpha}^{r-}(t,t') + (t \leftrightarrow t')\,, \tag{4.6}$$

for the metallic case with $\Delta_N = E_{N+1} - E_N$.

Using these results together with the expressions for $\tilde{\gamma}$ and $\tilde{\alpha}$, derived in section 3.2.1, one can, in principle, calculate the full time dependent solution starting from an arbitrary initial state.

For periodic voltages we have shown in section 3.1.3 that it is more convenient to work in Fourier-Laplace space. Our diagrammatic rules in energy space give for this case

$$\Sigma^{r+,n}_{ss'}(z) = i\int d\omega \tilde{\gamma}^{r,+,n}_{ss',s's}(\omega)\left\{\frac{1}{E_s - E_{s'} - \omega + n\Omega + z} + \frac{1}{E_{s'} - E_s + \omega + z}\right\}\,, \tag{4.7}$$

and a corresponding equation for $\Sigma^{r-,n}_{s's}(z)$ if we replace $\tilde{\gamma}^{r,+,n}$ by $\tilde{\gamma}^{r,-,n}$. The metallic case follows from using $\tilde{\alpha}^{\pm,n}_r$ instead of $\tilde{\gamma}^{r,\pm,n}_{ss',s's}$.

For the calculation of the stationary state one needs only the quantities $\Sigma^{r\pm,nm}_{ss'} = \Sigma^{r\pm,n}_{ss'}(-m\Omega + i\eta)$ as defined in Eq. (3.26). Without heat bath and using the Coulomb blockade model for the quantum dot, the stationary current has been calculated from these rates in Ref. [14] by using the kinetic equation (3.24) together with Eq. (3.25) for the tunneling current and Eq. (2.36) for the displacement current. For the calculation of the stationary DC-current in the presence of time-dependent transitions, where (3.64) has to be used, we refer to Refs. [15, 131].

Finally, we can easily set up the connection to the golden rule rates discussed in section 2.4. Here we assume $\Omega \gg$ , (quantum dot case) or $\Omega \gg \alpha_0 E_C$ (metallic island), so that we need only the DC-components $\Sigma^{r\pm}_{ss'} = \Sigma^{r\pm,0}_{ss'}(z = i\eta)$ as explained in section 3.1.3. As a consequence we obtain a $\delta(E_s - E_{s'} - \omega)$-function from the resolvents in (4.7) which gives

$$\Sigma^{r+}_{ss'} = 2\pi\tilde{\gamma}^{r,+}_{ss',s's}(E_s - E_{s'}) \quad , \quad \Sigma^{r-}_{ss'} = 2\pi\tilde{\gamma}^{r,-}_{s's,ss'}(E_{s'} - E_s) \tag{4.8}$$

for the quantum dot case, and

$$\Sigma^{r+}_{N+1,N} = 2\pi\tilde{\alpha}^{+}_{r}(\Delta_N) \quad , \quad \Sigma^{r-}_{N,N+1} = 2\pi\tilde{\alpha}^{-}_{r}(\Delta_N) \tag{4.9}$$

for the metallic case. For AC-voltages of the form (2.27) we can use (3.67) and (3.68), and we obtain directly the golden rule rates (2.134) and (2.135) for the quantum dot case, and (2.170) and (2.171) for the metallic case.

Finally we mention that the kernels in lowest order perturbation theory remain the same for the metallic case even if the channel number $Z$ is finite, since the lowest order diagrams can contain at most one fermionic loop.

## 4.2 "Noninteracting" quantum dot

In this section we consider the special case of a quantum dot containing only one single excitation energy or, equivalently as explained in section 2.3.3, a quantum dot with one single-particle state. We consider the case without time-dependent fields and the heat bath. The Hamiltonian is given by (2.71)

$$H(t) = \sum_{kr} \epsilon_{kr} a^{\dagger}_{kr} a_{kr} + \epsilon c^{\dagger} c + \sum_{kr} (\bar{T}^{r}_{k}(t) a^{\dagger}_{kr} c \; + \; h.c.) \, , \tag{4.10}$$

where $c, c^{\dagger}$ are the field operators of the dot, and the time dependence of the tunneling matrix elements involves only the static effective potentials of the reservoirs $\bar{T}^{r}_{k}(t) = T^{r}_{k} \exp\left(i\mu_r(t-t_0)\right)$.

The nonequilibrium problem corresponding to the Hamiltonian (4.10) has been solved exactly by many authors. We mention the Landauer-Büttiker formalism [88, 16, 17], Keldysh formalism [20, 146, 130], equation of motion methods [102], and golden rule theory with lorentzian broadening of the energy conservation [14]. Here we will rederive the solution by using the resonant tunneling approximation. This shows that all diagrams which have been neglected within this approximation cancel each other

exactly for the noninteracting limit. In fact, one can show that all the diagrams which give zero in sum can be classified into pairs such that each pair gives zero contribution separately [79]. In this way it is possible to control systematically wether an approximation set up for interacting systems will contain the noninteracting limit correctly or not. Usually this is hard to see within theories set up for strongly correlated fermions like e.g. slave boson methods [8, 72, 11, 60].

We denote the empty and singly occupied dot state by $|0>$ and $|1>$, respectively. In the stationary state the kinetic equation and the tunneling current follow from (3.28) and (3.29)

$$0 = \Sigma_{01} P_1 - \Sigma_{10} P_0 \,, \tag{4.11}$$

$$I_r = -e(\Sigma^r_{00} P_0 + \Sigma^r_{01} P_1) \,, \tag{4.12}$$

where we used $\Sigma^r_{10} = \Sigma^r_{11} = 0$ which follows directly from their definition. Furthermore, we have $P_0 + P_1 = 1$, $\Sigma_{00} = \sum_r \Sigma^r_{00}$ and $\Sigma_{01} = \sum_r \Sigma^r_{01}$. The latter two equations are valid since all the other diagrams which contribute to the kernels $\Sigma$ are zero here. Together with $\Sigma_{00} + \Sigma_{10} = 0$, which follows from (3.9), we get

$$\Sigma_{10} = -\sum_r \Sigma^r_{00} \quad , \quad \Sigma_{01} = \sum_r \Sigma^r_{01} \,. \tag{4.13}$$

Thus, we need $\Sigma^r_{00}$ and $\Sigma^r_{01}$ to solve the problem. We use the resonant tunneling approximation described in section 3.2.4 and show the analytical result here. For the technical details the reader is refered to [79, 78]. We obtain

$$\Sigma^r_{01} = 2\pi \left\{ \frac{\lambda_r \lambda^-}{\lambda} - M \sum_{r'} \int d\omega |\Pi(\omega)|^2 [\gamma^-_{r'}(\omega)\gamma^+_r(\omega) - \gamma^+_{r'}(\omega)\gamma^-_r(\omega)] \right\} , \tag{4.14}$$

$$\Sigma^r_{00} = \Sigma^r_{01} - 2\pi \frac{\lambda_r}{\lambda} \,, \tag{4.15}$$

where $\gamma^\pm_r(\omega) = \frac{1}{2\pi}, ^r(\omega) f^\pm_r(\omega)$ has already been introduced in Eq. (2.164),

$$\lambda = \int d\omega |\Pi(\omega)|^2 \quad , \quad \lambda^\pm = \int d\omega \sum_r \gamma^\pm_r(\omega) |\Pi(\omega)|^2 \quad , \quad \lambda_r = \int d\omega \gamma_r(\omega) |\Pi(\omega)|^2 \,, \tag{4.16}$$

and

$$\Pi(\omega) = \frac{1}{\omega - \epsilon - \sigma(\omega)} \quad , \quad \sigma(\omega) = \int d\omega' \frac{\sum_r \gamma_r(\omega')}{\omega - \omega' + i\eta} \,. \tag{4.17}$$

Furthermore we have used the definition

$$\gamma_r(\omega) = M\gamma_r^+(\omega) + \gamma_r^-(\omega) \,, \tag{4.18}$$

and note the property that

$$\sum_r \lambda_r = M\lambda^+ + \lambda^- = 1 \,. \tag{4.19}$$

The factor $M$ occuring in these equations is the degeneracy of the dot state and thus is given by $M = 1$ here. It is introduced because we will see in the next section that the same solution with $M > 1$ will hold for the interacting quantum dot as well. We note that for $M = 1$ we have $\gamma_r(\omega) = , ^r(\omega)/(2\pi)$ since the Fermi functions cancel.

Using the above solution and (4.13) we obtain for the transition rates entering the kinetic equation $\Sigma_{10} = 2\pi\lambda^+/\lambda$ and $\Sigma_{01} = 2\pi\lambda^-/\lambda$, or more explicitly

$$\Sigma_{10} = \frac{1}{\lambda}\int d\omega \frac{\sum_r , ^r(\omega) f_r^+(\omega)}{|\omega - \epsilon - \sigma(\omega)|^2} \quad , \quad \Sigma_{01} = \frac{1}{\lambda}\int d\omega \frac{\sum_r , ^r(\omega) f_r^-(\omega)}{|\omega - \epsilon - \sigma(\omega)|^2} \,. \tag{4.20}$$

In the numerator of these equations we recognize the golden rule transition rates. The denominator describes a renormalization and a broadening of the dot excitation energy $\epsilon$ by the real and imaginary part of $\sigma(\omega)$. Since $M = 1$ we get

$$\mathrm{Re}\sigma(\omega) = \frac{1}{2\pi} P \int d\omega' \frac{, (\omega')}{\omega - \omega'} \quad , \quad \mathrm{Im}\sigma(\omega) = -\frac{1}{2}, (\omega) \,, \tag{4.21}$$

where , $= \sum_r , ^r$ and $P\int$ denotes the principal value integral. The renormalization and broadening are independent of temperature and bias voltage. This is the reason why quantum fluctuations in noninteracting systems do not result in anomalies in the zero-temperature limit. Furthermore, for nearly constant density of states in the reservoirs the energy dependence of , $(\omega)$ will be weak. This means that the renormalization is small and the broadening nearly a constant.

If , is energy independent we have $\sigma = i, /2, \lambda = 2\pi/, ,$ and $\lambda_r = , {}^r/, ,$ which gives for the transition rates

$$\Sigma_{10} = \int d\omega \sum_r , {}^r f_r^+(\omega)\delta_\Gamma(\omega - \epsilon) \quad , \quad \Sigma_{01} = \int d\omega \sum_r , {}^r f_r^-(\omega)\delta_\Gamma(\omega - \epsilon)\,, \tag{4.22}$$

and, after some algebra, for the current rates

$$\Sigma_{01}^r = \int d\omega, {}^r f_r^-(\omega)\delta_\Gamma(\omega - \epsilon) \quad , \quad \Sigma_{00}^r = -\int d\omega, {}^r f_r^+(\omega)\delta_\Gamma(\omega - \epsilon)\,, \tag{4.23}$$

where the function

$$\delta_\Gamma(\omega) = \frac{1}{\pi}\frac{, /2}{\omega^2 + (, /2)^2} \tag{4.24}$$

has been introduced which has a lorentzian form with half-width , . If we replace this function by a Dirac delta function we would obtain the golden rule theory. This result expresses a very important feature of noninteracting systems with constant , . One can just use elementary golden rule theory and obtains the exact solution by simply smearing out the energy conservation by , ! It is remarkable that this property even holds when time-dependent fields are present [14]. It is basically due to the fact that the broadening of the dot excitation energy is a constant and does not depend on energy, temperature or bias voltage. We will see in the next section that the behaviour is very different in interacting systems.

Using (4.11), (4.12), (4.14), (4.15), and (4.20), we find for the stationary tunneling current after some elementary manipulations

$$I_r = \frac{e}{h}\sum_{\substack{r' \\ r' \neq r}} \int d\omega T_{rr'}(\omega)\left[f_r(\omega) - f_{r'}(\omega)\right] , \tag{4.25}$$

where the one-particle transmission probability is given by

$$T_{rr'}(\omega) = \frac{M, {}^r(\omega), {}^{r'}(\omega)}{(\omega - \epsilon - \mathrm{Re}\sigma(\omega))^2 + (\mathrm{Im}\sigma(\omega))^2}\,. \tag{4.26}$$

This formula agrees with the well-known Landauer-Büttiker formalism [88, 16] and is discussed in detail in Ref. [17]. In linear response, we have $\mu_r = \mu + \delta\mu_r$. With

$e\delta\bar{V}_r = \delta\mu_r$ we obtain $I_r = \sum_{r'} G_{rr'}(\delta\bar{V}_r - \delta\bar{V}_{r'})$ with the conductance matrix given by the Breit-Wigner formula

$$G_{rr'} = -2\pi\frac{e^2}{h}\frac{, ^r, ^{r'}}{,}\int d\omega\delta_\Gamma(\omega)f'(\omega+\epsilon-\mu)\,, \tag{4.27}$$

where we have neglected the energy dependence of $, ^r(\omega)$.

For $T \gg ,$ (incoherent or sequential tunneling limit), we obtain

$$G_{rr'} = -2\pi\frac{e^2}{h}\frac{, ^r, ^{r'}}{,}f'(\epsilon-\mu) \quad , \quad G^{max}_{rr'} = 2\pi\frac{e^2}{h}\frac{, ^r, ^{r'}}{, ^2}\frac{,}{T}\,, \tag{4.28}$$

i.e. a symmetric line shape of the resonance around $\epsilon = \mu$ with exponential tails. With decreasing temperature the line width decreases $\sim T$ and the height of the resonance increases $\sim 1/T$.

For $T \ll ,$ (coherent or resonant tunneling limit), we obtain

$$G_{rr'} = 2\pi\frac{e^2}{h}\frac{, ^r, ^{r'}}{,}\delta_\Gamma(\epsilon-\mu) \quad , \quad G^{max}_{rr'} = \frac{e^2}{h}\frac{, ^r, ^{r'}}{(, /2)^2}\,, \tag{4.29}$$

i.e. the line shape saturates at zero temperature to a lorentzian form reflecting the energy dependence of the transmission probability. For the special case of two reservoirs which couple symmetrically to the dot, the height of the resonance is given by the quantum conductance $e^2/h$. Compared to the incoherent limit we see that quantum fluctuations tend to suppress the conductance and broaden the line shape. The same qualitative behaviour will also be obtained in the interacting case described in the following sections. However, we will see that the line shape has no longer to be symmetrically, there can be logarithmic temperature or bias voltage dependences of peak position, peak height and broadening, and we will find interesting anomalies for the differential conductance as function of the bias voltage. All these features are completely absent in the noninteracting case, since the renormalization and broadening of the dot level have no interesting structure.

## 4.3 Interacting quantum dot

In this section we will study a more realistic and interesting case, namely the presence of two relevant excitation energies $\epsilon_\sigma = E_{s_\sigma} - E_{s_0}$, with $\sigma = \uparrow, \downarrow$, in the dot. As explained in section 2.3.3, this model is equivalent to the infinite-U impurity Anderson model in nonequilibrium which is described by the Hamiltonian (2.73)

$$H(t) = \sum_{k\sigma r} \epsilon_{kr} a^\dagger_{k\sigma r} a_{k\sigma r} + \sum_\sigma \epsilon_\sigma c^\dagger_\sigma c_\sigma + U n_\uparrow n_\downarrow + \sum_{k\sigma r} (\bar{T}^r_k(t) a^\dagger_{k\sigma r} c_\sigma \; + \; h.c.)\,, \qquad (4.30)$$

with $U \to \infty$ being the largest energy scale.

The significance of this equivalence lies in the fact that it is known from equilibrium theory that the Anderson model reveals a very interesting low-temperature behaviour. For degenerate energies $\epsilon = \epsilon_\uparrow = \epsilon_\downarrow$ and in the Kondo regime $\epsilon \ll -,$ , the system shows resonant transmission at zero temperature although the level position is far away from the Fermi level (defined at zero energy). The reason is that the transmission probability develops a Kondo resonance at the Fermi level by decreasing temperature below the Kondo temperature $T_K \sim (U,\ )^{1/2} \exp(\pi\epsilon/,\ )$ [11, 96, 60]. The height of this resonance increases $\sim \ln(T_K/T)$ and saturates for very low temperatures. At zero temperature the Kondo resonance is decreasing when the level $\epsilon$ approaches $-,$ from below since the system leaves the Kondo regime. However, at finite temperatures the situation is different. The Kondo resonance is only significant for $T < T_K$ which means that $|\epsilon| <$ , $\ln(U,\ /T^2)$. For reasonable temperatures this implies that the Kondo resonance is only visible for $\epsilon \sim -,$ . This is the cross-over from the Kondo regime to the mixed valence regime and corresponds roughly to the optimal value for the height of the resonance at the Fermi level.

The idea to test these features by measuring zero-bias anomalies of the differential conductance has a long history and many experiments have been performed [2, 65, 26, 147]. The disadvantage there is that the current is measured through an ensemble of

impurities and the control over physical parameters like coupling constants or impurity level positions is weak. Therefore the idea was formulated to test such features by measuring the conductance through quantum dots [109, 43, 71]. Various calculations were performed for the differential conductance as function of the bias voltage [58, 103, 107, 148] with the result of a zero-bias anomaly in the form of a maximum in the Kondo regime. It was predicted that the Kondo resonance splits by an applied bias and is shifted by Zeeman splitting [103]. The latter leads to a splitting of the zero-bias maximum. These features have been observed experimentally by Ralph & Buhrman [118]. They measured the differential conductance through single charge traps in a metallic quantum point contact. Although this system does not allow a controlled variation of the level position, the appearance of a zero bias maximum with a peak height varying logarithmically with temperature clearly demonstrates the mechanism of Kondo assisted tunneling. A detailed comparism of the line shape between experiment and theory can be found in Ref. [78]. The influence of external time dependent fields or bosonic environments was studied in Refs. [59, 77, 78] with the result of side band anomalies in the differential conductance and pump effects. A closer investigation of the zero-bias anomaly reveals a cross-over of the zero-bias maximum to a zero-bias minimum by shifting the level position of the dot through the Fermi level [77]. Further studies of the Kondo effect in quantum dots involve the AC-conductance in linear response [108], Aharonov-Bohm oscillations [13], and the study of double dots or dots with multiple levels [116].

To understand some of these results let us apply the resonant tunneling approximation. It can be evaluated analytically for the degenerate case which we will consider from now on. First we note that due to spin conservation the reduced density matrix of the dot is diagonal once it is diagonal at the initial time. Analog to (4.11)-(4.13) we

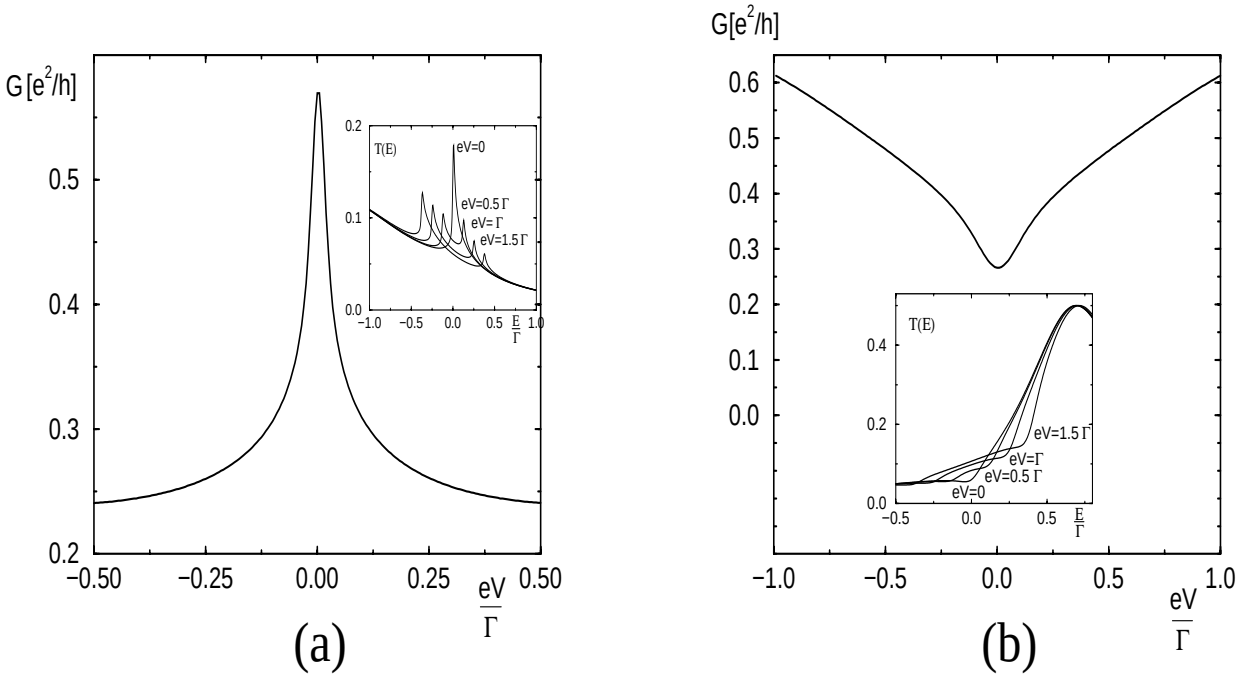


Figure 4.2: (a) The differential conductance vs. bias voltage for , $^L$ = , $^R$ = , /2, $T$ = 0.01, , $V_D$ = 0, $\epsilon$ = −4, and $E_C$ = 100, . The curve shows a maximum at zero bias. Inset: increasing voltage leads to an overall decrease of the transmission probability in the range $|E| < eV$. (b) The differential conductance vs. bias voltage for , $^L$ = , $^R$ = , /2, $T$ = 0.05, , $V_D$ = 0, $\epsilon$ = 0 and $E_C$ = 100, . The curve shows a minimum at zero bias. Inset: increasing voltage leads to an overall increase of the transmission probability in the range $|E| < eV$.

get

$$0 = \Sigma_{0\sigma} P_\sigma - \Sigma_{\sigma 0} P_0 \,, \tag{4.31}$$

$$I_r = -e(\Sigma^r_{00} P_0 + 2\Sigma^r_{0\sigma} P_\sigma) \,, \tag{4.32}$$

and

$$\Sigma_{\sigma 0} = -\frac{1}{2}\sum_r \Sigma^r_{00} \quad , \quad \Sigma_{0\sigma} = \sum_r \Sigma^r_{0\sigma} \,, \tag{4.33}$$

where $|\sigma>$ denotes the singly occupied dot with spin $\sigma$. The solution for $\Sigma^r_{0\sigma}$ and $\Sigma^r_{00}$ is given by (4.14) and (4.15) with $M = 2$. The transition rates $\Sigma_{\sigma 0}$ and $\Sigma_{0\sigma}$ follow from (4.20) and the tunneling current from (4.25) and (4.26).

The essential difference to the noninteracting case is the different value for $M$. Since there are $M = 2$ possibilities for an electron to tunnel onto the dot, we have to

multiply the golden rule tunneling "in" rate $\gamma_r^+$ in (4.18) with $M$. Adding the golden rule tunneling "out" rate $\gamma_r^-$, we obtain an estimate for the inverse finite life-time of the dot excitation. This is expressed by the imaginary part of $\sigma(\omega)$ which is proportional to this sum

$$\mathrm{Im}\sigma(\omega) = -\pi \sum_r \gamma_r(\omega) = -\frac{1}{2}\sum_r ,^r(\omega)(1 + f_r(\omega)) . \tag{4.34}$$

We see that the broadening depends now on the Fermi functions and is therefore temperature and voltage dependent. When energy increases the broadening decreases, i.e. we expect quantum fluctuations to become weaker if we increase $\epsilon$. From the Kramers-Kronig relation we have necessarily also a renormalization which is given by the real part of $\sigma(\omega)$. We obtain

$$\mathrm{Re}\sigma(\omega) = \frac{1}{2\pi}\sum_r ,^r(\omega)\left[\psi(\frac{1}{2} + \frac{\beta E_C}{2\pi}) - \mathrm{Re}\psi(\frac{1}{2} + i\frac{\beta}{2\pi}(\mu_r - \omega)) + \pi\frac{\omega - \mu_r}{2E_C}\right] , \tag{4.35}$$

where $\psi$ is the digamma function and we have chosen a lorentzian form for the energy dependence of $,^r(\omega)$ with half-width $E_C$

$$,^r(\omega) = ,^r\frac{E_C^2}{(\omega - \mu_r)^2 + E_C^2} . \tag{4.36}$$

The cut-off will be of the order of the charging energy $E_C$ since we do not allow for two electrons to tunnel onto the dot. The renormalization depends logarithmically on temperature and voltage

$$\mathrm{Re}\sigma(\omega) \approx \frac{1}{2\pi}\sum_r ,^r \ln\frac{E_C}{\max(2\pi T, |\mu_r - \omega|)} . \tag{4.37}$$

For low enough temperatures this leads to a logarithmic increase of the renormalization when $\omega$ approaches the effective potentials $\mu_r$ of the reservoirs. As a consequence the transmission probability (4.26) has a maximum near $\omega \approx \mu_r$ since there is a solution of $\omega - \epsilon - \mathrm{Re}\sigma(\omega) = 0$ near these values. This indicates the occurence of the Kondo resonance and explains the splitting when the potentials $\mu_r$ are not equal (see inset of

Fig. 4.2a). Since $\mathrm{Re}\sigma(\mu_r) \sim \, , /(2\pi)\ln(E_C/(2\pi T)$ for $|\mu_r - \mu_{r'}| \sim T \ll E_C$, the Kondo resonance can only occur for

$$\mu_r - \epsilon < \frac{,}{2\pi} \ln \frac{E_C}{2\pi T} \,, \tag{4.38}$$

and $\epsilon < \mu_r$. This gives roughly $T < T_K \sim E_C/(2\pi)\exp\left(-2\pi(\mu_r - \epsilon)/, \right)$ which agrees qualitatively but not quantitatively with the Kondo temperature given above due to the different factor in the exponent. This factor cannot be determined precisely within the resonant tunneling approximation because not all logarithmic terms of the kernels $\Sigma$ in $0(, )^3$ have been taken into account. Nevertheless, the qualitative form of the solution is correct.

To illustrate the consequences for the current let us start with the incoherent limit $T \gg , \,.$ In this case we can neglect the renormalization and the transmission probability is a sharp function around $\omega \sim \epsilon$. Neglecting the energy dependence of $, ^r(\omega)$ we can replace the transmission probability in formula (4.25) by

$$T_{rr'}(\omega) \to -2\pi \frac{, ^r , ^{r'}}{\mathrm{Im}\sigma(\epsilon)} \delta(\omega - \epsilon) \,, \tag{4.39}$$

which, using (4.34), gives for the conductance matrix in linear response

$$G_{rr'} = -4\pi \frac{e^2}{h} \frac{, ^r , ^{r'}}{,} \frac{1}{1 + f(\epsilon - \mu)} f'(\epsilon - \mu) \,, \tag{4.40}$$

which agrees with (2.145). As expected the line shape is asymmetric since the broadening of $\epsilon$ depends on $\mu$. This result shows a clear difference to the noninteracting case where the line shape is symmetric. It shows up already in the high temperature regime and can be calculated also from the golden rule approach as shown in section 2.4.2. The asymmetry was first predicted in Ref. [9] but has never been identified experimentally.

In the coherent regime $T \ll , \,,$ the real part of $\sigma(\omega)$ becomes important. As already explained above, the resonance of the transmission probability at the Fermi levels is

only significant for $\mu_r - \epsilon \sim$ , since the Kondo temperature depends exponentially on $\mu_r - \epsilon$. In this regime the relevant energy scale for the onset of quantum fluctuations is , . In Fig. 4.2 we show the differential conductance $G = dI/dV$ $(I = I_R = -I_L)$ as function of the bias voltage $V = V_L - V_R$ for $\epsilon + eV_D \sim -$, and $\epsilon + eV_D \sim 0$. Thereby we have chosen $V_L = -V_R = V/2$ and used (2.25) for $eV_D$ with symmetric capacitances $C_L = C_R$. This gives $eV_D = C_g/CeV_g$ independent of the bias voltage. For a low lying level a pronounced zero bias maximum is developed which is due to the fact that the Kondo resonances of the transmission probability at $\omega = \mu_r$, $r = L, R$, are split by the bias voltage and decrease in magnitude (see inset of Fig. 4.2a). In contrast, for $\epsilon + V_D$ near the electrochemical potentials of the reservoirs, a zero bias minimum is observed although the Kondo resonances are absent. This is due to the fact that the nontrivial structure of the real part of $\sigma(\omega)$ is still present and influences the differential conductance always for $T \ll$ , independent wether the transmission probability shows Kondo resonances or not. The striking difference of the zero-bias anomaly for different values of $V_D$ or $V_g$ motivates an interesting experiment which can only be performed with devices where the effective positions of the dot excitations can be varied by an external gate voltage.

## 4.4 Metallic island

In this section we study quantum fluctuation effects for the infinite-Z metallic island. For the single channel case we refer to Refs. [45, 99, 38]. As already explained in section 2.2 and 2.4.3, single-electron phenomena are usually described within the "orthodox theory" [85, 5] which treats tunneling in lowest order perturbation theory (golden rule) and corresponds to the classical picture of incoherent tunneling processes (sequential tunneling). As a necessary condition one needs weak tunneling, i.e., the conductance of the barriers has to be low $\alpha_0 \ll$. Despite the success of this straighforward approach,

it was found experimentally and theoretically that there are several regimes where coherent tunneling processes have to be taken into account.

First, in the Coulomb blockade regime, sequential tunneling is exponentially suppressed. The most simple contribution to the current is a second-order coherent process in which electrons tunnel via a virtual state of the island. Averin and Nazarov calculated the contribution of this "inelastic cotunneling" process to the current via the transition rate from the initial to the final state at zero temperature [6]. At finite temperature, divergences occur, but the authors of Ref. [6] gave an approximate estimation which is valid far away from the resonances and supposed that some regularization procedure has overcome the divergences. The results were confirmed experimentally [40, 104] (for more details see chapter 6 of Ref. [48]). However, attempts to regularize the expression of electron cotunneling at resonance by introducing a constant finite-life time of the charge excitations did not reveal any significant change of the maximal conductance [81, 106, 7, 87, 112, 41].

Second, it was found recently [123, 76, 80] that even at resonance, where sequential tunneling is not suppressed, higher order processes are important and can lead to a significant change of the conductance. Similiar effects were discussed for the average charge of the single-electron box in the equilibrium situation [86, 98, 47, 29, 49, 150]. The diagrammatic real-time technique described in chapter 3 was used within the resonant tunneling approximation in order to give a systematic description of the various tunneling processes [123, 76]. The effects from quantum fluctuations were shown to become observable either for strong tunneling $\alpha_0 \sim 1$ or at low enough temperatures $\alpha_0 \ln E_C/T \sim 1$, where $E_C$ denotes the charging energy. The predicted broadening of the conductance peak as well as the reduction of its height was confirmed qualitatively in an experiment by Joyez et al. [69] in the strong tunneling regime. Within the theory, only processes where the two classically occupied charge states are involved (even

virtually) were included. Therefore, it was necessary to introduce a band-width cut-off $\sim E_C$, which prohibits a comparism with experiment without fitting parameters. In a subsequent paper [80], the same diagrammatic technique was used to obtain the total current in second order in $\alpha_0$ including all relevant processes such that no cut-off remained. All terms were regularized in a natural way. At resonance new contributions were obtained compared to the previous theory of electron cotunneling. A comparism with recent experiments [69] showed good agreement without fitting any parameter.

Let us show the results of the resonant tunneling approximation more explicitly. We assume that only one excitation energy $\Delta_N = E_{N+1} - E_N$ with $E_N = E_C N^2$ lies within the relevant energy range of the effective potentials $e\bar{V}_r = eV_r - eV_D$ of the reservoirs. This means that the charging energy $E_C$ is assumed to be much larger than temperature and bias voltage so that the other excitations are irrelevant. Without loss of generality we can set $N = 0$.

In the absence of time-dependent fields and the heat bath, the Hamiltonian follows from (2.82) and (2.83)

$$H(t) = \sum_{qr} \omega_q^r (c_{qr}^\dagger c_{qr} + d_{qr}^\dagger d_{qr}) + \Delta_0 \hat{P}_1 + \sum_{qr} (\bar{g}_q^r(t)(c_{qr}^\dagger + d_{qr})\hat{P}_{01} + h.c.)\,, \qquad (4.41)$$

where the time dependence of the coupling constants is only due to the static voltages $\bar{g}_q^r(t) = g_q^r \exp(i\mu_r(t - t_0))$. This Hamiltonian looks very similiar to (2.70) or (4.10) where we considered a quantum dot with one excitation energy. However, the important difference here is that the field operators $c, d$ correspond to bosons whereas in (2.70) we had to deal with Fermi statistics. Therefore, the resonant tunneling approximation does not turn out to be exact here, since the cancellation of all diagrams left out within this approximation is essentially due to the sign which occurs by changing the order of Fermi field operators. Nevertheless, we can apply the resonant tunneling approximation here as well and we obtain the same solution as in the fermionic case

for $M = 1$ but with the replacements , ${}^{r}(\omega) \to 2D_r(\omega - \mu_r)$, $f_r^{\pm} \to n_r^{\pm}$, $\gamma_r^{\pm} \to \alpha_r^{\pm}$, and $\gamma_r \to \alpha_r = \alpha_r^{+} + \alpha_r^{-}$, where $D_r(\omega)$ and $\alpha_r^{\pm}$ are defined in (2.89) and (2.174).

The tunneling current is given by (4.25) but the Fermi functions in this expression are replaced by Bose distributions. Therefore, $T_{rr'}$ is a transmission probability between Bose reservoirs [16]. Inserting (4.26) together with the above mentioned replacements, and performing some elementary manipulations, we can rewrite the current as

$$I_r = \frac{e}{h} \sum_{\substack{r' \\ r' \neq r}} \int d\omega T^F_{rr'}(\omega) \left[ f_r(\omega) - f_{r'}(\omega) \right] , \tag{4.42}$$

where $T^F_{rr'}$ is the transmission probability between the original Fermi reservoirs

$$T^F_{rr'}(\omega) = 4\pi^2 \frac{\alpha_r(\omega)\alpha_{r'}(\omega)}{(\omega - \Delta_0 - \mathrm{Re}\sigma(\omega))^2 + (\mathrm{Im}\sigma(\omega))^2} . \tag{4.43}$$

Renormalization and broadening effects are described by the real and imaginary part of $\sigma(\omega)$

$$\sigma(\omega) = \int d\omega' \frac{\sum_r \alpha_r(\omega')}{\omega - \omega' + i\eta} . \tag{4.44}$$

We see that in contrast to the fermionic case the bosonic distribution functions $n_r^{\pm}$ occuring in $\alpha_r^{\pm}$ do not cancel in the sum $\alpha_r$. Like in the quantum dot case with two excitations, this gives rise to a broadening which depends on energy, temperature and voltage, and via Kramers Kronig to a nontrivial renormalization. Explicitly, we get

$$\mathrm{Im}\sigma(\omega) = -\sum_r D_r(\omega - \mu_r)(1 + 2n_r(\omega)) , \tag{4.45}$$

$$\mathrm{Re}\sigma(\omega) = -\frac{1}{\pi} \sum_r D_r(\omega - \mu_r)[\psi(\frac{E_C}{2\pi T}) + \psi(1 + \frac{E_C}{2\pi T}) - 2\mathrm{Re}\psi(i\frac{|\omega - \mu_r|}{2\pi T})] , \tag{4.46}$$

where we have chosen a lorentzian form for $D_r(\omega)$ with half-width $E_C$

$$D_r(\omega) = \pi \alpha_0^r \omega \frac{E_C^2}{\omega^2 + E_C^2} , \tag{4.47}$$

and $\alpha_0^r$ is the dimensionless conductance of barrier $r$ defined in (2.90). For very low temperatures we get

$$\mathrm{Im}\sigma(\omega) \approx -\pi \sum_r \alpha_0^r |\omega - \mu_r| \,, \tag{4.48}$$

$$\mathrm{Re}\sigma(\omega) \approx -2 \sum_r \alpha_0^r (\omega - \mu_r) ln \frac{E_C}{|\omega - \mu_r|} \,. \tag{4.49}$$

The broadening is proportional to energy since the number of available states for tunneling on or off the island is also proportional to energy (compare (2.17)). In contrast to the interacting quantum dot in the previous section, the renormalization is zero for $\omega \sim \mu_r$. Therefore, no additional resonances occur here for the transmission probability but we still have a logarithmic shift of the excitation energy $\Delta_0$.

The renormalization of $\Delta_0$ is determined by finding the maximum of the transmission probability (4.43) which is approximately determined by solving the self-consistent equation

$$\tilde{\Delta}_0 = \Delta_0 + \mathrm{Re}\sigma(\tilde{\Delta}_0) \,. \tag{4.50}$$

In a first approximation we use $\tilde{\Delta}_0$ for the value of $\omega$ inside the $\psi$-function of the real part of $\sigma$ given by (4.46). We obtain for $\omega \ll E_C$

$$\omega - \Delta_0 - \mathrm{Re}\sigma(\omega) = Z^{-1}(\omega - \tilde{\Delta}_0) \,, \tag{4.51}$$

with the renormalization factor $Z$ defined by

$$Z^{-1} = 1 + \sum_r \alpha_0^r [\psi(\frac{E_C}{2\pi T}) + \psi(1 + \frac{E_C}{2\pi T}) - 2\mathrm{Re}\psi(i\frac{|\tilde{\Delta}_0 - \mu_r|}{2\pi T})] \,. \tag{4.52}$$

Within this approximation the transmission probability reads

$$T_{rr'}^F(\omega) = 4\pi^2 \frac{\tilde{\alpha}_r(\omega)\tilde{\alpha}_{r'}(\omega)}{(\omega - \tilde{\Delta}_0)^2 + (\mathrm{Im}\tilde{\sigma}(\omega))^2} \,, \tag{4.53}$$

where $\tilde{\alpha}_r$ and $\tilde{\sigma}$ are defined as before but multiplied with $Z$. This can be interpreted as a renormalization of the dimensionless conductance $\alpha_0^r$

$$\tilde{\alpha}_0^r = Z\alpha_0^r \,. \tag{4.54}$$

What we mean by renormalization becomes clear when we neglect the broadening in (4.53) which is described by the imaginary part of $\tilde{\sigma}$. This is justified if $\tilde{\alpha}_0^r \ll 1$. We obtain

$$T_{rr'}^F(\omega) = 4\pi^2 \frac{\tilde{\alpha}_r(\tilde{\Delta}_0)\tilde{\alpha}_{r'}(\tilde{\Delta}_0)}{\tilde{\alpha}(\tilde{\Delta}_0)} \delta(\omega - \tilde{\Delta}_0)\,. \tag{4.55}$$

This is precisely the golden rule result (2.178) for the transmission probability but with renormalized parameters.

In certain limits we can estimate the renormalized parameters. We take $V_L = -V_R = V/2$, $V_D = 0$ (otherwise one has to shift the excitation energy $\Delta_0$ by $V_D$), and $\alpha_0^L = \alpha_0^R = \alpha_0/2$. If one of the energy parameters $\tilde{\Delta}_0$, $T$, or $eV$ is large compared to the other two ones but small compared to the charging energy, we obtain for the renormalization factor

$$Z = \frac{1}{1 + 2\alpha_0 \ln \frac{E_C}{\max(|\tilde{\Delta}_0|, 2\pi T, |eV|/2)}}\,. \tag{4.56}$$

We note that $\alpha_0$ is the sum of the dimensionless conductances of all barriers. The renormalized parameters follow from

$$\tilde{\Delta}_0 = Z\Delta_0 \quad , \quad \tilde{\alpha}_0^r = Z\alpha_0^r\,. \tag{4.57}$$

For the derivation we have used the asymptotic expansion $\psi(z) = \ln(z)$, for $|z| \to \infty$. These equations agree with the renormalization group results performed for the equilibrium case $V_r = 0$ [98, 29]. This shows that the leading logarithmic terms are included within the resonant tunneling approximation. However, we have achieved more than renormalization group here since we do not need all the approximative steps used so far. We can handle all intermediate regimes for the three energy parameters described before and can account for the broadening of the charge excitations by not neglecting the imaginary part of $\sigma$ in (4.53). The latter can be estimated to be of the

order $\hbar/\tau \sim \mathrm{Im}\sigma(\tilde{\Delta}_0)$ which gives within the same limits discussed before

$$\frac{\hbar}{\tau} \sim \pi\tilde{\alpha_0}\max(|\tilde{\Delta}_0|, 2T, |eV|/2)\,. \tag{4.58}$$

which agrees with (2.17). We see that broadening effects are important for $\tilde{\alpha}_0 > 0.1$ which means that they can only be enhanced by lowering the tunneling barriers. Renormalization effects are important for

$$\max(|\tilde{\Delta}_0|, 2\pi T, |eV|/2) < E_C e^{-1/(2\alpha_0)}\,, \tag{4.59}$$

which means that they can be enhanced either by lowering the tunneling barriers or by lowering all the other energy parameters.

Let us demonstrate the influence of quantum fluctuations on the differential conductance as function of the gate voltage. Again we set $V_L = -V_R = V/2$ and $\alpha_0^L = \alpha_0^R = \alpha_0/2$. We study $G = dI/dV$, with $I = I_R = -I_L$, as function of $\Delta_0$ and set $V_D = 0$ (equivalently we could study $G$ as function of $eV_D = C_g/CeV_g$ and keep $\Delta_0$ fixed). We insert the transmission probability (4.53) including the broadening into the current formula (4.42). Using the result (4.56) for the renormalization factor, we find in the two limits $T \ll |eV|$ and $|eV| \ll T$ that the differential conductance at $\Delta_0 = \tilde{\Delta}_0 = 0$ is given by

$$2G(\Delta_0 = 0)R_T = \frac{Z}{2} = \frac{1}{2}\frac{1}{1 + 2\alpha_0 \ln \frac{E_C}{\max(2\pi T, |eV|/2)}}\,, \tag{4.60}$$

where $R_T = R_T^L = R_T^R$ is the resistance of a single barrier. The golden rule result (2.185) is $2G(\Delta_0 = 0)R_T = 1/2$ and corresponds to $1/2$ of the ohmic resistance since all the other excitation energies are suppressed by the Coulomb blockade. We see that due to quantum fluctuations, the differential conductance is no longer a constant at the symmetry point but decreases logarithmically with bias voltage or temperature. We note that the qualitative effect of quantum fluctuations is again a suppression of the

differential conductance like it was the case for quantum dots. It is not suprising that the differential conductance for the noninteracting quantum dot case saturates at low temperatures whereas it decreases for the metallic island since the golden rule results are already different for the two cases.

The broadening of the line shape of the differential conductance can be estimated by noting that the integral of $G(\Delta_0)$ over $\Delta_0$ is not influenced by quantum fluctuations and can be directly calculated from (4.42) and (4.43) as

$$\int d\Delta_0 G(\Delta_0) R_T = \frac{1}{3}|eV| \quad , \quad \text{for } T \ll |eV| \,, \tag{4.61}$$

$$= \frac{\pi^2}{8} T \quad , \quad \text{for } |eV| \ll T \,. \tag{4.62}$$

Together with the value at the symmetry point we conclude that quantum fluctuations lead to a broadening that increases logarithmically with bias voltage or temperature if we measure $\Delta_0$ in units of $|eV|$ or $T$.

Both features, the logarithmic decrease of $G(\Delta_0 = 0)$ and the logarithmic increase of the broadening with bias voltage or temperature is demonstrated in Fig. 4.3. In linear response these effects have been observed experimentally [69] and a detailed fit between experiment and theory can be found in Ref. [80].

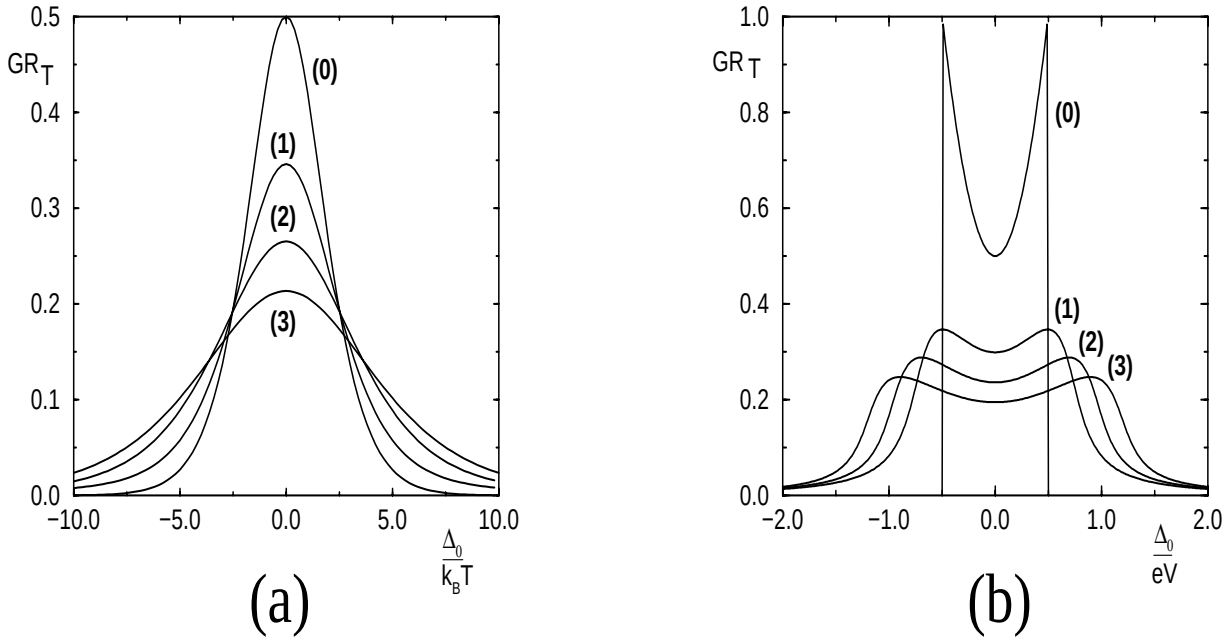


Figure 4.3: (a) The differential conductance in linear response (V=0) for the metallic island as a function of the excitation energy $\Delta_0$ normalized to the temperature $T$ with $\alpha_0^L = \alpha_0^R = 0.05$ and (1) $T/E_C = 0.1$, (2) $T/E_C = 0.01$, (3) $T/E_C = 0.001$. For comparison, (0) shows the golden rule result, which is independent of the temperature $T$. (b) The differential conductance in nonlinear response for the metallic island as a function of the excitation energy $\Delta_0$ normalized to the transport voltage $eV$ with $\alpha_0^L = \alpha_0^R = 0.05$, $T = 0$ and (1) $eV/E_C = 0.1$, (2) $eV/E_C = 0.01$, (3) $eV/E_C = 0.001$. For comparison, (0) shows the golden rule result, which is independent of the transport voltage $eV$.

# Chapter 5

# Conclusions

Within this paper we have tried to analyse some aspects related to a very fundamental problem of statistical mechanics, namely the interaction between a large environment and a small mesoscopic system. To make contact to experimentally realizable systems, we concentrated on particle exchange through high tunneling barriers and heat exchange in the form of a fluctuating voltage. For the environment we have chosen metallic electronic reservoirs with different electrochemical potentials and a heat bath consisting of free bosonic modes. The mesoscopic system is realized by a strongly interacting quantum dot. From statistical mechanics for macroscopic systems being in contact with large particle reservoirs we would expect a grandcanonical ensemble for the equilibrium case. There are three interesting aspects which come into play if we make the system smaller. First, the energy scale associated with the coupling between system and environment can be so large that quantum fluctuations lead to a complete deviation from a grandcanonical ensemble. In macroscopic systems, the coupling to the environment is always a surface effect which can be negleted in the thermodynamic limit. Second, the energy scale characterizing the distance between the one-particle excitation energies of the mesoscopic system can be so large that the discreteness of the density of states becomes visible on experimentally contrallable voltage scales. This demands the consideration of finite size effects and strong capacitive interactions. Third,

the nonequilibrium stationary state induced by different electrochemical potentials on the reservoirs can no longer be described by a local equilibrium distribution.

Therefore, we have aimed at presenting a nonequilibrium theory in chapter 3 which is capable of providing a nonperturbative analysis in the coupling between an environment and a strongly correlated finite system. The approach is similiar to techniques used for two- or multi-level systems in connection with a heat bath [140]. We have generalized the environment to include particle reservoirs. They can have different electrochemical potentials so that a nonequilibrium stationary state results which cannot be described by a grandcanonical ensemble. As a consequence, a stationary current will flow through the system which can easily be measured experimentally. We have derived formally exact kinetic equations together with systematic rules how to calculate the kernels entering these equations. The kernels in lowest order perturbation theory in tunneling provide a generalization of golden rule theory to the description of time-dependent stationary states and transient phenomena. This is similiar to the noninteracting blip approximation in spin boson models [89, 140]. Furthermore, we have presented an approximation to resum an infinite series of higher order diagrams which describe quantum fluctuations. This is similiar to the study of the Lamb shift in quantum optics [39]. This provides the possibility to describe coherence between the environment and the mesoscopic system, e.g. in the form of coherent transport through the device. In noninteracting systems this is a well-established theory where the scattering formalism can be used [88, 16]. Famous coherent phenomena are weak localization in disordered systems from interference of time-reversed paths, and Aharonov-Bohm oscillations occuring by interference of paths which enclose a magnetic flux. The double barrier devices which are studied in this paper reveal another type of interference. An electron tunneling through the system can be reflected back and forth between the barriers. Depending on the number of reflections, many paths are possible which can

interfere in a constructive way if the length of the system is compatible with the Fermi wave length. This can lead to perfect transmission through the whole device even if the individual barriers are very high. For noninteracting systems, this phenomenon is usually described within a scattering formalism by simply calculating the transmission coefficient from elementary quantum mechanics. A different point of view is the usage of a tunneling Hamiltonian which has the advantage that a straightforward generalization to interacting systems can be achieved. Here one uses a basis of standing waves in the leads and the mesoscopic systems. The various processes are electrons hopping back and forth between reservoir and system using these states. Resumming processes from all orders of perturbation theory in tunneling within this picture is equivalent to studying interference of paths from electrons being reflected back and forth between the barriers. We have demonstrated this explicitly in section 4.2 for the simplest model of a quantum dot consisting of one single state. Therefore, the applications presented in this paper for strongly correlated quantum dots and metallic islands can be viewed as an attempt to generalize interference phenomena in mesoscopic systems in the presence of interactions. A challenge for future research is the implementation of renormalization group methods within nonequilibrium techniques based on kinetic equations and the generalization to open systems with perfectly transmitting channels to the reservoirs.

We have demonstrated that the measurement of the differential conductance $G$ as function of the gate voltage $V_g$ or the bias voltage $V$ can reveal all aspects described above. The discreteness of the dot excitation spectrum leads to resonances separated by the sum of level spacing and charging energy. This demonstrates the quantization of charge and energy. These single-electron phenomena are important tools for technological applications like single-electrometry, metrology and single-electronics. They can be understood on the level of golden rule theory which has been summarized in

chapter 2 for discrete and continuous spectra of the dot. Furthermore we have included bosonic baths and time-dependent fields which are of recent experimental interest.

Quantum fluctuations set on by lowering temperature or increasing tunneling. Whereas for noninteracting systems the effects on $G(V_g)$ are already well-known from Landauer-Büttiker theory, the presence of interactions can lead to an anomalous temperature dependence of height, broadening or position of the resonances. This reflects the presence of strong correlations.For spin degenerate and discrete excitation energies quantum fluctuations can create zero bias anomalies of $G(V)$ at fixed gate voltage as has been described in section 4.3. They can occur in the form of zero bias maxima or minima dependent on the postion of the excitation energies relative to the electrochemical potentials of the reservoirs. Metallic islands are described in section 4.4. Here, we have seen that a renormalization and a broadening of the charge excitations occur which depend on temperature, bias voltage and energy in a nontrivial way. As a consequence, the "orthodox" theory and the theory of electron cotunneling had to be generalized to include higher order processes which we have called resonant tunneling processes. Recent experiments demonstrate the observability of these effects. Due to the enormous variety of possible arrangements of dot systems and the experimental progress in realizing such devices, we expect that future research will reveal many more motivations for studying quantum fluctuations induced by strong coupling between mesoscopic systems and particle reservoirs.

# Acknowledgements

It is a pleasure to thank all my collaborators Y. Blanter, C. Bruder, P. Brune, R. Fazio, M. Hettler, J. König, T. Pohjola, M.M. Salomaa, J. Schmid, G. Schön, J. Stampe, and R. Ziegler who helped to find many of the results presented in this paper and in related subjects. Furthermore I acknowledge many helpful discussions with M. Büttiker, D. Esteve, P. Falci, H. Grabert, L.P. Kouwenhoven, D. Loss, Y.V. Nazarov, J. von Delft, A. Odintsov, U. Weiss, P. Woelfle, A. Zawadowski, A.D. Zaikin, G. Zimanyi and W. Zwerger. This work was supported by the Swiss National Science foundation and by the Deutsche Forschungsgemeinschaft through Sonderforschungsbereich 195.

# Appendix A

# Deutsche Zusammenfassung

In den letzten Jahren hat der Fortschritt in der Nanotechnologie zu einem großem Interesse an sehr kleinen leitenden Inseln geführt, die mit makroskopischen Zuleitungen kontaktiert werden. In diesen Systemen kann sowohl die Quantisierung der Ladung als auch der Energie experimentell beobachtet werden. Fügt man ein Elektron, d.h. eine Elementarladung, zu einem neutralen Elektronengas der Ausdehnung $L$ hinzu, so muß aufgrund der Coulomb-Wechselwirkung die Ladungsenergie $E_C \sim e^2/(\epsilon L) \sim e^2/(2C)$ aufgebracht werden, wobei $\epsilon$ die Dielektrizitätskonstante und $C$ die Selbstkapazität des Systems bezeichnen. Für Längen im Nanobereich ergeben sich Ladungsenergien in der Größenordnung $1-10K$, d.h. der Elektronentransport wird für Temperaturen $T < 1K$ signifikant durch diese Energieskala bestimmt. Dies führt u.a. zu dem Phänomen der Coulomb-Blockade, d.h. der Transport kann für bestimmte Werte der elektrochemischen Potentiale vollständig unterdrückt werden. Dies bedeutet das die mittlere Ladung auf der Insel durch externe Gatterspannungen diskret reguliert werden kann. In der gleichen Weise wird der Strom durch diskrete Energiespektren auf der Insel beeinflußt. Hier muß der Niveauabstand $\delta E$ aufgebracht werden. Speziell in Halbleiter-Quantenpunkten ist der Niveauabstand vergleichbar mit der Ladungsenergie. Dies impliziert die Möglichkeit Quantenpunkte mit künstlichen Atomen oder Molekülen zu vergleichen, deren Spektren durch Kontaktierung mit makroskopischen Zuleitungen

gemessen werden können.

Das Studium dieser Systeme ist von vielseitigem Interesse sowohl für Experimentatoren als auch für Theoretiker. Die Sensitivität gegenüber dem Hinzufügen einer einzigen Ladung kann für messtechnische Zwecke ausgenützt werden, wie z.B. die Messung einzelner Ladungen oder die Festsetzung eines Stromstandards. Elektronische Anwendungen sind Gegenstand intensiver Forschung und werden immer realistischer da die Arbeitstemperatur von Quantenpunkten immer weiter nach oben geführt wird. Weiterhin können Einzelelektron-Effekte für spektroskopische Messungen ausgenützt werden. Für Theoretiker stellen Quantenpunkte interessante stark korrelierte Systeme im Gleichgewicht oder Nichtgleichgewicht dar. Tieftemperatur-Methoden können durch direkten Vergleich mit dem Experiment getestet werden. Quantenpunkte weisen viele Analogien zu verallgemeinerten Kondo- und Anderson-Modellen auf. Diese Systeme sind von fundamentalem Interesse in der Theorie der stark korrelierten Fermionen. Gitter von Quantenpunkten können durch Hubbard-artige Modelle dargestellt werden. Die Kopplung eines Quantenpunktes an makroskopische Teilchen- und Wärmebäder stellt ein fundamentales Problem der statistischen Mechanik dar, nämlich die Zerstörung der Kohärenz in einem mesoskopischen System aufgrund des Austausches von Teilchen und Energie mit der Umgebung.

Viele Phänomene in Quantenpunkten können in Störungstheorie im Tunneln verstanden werden. Dies bedeutet, daß die Kopplung der Insel an die Reservoire klein ist und nicht zu einer Änderung der Spektraldichte des Quantenpunktes führt. In diesem Fall können klassische Mastergleichungen mit Raten in goldener Regel verwendet werden. Dieser Zugang wird als "orthodoxe" Theorie bezeichnet und beschreibt inkohärenten Transport, d.h. die Prozesse der herein- und heraustunnelnden Elektronen sind nicht zueinander korreliert. Zur Rechtfertigung der Störungstheorie muß angenommen werden, daß die intrinsische Verbreiterung der Einteilchen-Anregungen

der Insel klein gegenüber der Temperatur ist. Experimentell kann dies leicht erreicht werden indem man Tunnelbarrieren mit einem Widerstand $R_T$ verwendet, der wesentlich höher als der Quantenwiderstand $R_K = h/e^2 = 25.81281 \ldots k\Omega$ ist. Daher existiert ein wohldefinierter experimenteller Bereich wo Störungstheorie ausreichend ist um Einzelelektron-Transport bei Anwesenheit von diskreten Energiespektren zu beschreiben.

Es ist wichtig zu beachten, daß eine klassische Mastergleichung mit Raten in goldener Regel nur das Tunneln, aber nicht die Korrelationen auf der Insel störungstheoretisch behandelt. Daher muß dieser Zugang vom wohlbekannten Landauer-Büttiker Formalismus unterschieden werden, der zwar kohärenten Transport für beliebige Tunnelbarrieren und Temperaturen beschreiben kann, aber nur in wechselwirkungsfreien Systemen angewendet werden darf. Es ist daher wichtig eine Theorie zu formulieren, die zwischen diesen beiden Zugängen interpolieren kann. Es ist ein wesentlicher Bestandteil dieser Arbeit eine Technik mit dieser Eigenschaft vorzustellen, d.h. unser Ziel ist die Beschreibung von kohärentem Transport durch stark wechselwirkende Quantenpunkte.

Es gibt verschiedene experimentelle Motivationen für das Studium von kohärentem Transport in Einzelelektron-Systemen. Im Coulomb-Blockade Bereich ist inkohärenter Transport exponentiell unterdrückt. Hier wird der Strom durch das sogenannte Cotunneln bestimmt. Dies sind Prozesse höherer Ordnung bei denen das Elektron über einen virtuellen Zwischenzustand kohärent durch den gesamten Quantenpunkt transportiert wird. Falls Quantenpunkte in Aharonov-Bohm Ringe eingebaut sind, werden nur die kohärenten Prozesse eine Flußabhängigkeit zeigen und zu Aharonov-Bohm Oszillationen des Stromes führen. Weiterhin können Experimente durchgeführt werden bei denen der Tunnelwiderstand einer Barriere den Quantenwiderstand erreicht ohne daß Einzelelektron-Effekte zerstört werden. Hier führen Quantenfluktuationen zu

einer signifikanten Abweichung von der "orthodoxen" Theorie auch in Bereichen wo die inkohärenten Prozesse nicht unterdrückt sind. Die Spektraldichte der Insel wird hier stark durch die äußere Umgebung beeinflußt was sich in nichttrivialen Renormierungen und Verbreiterungen der Einteilchen-Anregungen ausdrückt. Dieselben Effekte können auch bei schwacher Transmission der Barrieren vorhanden sein falls die Temperatur klein genug ist.

In wechselwirkungsfreien Systemen ist es sehr einfach Quantenfluktuationen zu berücksichtigen indem man einfach die Energieerhaltung der goldenen Regel durch eine Lorentzartige Funktion mit Halbwertsbreite , ersetzt, wobei , ein Maß für die intrinsische Verbreiterung der Einteilchenzustände bzw. die inverse Lebensdauer der Anregungen darstellt. Für Temperaturen in der Größenordnung $T \sim$ , $\ll E_C$, wird die Linienform der Leitwert-Resonanzen durch die wohlbekannte Breit-Wigner Formel beschrieben. In wechselwirkenden Systemen hingegen zeigt die Verbreiterung der Anregungen eine komplizierte Abhängigkeit von Energie, Temperatur und Transportspannung. Dies induziert starke Renormierungen der Niveaus und der Kopplungskonstanten. Für Quantenpunkte, die durch ein einziges spinentartetes Niveau beschrieben sind, kann die Spektraldichte sogar neue Kondo-artige Resonanzen aufweisen. Diese führen zu verschiedenen zero-bias Anomalien des differentiellen Leitwertes als Funktion der Transportspannung. Quantenpunkte mit kontinuierlichen Einteilchen-Spektren, aber endlicher Ladungsenergie, sind in der Zwei-Zustands-Näherung äquivalent zu Vielkanal-Kondo-Modellen. Auch hier beobachtet man ein anomales Temperaturverhalten des Leitwertes. Durch Veränderung des Niveauabstandes, der Niveaupositionen oder unter Benützung von gekoppelten Quantenpunkten können eine Vielzahl von verschiedenartigen Vielteilchensystemen realisiert werden. Deren Tieftemperatur-Verhalten ist für die meisten Fälle bis jetzt noch nicht bekannt.

Falls die Transmission pro Kanal einer Barriere nahe bei eins liegt, so ist es nicht

mehr möglich zwischen Elektronen im System und in den Reservoiren zu unterscheiden. Dieses Problem wird in dieser Arbeit nicht behandelt, da hier bis jetzt noch keine zufriedenstellende Theorie vorhanden ist. Wir betrachten hier Barrieren mit kleiner Transmission pro Kanal, so daß eine wohldefinierte Beschreibung mit Hilfe eines Tunnel-Hamiltonoperators möglich ist. Für große Kanalzahl enthält dies aber auch die Möglichkeit, daß die gesamte Transmission einer Barriere nahe bei eins liegt. Experimente in diesem Bereich sind kürzlich in metallischen Quantenpunkten durchgeführt worden mit einer klaren Evidenz für Abweichungen von der "orthodoxen" Theorie. Weiterhin können Quantenfluktuationen durch Erniedrigung der Temperatur sichtbar gemacht werden. Insbesondere vertikale Quantenpunkt-Strukturen, ultrakleine metallische Teilchen, Karbon-Quantendrähte oder Moleküle, wo der Niveauabstand und auch die Kopplung an die Reservoire sehr groß sein können, sind vielversprechende Systeme um Quantenfluktuationen im Bereich schwacher Transmission bei realistischen Temperaturen zu beobachten.

Die Arbeit ist folgendermaßen gegliedert. Nach einigen einführenden Abschnitten in denen das System, die zugrundeliegende Physik und Zusammenhänge zu anderen Modellen ausführlich beschrieben werden, wird am Ende des Kapitels 2 die Theorie der Mastergleichung in goldener Regel dargestellt. Wir behandeln sowohl Quantenpunkte mit diskreten Spektren als auch metallische Systeme und diskutieren den Übergang zwischen diesen beiden Grenzfällen. In Anbetracht kürzlicher Experimente werden auch die Ankopplung von bosonischen Bädern und zeitabhängigen Feldern ausführlich dargestellt. Wir vergleichen mit den Ergebnissen der Landauer-Büttiker Theorie und diskutieren die Unterschiede, die durch die starken Korrelationen auf der Insel hervorgerufen werden.

In Kapitel 3 stellen wir eine Theorie vor, die es erlaubt die goldene Regel systematisch auf zeitabhängige Phänomene und höhere Ordnungen im Tunneln zu ver-

allgemeinern. Diese Theorie beruht auf kürzlich entwickelten Real-Zeit diagrammatischen Methoden und steht in engem Zusammenhang mit Wegintegral-Methoden, die für dissipative Systeme oder einzelne metallische Tunnelkontakte entwickelt worden sind. Die zugrundeliegende Idee ist die Ausintegration der wechselwirkungsfreien Reservoire und der bosonischen Bäder, so daß eine effektive Beschreibung in den Freiheitsgraden des lokalen Systems möglich wird. Wir leiten eine formal exakte kinetische Gleichung her und stellen systematische Regeln auf um den Integralkern in jeder Ordnung Störungstheorie im Tunneln zu berechnen. Die starken Korrelationen auf der Insel werden dabei immer vollständig berücksichtigt. Schliesslich formulieren wir die sogenannte Resonanztunnel-Näherung, die eine Aufsummation einer unendlichen Reihe in allen Ordnungen im Tunneln erlaubt.

Die Theorie wird in Kapitel 4 auf verschiedene Probleme angewendet. Zunächst zeigen wir, daß sowohl die Grenzfälle der goldenen Regel als auch die wechselwirkungsfreie Landauer-Büttiker Theorie vollständig reproduziert werden können. Anschließend diskutieren wir Quantenfluktuationen in wechselwirkenden Quantenpunkten jenseits der Störungstheorie. Diese äussern sich in Kondo-artigen Phänomenen, zero-bias Anomalien und weiteren anomalen Abhängigkeiten der Linienformen von Temperatur und Transportspannung. Wir berechnen explizit die Verbreiterung und Renormierung der Einteilchen-Anregungen und vergleichen mit Ergebnissen der Renormierungsgruppe.

# Bibliography


[1] P. W. Anderson, Phys. Rev. **124**, 41 (1961).

[2] J. Appelbaum, Phys. Rev. Lett. **17**, 91 (1966).

[3] D. V. Averin and A. N. Korotkov, Zh. Eksp. Teor. Fiz. **97**, 1661 (1990) [Sov. Phys. JETP **70**, 937 (1990)].

[4] D. V. Averin, A. N. Korotkov, and K. K. Likharev, Phys. Rev. **B44**, 6199 (1991).

[5] D. V. Averin and K. K. Likharev, in *Mesoscopic Phenomena in solids*, eds. B. Altshuler, P.A. Lee, and R.A. Webb (North-Holland, Amsterdam, 1991).

[6] D. V. Averin and Y. V. Nazarov, Phys. Rev. Lett. 65 (1990) 2446; D. V. Averin and Y. V. Nazarov, in *Single Charge Tunneling*, eds. H. Grabert and M. H. Devoret (Plenum Press, New York, 1992).

[7] D. V. Averin, Physica B **194-196**, 979 (1994).

[8] S. E. Barnes, J. Phys. F: Metal Phys. **6**, 1375 (1976); **7** (1977) 2637; Phys. Rev. B 33 (1986) 3209.

[9] C. W. J. Beenakker, Phys. Rev. B **44**, 1646 (1991).

[10] C. W. J. Beenakker and A. A. M. Staring, Phys. Rev. B **46**, 9667 (1992).

[11] N.E. Bickers, Rev. Mod. Phys. **59**, 845 (1987).

[12] R. H. Blick, R. J. Haug, J. Weis, D. Pfannkuche, K. von Klitzing and K. Eberl, Phys. Rev. B **53**, 7899 (1996).

[13] C. Bruder, R. Fazio, and H. Schoeller, Phys. Rev. Lett. **76**, 114 (1995).

[14] C. Bruder and H. Schoeller, Phys. Rev. Lett. **72**, 1076 (1994).

[15] P. Brune, C. Bruder and H. Schoeller, preprint.

[16] M. Büttiker, Phys. Rev. Lett. **57**, 1761 (1986); Phys. Rev. B **46**, 12485 (1992).

[17] M. Büttiker, IBM J. Res. Dev. **32**, 317 (1988).

[18] M. Büttiker and H. Thomas, in *Quantum-Effect Physics, Electronics and Applications*, eds. K. Ismail *et al.*, (Institute of Physics Conference Series Number 127, Bristol, 1992); M. Büttiker, A. Prêtre, and H. Thomas, Phys. Rev. Lett. **70**, 4114 (1993); M. Büttiker and T. Christen, in *Mesoscopic Electron Transport*, NATO ASI, Series E, eds. L.P. Kouwenhoven et al., Kluwer, to be published.

[19] A. O. Caldeira and A. J. Leggett, Physica A **121**, 587 (1983); Ann. Phys. (N.Y.) **149**, 374 (1983); **153**, 445(E) (1983).

[20] C. Caroli, R. Combescot, P. Nozières and D. Saint-James, J.Phys. C **4**, 916 (1971); J.Phys. C **5**, 21 (1972).

[21] S. Datta, Phys. Rev. B **45**, 1347 (1992).

[22] M.H. Devoret, D. Esteve, H. Grabert, G.-L. Ingold, H. Pothier, and C. Urbina, Phys. Rev. Lett. **64**, 1824 (1990).

[23] M. H. Devoret, D. Esteve and C. Urbina, Nature **360**, 547 (1992).

[24] I.A. Devyatov and K.K. Likharev, Physica B **194-196**, 1341 (1994).

[25] P. D. Dresselhaus, L. Ji, S. Han, J. E. Lukens and K. K. Likharev, Phys. Rev. Lett. **72**, 3226 (1994).

[26] A.M. Duif, A.G. Jansen, and P. Wyder, J.Phys.: Cond. Matt. **1**, 3157 (1989).

[27] T. W. Ebbesen, Physics Today **49(6)**, 26 (1996).

[28] U. Eckern, G. Schön and V. Ambegaokar, Phys. Rev. B **30**, 6419 (1984).

[29] G. Falci, G. Schön and G.T. Zimanyi, Phys. Rev. Lett. **74**, 3257 (1995).

[30] U. Fano, Phys. Rev. **124**, 1866 (1961).

[31] R.P. Feynman and F.L. Vernon, Ann. Phys. (N.Y.) 24 (1963) 118.

[32] E. Fick and G. Sauermann, *The Quantum Statistics of Dynamic Processes*, Springer Series in Solid-State Sciences 86 (Springer-Verlag, Berlin, 1990).

[33] K. Flensberg, Phys. Rev. B **48**, 11156 (1993).

[34] K. Flensberg, S.M. Girvin, M. Jonson, D.R. Penn, and M.D. Stiles, Phys. Scripta **T42**, 189 (1992).

[35] E. B. Foxman, P. L. McEuen, U. Meirav, N. S. Wingreen, Y. Meir, P. A. Belk, N. R. Belk, M. A. Kastner and S. J. Wind, Phys. Rev. B **47**, 10020 (1993).

[36] J. Fricke, Ann. Phys. (N.Y.) **252**, 479 (1996).

[37] T. A. Fulton and G. J. Dolan, Phys. Rev. Lett. **59**, 109 (1987).

[38] A. Furusaki, K. A. Matveev, Phys. Rev. B **52**, 16676 (1995).

[39] C. W. Gardiner, *Quantum Noise*, Springer Series in Synergetics 56 (Springer-Verlag, Berlin, 1991).

[40] L. J. Geerligs, D. V. Averin and J. E. Mooij, Phys. Rev. Lett. **65**, 3037 (1990).

[41] L. J. Geerligs, M. Matters and J. E. Mooij, Physica B **194-196**, 1267 (1994).

[42] L.I. Glazman and K.A. Matveev, Pis'ma Zh. Eksp. Teor. Fiz. **48**, 403 (1988), [JETP Lett **48**, 445 (1988)].

[43] L.I. Glazman and M.E. Raikh, Pis'ma Zh. Eksp. Teor. Fiz. **47**, 378 (1988) [JETP Lett. **47**, 452 (1988)].

[44] L.I. Glazman and R.I. Shekhter, Zh. Eksp. Teor. Fiz. **94**, 292 (1988 [Sov. Phys. JETP **67**, 163 (1988)].

[45] L. I. Glazman and K. A. Matveev, Zh. Eksp. Teor. Fiz. **98**, 1834 (1990) [Sov. Phys. JETP 71, 1031 (1990)].

[46] J. M. Golden and B. I. Halperin, Phys. Rev. B **53**, 3893 (1996).

[47] D.S. Golubev and A.D. Zaikin, Phys. Rev. B **50**, 8736 (1994).

[48] H. Grabert and M.H. Devoret, *Single Charge Tunneling*, NATO ASI Series, Vol.294 (New York, Plenum Press 1992).

[49] H. Grabert, Phys. Rev. B **50**, 17364 (1994).

[50] M. Grifoni, M. Sassetti, P. Hänggi and U. Weiss, Phys. Rev. B **52**, 3596 (1995).

[51] M. Grifoni, M. Sassetti and U. Weiss, Phys. Rev. E **53**, R2033 (1996).

[52] P. Guéret, N. Blanc, R. Germann and H. Rothuizen, Phys. Rev. Lett. **68**, 1896 (1992).

[53] O. Gunnarsson and K. Schönhammer, Phys. Rev. Lett. **50**, 604 (1983); Phys. Rev. B **28**, 4315 (1983).

[54] W. Häusler, Ann. Physik **5**, 401 (1996).

[55] C. J. P. M. Harmans, Physics World **5**, 50 (1992).

[56] F. Hekking, Yu. V. Nazarov and G. Schön, Europhys. Lett. **14**, 489 (1991); Europhys. Lett. **20**, 255 (1992).

[57] J. M. Hergenrother, M. T. Tuominen, J. G. Lu, D. C. Ralph and M. Tinkham, Physica B **203**, 327 (1994); J. M. Hergenrother, J. G. Lu, M. T. Tuominen, D. C. Ralph and M. Tinkham, Phys. Rev. B **51**, 9407 (1995).

[58] S. Hershfield, J.H. Davies, and J.W. Wilkins, Phys. Rev. Lett. **67**, 3720 (1991); Phys. Rev. **B46**, 7046 (1992).

[59] M.H. Hettler and H. Schoeller, Phys. Rev. Lett. **74**, 4907 (1995).

[60] A.C. Hewson, *The Kondo Problem to Heavy Fermions*, (Cambridge University Press, 1993).

[61] H. van Houten, C.W.J. Beenakker, and A.A.M. Staring, in *Single Charge Tunneling*, NATO ASI Series, Les Houches, eds. H. Grabert and M. Devoret (Plenum, New York, 1992).

[62] R. Howard and P. Mankiewich, to be published in *Nano-Science and Technology*, ed. G. Timp (AIP Press, New York).

[63] H.T. Imam, V.V. Ponomarenko, and D.V. Averin, Phys. Rev. B **50**, 18288 (1994).

[64] G. Ingold and Yu.V. Nazarov, in *Single Charge Tunneling*, NATO ASI Series, Les Houches, eds. H. Grabert and M. Devoret (Plenum, New York, 1992).

[65] A.G.M. Jansen, A.P. van Gelder, P. Wyder, and S. Strassler, J. Phys. C **13**, 6073 (1980).

[66] K. Jauregui, W. Häusler, D. Weinmann, and B. Kramer, Phys. Rev. B **53** R1713 (1996).

[67] M. Jonson, Phys. Rev. **B39**, 5924 (1989).

[68] A. T. Johnson, L. P. Kouwenhoven, W. de Jong, N. C. van der Vaart, C. J. P. M. Harmans and C. T. Foxon, Phys. Rev. Lett. **69**, 1592 (1992).

[69] P. Joyez, V. Bouchiat, D. Esteve, C. Urbina and M. H. Devoret, preprint.

[70] M. A. Kastner, Rev. Mod. Phys. **64**, 849 (1992); Physics Today **46**, 24 (1993).

[71] A. Kawabata, J. Phys. Soc. Japan **60**, 3222 (1991).

[72] H. Keiter and G. Morandi, Phys. Rep. **109**, 227 (1984).

[73] J. M. Kinaret, Y. Meir, N. S. Wingreen, P. A. Lee and Xiao-Gang Wen, Phys. Rev. B **46**, 4681 (1992).

[74] D. L. Klein, P. L. McEuen, J. E. Bowen Katari, R. Roth, A. P. Alivisatos, Appl. Phys. Lett. **68**, 2574 (1996).

[75] G. Klimeck, G. Chen and S. Datta, Phys. Rev. B **50**, 2316 (1994); Phys. Rev. B **50**, 8035 (1994).

[76] J. König, H. Schoeller and G. Schön, Europhys. Lett. **31**, 31 (1995); and in *Quantum Dynamics of Submicron Structures*, eds. H. A. Cerdeira *et al.*, NATO ASI Series E, Vol. 291 (Kluwer, 1995), p.221

[77] J. König, H. Schoeller and G. Schön, Phys. Rev. Lett. **76**, 1715 (1996); and in *Festkörperprobleme / Advances in Solid State Physics*, Vol. 35, ed. R. Helbig (Vieweg, Braunschweig/Wiesbaden), p.215 (1996).

[78] J. König, J. Schmid, H. Schoeller, and G. Schön, Phys. Rev. B **54**, 16820 (1996).

[79] J. König, diploma thesis, Karlsruhe 1995.

[80] J. König, H. Schoeller and G. Schön, preprint.

[81] A. N. Korotkov, D. V. Averin, K. K. Likharev and S. A. Vasenko, in *Single-Electron Tunneling and Mesoscopic Devices*, ed. H. Koch and H. Lübig (Springer, Berlin, 1992).

[82] R. Kotlyar and S. Das Sarma, cond-mat/9611200.

[83] L. P. Kouwenhoven, N. C. van der Vaart, A. T. Johnson, W. Kool, C. J. P. M. Harmans, J. G. Williamson, A. A. M. Staring and C. T. Foxon, Z. Phys. B **85**, 367 (1991).

[84] L.P. Kouwenhoven, S. Jauhar, K. McCormick, D. Dixon, P.L. McEuen, Yu. V. Nazarov, N.C. van der Vaart, and C.T. Foxon, Phys. Rev. B **50**, 2019 (1994).

[85] I.O. Kulik and R.I. Schekhter, Zh. Eksp. Teor. Fiz. **68**, 623 (1975) [Sov. Phys. JETP 41 (1975) 308].

[86] P. Lafarge, H. Pothier, E. R. Williams, D. Esteve, C. Urbina and M. H. Devoret, Z. Phys. B **85**, 327 (1991).

[87] P. Lafarge and D. Esteve, Phys. Rev. B **48**, 14309 (1993).

[88] R. Landauer, IBM J. Res. Dev. **1**, 233 (1957).

[89] A.J. Leggett, S. Chakravarty, A.T. Dorsey, M.P.A. Fisher, A. Garg, and W. Zwerger, Rev. Mod. Phys. **59**, 1 (1987).

[90] C. S. Lent, P. D. Tougaw and W. Porod, Appl. Phys. Lett. **62**, 714 (1993).

[91] E. Lieb and D. Mattis, Phys. Rev. **125**, 164 (1962).

[92] K. K. Likharev, IEEE Trans. Magn. **23**, 1142 (1987); IBM J. Res. Dev. **32**, 144 (1988).

[93] K. K. Likharev and T. Claeson, Scientific American **266**, 50 (1992).

[94] S. Lloyd, Science **261**, 1569 (1993).

[95] D. Loss and D. P. DiVincenzo, cond-mat/9701055.

[96] G.D. Mahan, *Many-Particle Physics*, (Plenum, 1990).

[97] J. M. Martinis, M. Nahum and H. D. Jensen, Phys. Rev. Lett. **72**, 904 (1994).

[98] K.A. Matveev, Zh. Eksp. Teor. Fiz. **99**, 1598 (1991) [Sov. Phys. JETP 72 (1991) 892].

[99] K. A. Matveev, Phys. Rev. B **51** 1743 (1995).

[100] K. A. Matveev, L. I. Glazman and H. U. Baranger, Phys. Rev. B **53**, 1034 (1996); Phys. Rev. B **54**, 5637 (1996).

[101] P.L. McEuen and L.P. Kouwenhoven, to be published in *Nano-Science and Technology*, ed. G. Timp (AIP Press, New York).

[102] Y. Meir, N.S. Wingreen, and P.A. Lee, Phys. Rev. Lett. **66**, 3048 (1991).

[103] Y. Meir, N.S. Wingreen, and P.A. Lee, Phys. Rev. Lett. **70**, 2601 (1993); N.S. Wingreen and Y. Meir, Phys. Rev. **B49**, 11040 (1994).

[104] U. Meirav, M. A. Kastner and S. J. Wind, Phys. Rev. Lett. **65**, 771 (1990).

[105] L. W. Molenkamp, K. Flensberg and M. Kemerink, Phys. Rev. Lett. **75**, 4282 (1994).

[106] Yu. V. Nazarov, J. Low Temp. Phys. **90**, 77 (1993).

[107] T.K. Ng, Phys. Rev. Lett. **70**, 3635 (1993).

[108] T.K. Ng, Phys. Rev. Lett. **76**, 487 (1996).

[109] T.K. Ng and P.A. Lee, Phys. Rev. Lett. **61**, 1768 (1988).

[110] A.A. Odintsov, G. Falci, and G. Schön, Phys. Rev. B **44**, 13089 (1991).

[111] T. H. Oosterkamp, L. P. Kouwenhoven, A. E. A. Koolen, N. C. van der Vaart, and C. J. P. M. Harmans, preprint.

[112] C. Pasquier, U. Meirav, F. I. B. Williams and D. C. Glattli, Phys. Rev. Lett. **70**, 69 (1993).

[113] D. Pfannkuche and S.E. Ulloa, Phys. Rev. Lett. **74**, 1194 (1995).

[114] D. Pfannkuche, V. Gudmundsson and P. A. Maksym, Phys. Rev. B **47**, 2244 (1993).

[115] Physica B **189** (1993), special issue on *Few-electron Nanostructures.*

[116] T. Pohjola, J. König, M. M. Salomaa, J. Schmid, H. Schoeller and G. Schön, preprint.

[117] D.C. Ralph, C.T. Black and M. Tinkham, Phys. Rev. Lett. **74**, 3241 (1995); D.C. Ralph, C.T. Black, M. Tinkham, and R.C. Tiberio, preprint, submitted to *Science.*

[118] D.C. Ralph and R.A. Buhrman, Phys. Rev. Lett. **72**, 3401 (1994).

[119] M. A. Reed, J. N. Randall, R. J. Aggarwall, R. J. Matyi, T. M. Moore and A. E. Wetsel, Phys. Rev. Lett. **60**, 535 (1988).

[120] M. Reed, Scientific American **268**, 118 (1993).

[121] T. Schmidt, R. J. Haug, K. v. Klitzing, A. Förster and H. Lüth, Phys. Rev. Lett. **78**, 1544 (1997).

[122] H. Schoeller, Ann. Phys. (N.Y.) **229**, 273 (1994).

[123] H. Schoeller and G. Schön, Phys. Rev. **B50**, 18436 (1994); Physica **B203**, 423 (1994).

[124] G. Schön, to be published in *Quantum Processes and Dissipation*, Chapter 4, eds. B. Kramer *et al.*, (VCH Publishers).

[125] G. Schön and A.D. Zaikin, Phys. Rep. **198**, 237 (1990).

[126] C. Schönenberger, H. van Houten, H. C. Donkersloot, Europhys. Lett. **20**, 249 (1992).

[127] J. R. Schrieffer and P. A. Wolff, Phys. Rev. **149**, 491 (1966).

[128] J. H. F. Scott-Thomas, S. B. Field, M. A. Kastner, H. I. Smith and D. A. Antonadis, Phys. Rev. Lett. **62**, 583 (1989).

[129] J. H. Shirley, Phys. Rev. **138**, B979 (1965).

[130] C.A. Stafford, Phys. Rev. Lett. **77**, 2770 (1996).

[131] C. A. Stafford and N. S. Wingreen, Phys. Rev. Lett. **76**, 1916 (1996).

[132] B. Su, V. J. Goldman and J. E. Cunningham, Science **255**, 313 (1992).

[133] Y. Tanaka and H. Akera, Phys. Rev. B **53**, 3901 (1996).

[134] S. Tarucha, D.G. Austing, T. Honda, R.J. van der Hage, and L.P. Kouwenhoven, Phys. Rev. Lett. **77**, 3613 (1996).

[135] P. K. Tien and J. R. Gordon, Phys. Rev. **129**, 647 (1963).

[136] N. C. van der Vaart, A. T. Johnson, L. P. Kouwenhoven, D. J. Maas, W. de Jong, M. P. de Ruyter van Stevenick, A. van der Enden and C. J. P. M. Harmans, Physica B **189**, 99 (1993).

[137] N. C. van der Vaart, L. P. Kouwenhoven, S. F. Godijn, C. J. P. M. Harmans and J. E. Mooij, in *Superlattices and Microstructures*, NanoMES 1996 conference proceedings; N. C. van der Vaart, PhD thesis, Delft 1995.

[138] E. H. Visscher, S. M. Verbrugh, J. Lindeman, P. Hadley and J. E. Mooij, Appl. Phys. Lett. **66** 305 (1994).

[139] F. R. Waugh, M. J. Berry, D. J. Mar, R. M. Westervelt, K. L. Campman and A. C. Gossard, Phys. Rev. Lett. **75**, 705 (1995); F. R. Waugh, M. J. Berry, C. H. Crouch, C. Livermore, D. J. Mar, R. M. Westervelt, K. L. Campman and A. C. Gossard, Phys. Rev. B **53**, 1413 (1996).

[140] U. Weiss, *Quantum Dissipative Systems*, Series in Modern Condensed Matter Physics, Vol. 2 (World Scientific, 1993).

[141] D. Weinmann, W. Häusler, W. Pfaff, B. Kramer, and U. Weiss, Europhys. Lett. **26**, 467 (1994);

[142] D. Weinmann, W. Häusler and B. Kramer, Phys. Rev. Lett. **74**, 984 (1995).

[143] J. Weis, R. J. Haug, K. von Klitzing and K. Ploog, Phys. Rev B **46**, 12837 (1992).

[144] J. Weis, R. J. Haug, K. von Klitzing and K. Ploog, Phys. Rev. Lett. **71**, 4019 (1993).

[145] N.S. Wingreen, K.W. Jacobsen, and J.W. Wilkins, Phys. Rev. Lett. **61**, 1396 (1988); Phys. Rev. B **40**, 11834 (1989).

[146] N.S. Wingreen, A.P. Jauho, and Y. Meir, Phys. Rev. B **48**, 8487 (1993).

[147] E.L. Wolf, *Principles of Electron Tunneling Spectroscopy*, (Oxford Univ. Press, New York, 1989), Chap. 8.

[148] A.L. Yeyati, A. Martin-Rodero, and F. Flores, Phys. Rev. Lett. **71**, 2991 (1993).

[149] Zeitschrift für Physik B, Condensed Matter **85** (1991), special issue on *Single Charge Tunneling*.

[150] W. Zwerger, Z. Phys. B **93**, 333 (1994).

Ich versichere, diese Arbeit selbständig verfaßt und keine anderen als die angegebenen Quellen und Hilfsmittel benutzt zu haben.

Karlsruhe, März 1997